2010

# Structural and functional study of multidrug transporters

Feng Long
*Iowa State University*

**Structural and functional study of multidrug transporters**

by

**Feng Long**

A dissertation submitted to the graduate faculty

in partial fulfillment of the requirements for the degree of

DOCTOR OF PHILOSOPHY

Major: Molecular, Cellular and Developmental Biology

Program of Study Committee:
Edward W. Yu, Major Professor
Drena L. Dobbs
Gregory J. Phillips
Kai-Ming Ho
Qijing Zhang

Iowa State University

Ames, Iowa

2010

# TABLE OF CONTENTS

# ABSTRACT

Active efflux of antimicrobial agents is one of the most important strategies that bacteria use to ensure their survival in a toxic extracellular environment. Our interest is to elucidate the structural and functional relationships of bacterial multidrug efflux transporters that give rise to antibiotic resistance. In this dissertation, I focus on studying two specific groups, the multidrug and toxic compound extrusion (MATE) family and the resistance-nodulation-division (RND) family, of multidrug efflux transporters. The functions of the two MATE efflux pumps, NorM of *Neisseria gonorrhoeae* and YdhE of *Escherichia coli*, are characterized using a variety of biochemical assays, including drug susceptibility and transport assays. Direct measurements of efflux allow us to confirm that NorM behaves as a $Na^+$-dependent transporter. The capacity of NorM and YdhE to recognize structurally divergent compounds is also examined using steady-state fluorescence polarization assays. The results suggest that NorM and YdhE bind these antimicrobials with dissociation constants ($K_D$s) in the micromolar range.

In addition, I present the crystal structures of the CusA transporter, the only heavy-metal efflux (HME) pump of the RND family in *E. coli*, in the absence and presence of Cu(I) and Ag(I) ions. These are the first structures of any efflux pumps belonging to the HME-RND family. Surprisingly, the binding of Cu(I) and Ag(I) triggers significant conformational changes in both the periplasmic and transmembrane domains of the pump. Based on the crystal structures and biochemical studies, I put forward my hypothesis that CusA is capable of actively picking up metal ions from the cytoplasm as well as the periplasmic space, utilizing the methionine pairs/clusters in the pump to bind and export metal ions. A stepwise shuttle mechanism is probably employed by the pump to extrude these heavy metals.

# CHAPTER 1. General Introduction

## Bacterial multidrug resistance

Since the discovery of penicillin in 1928, antibiotics have had been used to cure many potentially lethal bacterial infections. As a consequence of the widespread use of these antibiotics, an increasing number of pathogens are becoming resistance to multiple antibiotics. One of the most serious threats to human health was posed with the emergence of vancomycin resistance in methicilllin-resistant *Staphylococcus aureus* (MRSA) (1). To date it has been found to be more difficult to treat bacterial infections with standard therapies. Bacteria can work against the action of antibiotics through various strategies (2). These include altering or modifying the target, enzymatic inactivating the drug, preventing an antibiotic from entering the bacterial cell, and actively transporting an antibiotic out of the cell. Except for the intrinsic resistance to given antibacterial drugs, bacteria can resist antibiotics in a broad range by acquiring resistance genes from other species (3).

Bacterial multidrug efflux transporters are currently categorized in five different families: the major facilitator (MF) superfamily (4-6), the resistance nodulation cell division (RND) family (7), the small multidrug resistance (SMR) family (8), the ATP binding cassette (ABC) family (9) and the multidrug and toxic compound extrusion (MATE) family (10). The ABC family transporters take the free energy generated from ATP hydrolysis to expel toxic substances out of cells. Efflux transporters in the other families, however, utilize the transmembrane electrochemical gradient of protons or sodium ions to extrude these harmful substrates from cells. In this dissertation, I mainly focus on the study of representative transporters belonging to the RND and MATE families.

Multidrug transporters have been identified in both mammalian and bacterial cells. An understanding of how these efflux transporters works would allow us to find better approaches for treating bacterial infections and cancer. The key to understand how these efflux pumps operate involves the determination of the structures of representative transporters and the elucidation of the conformational changes that accompany with drug translocation across the cell membrane.

## Multidrug efflux pumps of the MATE family

The MATE family is the most recently classified family with only about twenty transporters having been identified so far. MATE transporters are typically composed of 12 putative transmembrane domains, and have been found in all major kingdoms (Eukarya, Archaea, and Eubacteria). NorM of *Vibrio parahaemolyticus*, the first characterized MATE transporter, is a $Na^+$ /drug antiporter that confers resistance to dyes, fluoroquinolones and aminoglycosides (11). Subsequently, other MATE efflux pumps have been identified in many pathogenic bacteria, including *Acinetobacter baumannii* (12), *Brucella melitensis* (13), *Clostridium difficile* (14), *Haemophilus influenza* (15), *Neisseria gonorrhoeae* (16), *Neisseria meningitides* (16), *Pseudomonas aeruginosa* (17), *Staphylococcus aureus* (18), and *Vibrio cholera* (19-21). The main substrates for these MATE transporters are cationic and aromatic compounds. Until now, little knowledge has been obtained regarding the structures and fundamental mechanisms that give rise to multidrug resistance mediated by this novel MATE family of transporters. Nonetheless, the presence of these multidrug efflux pumps in pathogens highlights the potential clinical significance of this transporter family. In this

dissertation, I target the NorM pump of *N. gonorrhoeae* and the YdhE transporter of *Escherichia coli*, and characterize the functions of these two MATE-type proteins.

*N. gonorrhoeae*, a gram-negative diplococcus, is found only in humans and causes one of the most common sexually transmitted diseases. This pathogen is progressively shown to be resistant to multiple antibiotics, including penicillin, tetracycline, erythromycin, and ciprofloxacin. In April 2007, the Centers for Diseases Control and Prevention (CDC) officially added gonorrhea to the list of antibiotic resistant 'super bugs' (22). In the USA, it is estimated that 700,000-800,000 new cases occur each year, with a cost of about $1.1 billion annually for this infection (23). While we are aware of the growing public health concern resulted from the antimicrobial resistance developed in *N. gonorrhoeae*, four multidrug transporters have been identified in *N. gonorrhoeae*. These transporters are MtrD (RND) (24-26), FarB (MF) (27), MacB (ABC) (28) and NorM (MATE). The gonococcal NorM appears to recognize and export a number of cationic toxic compounds, including ethidium bromide, acriflavin, 2-N-methylellipticinium, and ciprofloxacin (16).

The *E. coli* YdhE multidrug transporter is homologous to *N. gonorrhoeae* NorM (11, 29, 30). These two MATE transporters share 34% identity and 70% similarity. Both YdhE and NorM are membrane proteins, consisting of 457 and 459 amino acid residues, respectively. Our goal is to understand the structural and functional relationship of these MATE transporters using x-ray crystallography and different biochemical methods. Particularly, I investigate the active molecular functions of *N. gonorrhoeae* NorM and *E. coli* YdhE by conducting heterogenous drug susceptibility test, *in vivo* transport assay, and a novel fluorescence polarization assay. The information has allowed us to understand the

fundamental rules that govern drug recognition and extrusion in the MATE family of multidrug efflux pumps.

## Multidrug efflux pumps of the RND family

The RND-type transporters play a major role in mediating clinically relevant antibiotic resistance in Gram-negative bacteria. These transporters can work against a broad range of structural unrelated toxic compounds. For example, *E. coli* AcrB is capable of extruding a variety of antibiotics, detergents, dyes and simple organic solvents (31). A typical RND efflux system consists of three fundamental components: an inner membrane RND transporter, a periplasmic membrane fusion protein (MFP) and an outer membrane protein (OMP) channel. The resulting tripartite complex spans both the inner and outer membranes and exports these toxic substrates directly out of the bacterial cell (32, 33). The energy source of the process comes from proton import, which is utilized by the inner membrane RND transporter.

The RND family can be further divided into two sub-families, the hydrophobic and amphiphilic efflux RND (HAE-RND) and heavy-metal efflux RND (HME-RND) sub-families. As a Gram-negative bacterium, *E. coli* possesses seven RND transporters. Six of these efflux pumps, AcrB (31, 34-41), AcrD (42), AcrF (43), MdtB (44, 45), MdtC (44, 45) and YhiV (46, 47), are categorized as the HAE-RND sub-family. These six transporters are responsible for the intrinsic tolerance of antibiotics and toxic organic compounds. The rest of the transporter CusA belongs to the HME-RND family and is found to be capable of exporting copper (I) and silver (I) ions out of *E. coli* cell (48, 49).

Among all known RND transporters, the X-ray structures of *E. coli* AcrB (35, 36, 38, 39) and *Pseudomonas aeruginosa* MexA (50) have been determined. Based on the crystal structures, the functional unit of these efflux pumps is a homotrimer. In each monomer of the AcrB pump, there are 12 transmembrane (TM) helices spanning the entire cytoplasmic membrane, and two large periplasmic loops protruding approximately 80Å into the periplasm. A large cavity with a diameter of approximate 35Å is formed in the transmembrane region within the trimer. The large periplasmic domain of the pump mainly comprises two distinct loops located between TM1 and 2, and TM7 and 8 (51). It has been well characterized that the AcrB transporter interacts with TolC (OMP) and AcrA (MFP) to form a functional tripartite RND efflux complex (52). The crystal structures of these three individual components are all available (53-55). A proposed assembled model of the tripartite RND efflux complex, based on cross-linking and computation method, has suggested that this efflux system is in the form of $AcrB_3$-$AcrA_3$-$TolC_3$ (56). A pathway for transporting substrates in the pump has been shown through a tunnel formed by the periplasmic domain using computational calculation (40, 50). However, the fundamental mechanisms involved in the assembly and drug transport of this tripartite system are still not clear and confirmative.

Towards our goal to elucidate the structures and fundamental mechanisms that give rise to the recognition and extrusion of toxic compounds in RND efflux transporters, we focus on studying the *E. coli* CusCBA HME-RND efflux system. This study has provided us with the understanding of heavy-metal tolerance in bacteria.

As an alternative clinical treatment of bacterial infections, both silver and copper exhibit antimicrobial activities against a broad range of microorganisms at low concentrations. Although copper is required by most microorganisms in trace amount to

maintain their lives, excess amount of copper is extremely toxic (57). It has been reported that silver and copper compounds effectively eliminate *Legionella* in drinking water pipelines (58). Silver compounds are comparatively more often used for clinical purposes. Colloidal silver was first approved for wound management by the US Food and Drug Administration (FDA) in the 1920s (59). To date, silver compounds are still widely used in the treatment of open wounds due to the limited prescription of antibiotics. Because of the widespread use of silver and copper as microcidal agents, concerns about the emergence of bacterial resistance are being raised (59, 60).

The Cus system is encoded by a single operon *cusCFBA*, which is located on the *E. coli* chromosome (48, 49, 61). The transcription of this operon is regulated by a two-component system, consisting of a membrane kinase sensor (CusS) and a transcriptional regulatory responder (CusR) (62). CusB and CusC are the MFP and OMP proteins, respectively. Presumably, in cooperation with the CusA efflux pump, they form a tripartite complex that spans both the inner and outer membranes of *E. coli*, resembling the AcrAB-TolC system. Distinct from most RND efflux complexes, the Cus system has an additional component - the small periplasmic protein CusF (63- 65). The crystal structure of CusF depicts that this protein forms a five-stranded β–barrel with the conserved residues H36, W44, M47 and M49 making up the Cu(I)/Ag(I) binding site. It has been proposed that CusF functions as a metallochaperone that delivers Cu(I) or Ag(I) in the periplasm to the CusCBA efflux machinery. The x-ray crystal structure of CusB has been solved recently in our lab (66). The multiple Cu(I)/Ag(I) binding sites were discovered at the potential hinge regions between the individual domains. One of the objectives of this dissertation is to understand the structure and function of the CusA inner membrane transporter, which is the most

important component of the Cus transport system. I have determined the crystal structures of CusA in the absence and presence of Cu(I) and Ag(I). Together with results from site-directed mutagenesis and different biochemical assays, I put forward to propose a molecular mechanism that governs the heavy-metal export in bacteria. It is expected that this information will provide us with important clues for the understanding of other HAE-RND efflux pumps.

## Organization of the dissertation

Chapter 1 gives the general introduction of multidrug resistance in bacteria and of multidrug efflux pumps. Two transporter families, including MATE and RND, are described in details. The rationale of the dissertation is also addressed in this chapter. Chapter 2 is a manuscript, published in *Antimicrobial Agents and Chemotherapy* in 2008, which characterizes two MATE transporters, *N. gonorrhoeae* NorM and *E. coli* YdhE.

Chapter 3 is a manuscript, submitted to the journal *Nature*, which describes the crystal structures of the HME-RND transporter CusA of *E. coli* in the absence and presence of Cu(I) and Ag(I). In this chapter, a variety of functional studies were also performed to elucidate the molecular mechanisms of the efflux pump. Chapter 4 summarizes the results and provides the overall conclusions of the dissertation.

## References

1. De Lencastre, H., D. Oliveira, A. Tomasz. 2007. Antibiotic resistant *Staphylococcus aureus*: a paradigm of adaptive powder. *Curr. Opin. Microbiol.* 10:428-35.

2. Nikaido, H. 2009. Multidrug resistance in bacteria. *Annu. Rev. Biochem.* 78:119-46.

3. Bennett, P. M. 2008. Plasmid encoded antibiotic resistance: acquisition and transfer of antibiotic resistance genes in bacteria. *J Pharmacol.* 153(S1):S347-57.

4. Griffith, J. K., M. E. Baker, D. A. Rouch, M. G. Page, R. A. Skurray, I. T. Paulsen, K. F. Chater, S. A. Baldwin, and P. J. Henderson. 1992. Membrane transport proteins: Implications of sequence comparisons. *Curr. Opin. Cell Biol.* 4:684-695.

5. Marger, M. D. and M. H. Saier, Jr. 1993. A major superfamily of transmembrane facilitators that catalyse uniporter, symporter and antiporter. *Trends Biochem. Sci.* 18: 13-20.

6. Pao, S. S., I. T. Paulsen, and M. H. Saier, Jr. 1998. Major facilitator superfamily. *Microbiol. Mol. Biol. Rev.* 62:1-34.

7. Tseng, T. T., Gratwick K. S., Kollman J., Park D., Nies D. H., Goffeau A., and M. H. Saier, Jr. 1999. The RND permease superfamily: an ancient, ubiquitous and diverse family that includes human disease and development proteins. *J. Mol. Microbiol. Biotechnol.* 1:107-125.

8. Paulsen, I. T., R. A. Skurray, R. Tam, M. H. Saier, Jr., R. J. Turner, J. H. Weiner, E. B. Goldberg, and L. L. Grinius. 1996. The SMR family: a novel family of multidrug efflux proteins involved with the efflux of lipophilic drugs. *Mol. Microbiol.* 19:1167-1175.

9. Higgins, C.F. 1992. ABC transporters: from microorganisms to man. *Annu. Rev. Cell Biol.* 8:67-113.

10. Brown, M. H., I. T. Paulsen, and R. A. Skurray. 1999. The multidrug efflux protein NorM is a prototype of a new family of transporters. *Mol. Microbiol.* 31:394-395.

11. Morita, Y., K. Kodama, S. Shiota, T. Mine, A. Kataoka, T. Mizushima, and T. Tsuchiya. 1998. NorM, a putative multidrug efflux protein, of *Vibrio parahaemolyticus* and its homolog in *Escherichia coli*. *Antimicrob. Agents Chemother.* 42:1778-1782.

12. Su, X.-Z., J. Chen, T. Mizushima, T. Kuroda, and T. Tsuchiya. 2005. AbeM, an $H^+$-coupled *Acinetobacter baumannii* multidrug efflux pump belonging to the MATE family of transporters. *Antimicrob. Agents Chemother.* 49:4362-4364.

13. Braibant, M., L. Guilloteau, and M. S. Zygmunt. 2002. Functional characterization of *Brucella melitensis* NorMI, an efflux pump belonging to the multidrug and toxic compound extrusion family. *Antimicrob. Agents Chemother.* 46:3050-3053.

14. Dridi, L., J. Tankovic, and J. C. Petit. 2004. CdeA of *Clostridium difficile*, a new multidrug efflux transporter of the MATE family. *Microb. Drug Resist.* 10:191-196.

15. Xu, X.-J., X.-Z. Su, Y. Morita, T. Kuroda, T. Mizushima, and T. Tsuchiya. 2003. Molecular cloning and characterization of the HmrM multidrug efflux pump from *Haemophilus influenzae* Rd. *Microbiol. Immunol.* 47:937-943.

16. Rouquette-Loughlin, C., S. A. Dunham, M. Kuhn, J. T. Balthazar, and W. M. Shafer. 2003. The NorM efflux pump of by *Neisseria gonorrhoeae* and *Neisseria meningitides* recognizes antimicrobial cationic compounds. *J. Bacteriol.* 185:1101-1106.

17. He, G.-X., T. Kuroda, T. Mima, Y. Morita, T. Mizushima, and T. Tsuchiya. 2004. An $H^+$- coupled multidrug efflux pump, PmpM, a member of the MATE family of transporters, from *Pseudomonas aeruginosa*. *J. Bacteriol.* 186:262-265.

18. Kaatz, G. W., F. McAleese, and S. M. Seo. 2005. Multidrug resistance in *Staphylococcus aureus* due to overexpression of a novel multidrug and toxin extrusion (MATE) transport protein. *Antimicrob. Agents Chemother.* 49:1857-1864.

19. Singh, A. K., R. Halder, D. Mandal, and M. Kundu. 2006. Analysis of the topology of *Vibrio cholerae* NorM and identification of amino acid residues involved in norfloxacin resistance. *Antimicrob. Agents Chemother.* 50:3717-3723.

20. Nazmul Huda, N., J. Chen, Y. Morita, T. Kuroda, T. Mizushima, and T. Tsuchiya. 2003. Gene cloning and characterization of VcrM, a $Na^+$-coupled multidrug efflux pump from *Vibrio cholerae* non-O1. *Microbiol. Immunol.* 47:419-427.

21. Begum, A., M. Rahaman, W. Ogawa, T. Mizushima, T. Kuroda, and T. Tsuchiya. 2005. Gene cloning and characterization of four MATE family multidrug efflux pumps from *Vibrio cholerae* non-O1. *Microbiol. Immunol.* 49:949-957.

22. http://www.cdc.gov/Gonorrhea/arg/default.htm.

23. http://www.thebody.com/content/art6532.html.

24. Maness, M. J., and P. F. Sparling. 1973. Multiple antibiotic resistance due to a single mutation in *Neisseria gonorrhoeae*. *J. Infect. Dis.* 128:321-330.

25. Hagman, K. E., W. Pan, B. G. Spratt, J. T. Balthazar, R. C. Judd, and W. M. Shafer. 1995. Resistance of *Neisseria gonorrhoeae* to anitmicrobial hydrophobic agents is modulated by the *mtrRCDE* efflux system. *Microbiology* 141:611-622.

26. Hagman, K. E., C. E. Lucas, J. T. Balthazar, L. A. Snyder, M. Nilles, R. C. Judd, and W. M. Shafer. 1997. The MtrD protein of *Neisseria gonorrhoeae* is a member of resistance/nodulation/division protein family constituting part of an efflux system. *Microbiology* 143:2117-2125.

27. Lee, E.-H., and W. M. Shafer. 1999. The *farAB*-encoded efflux pump mediates resistance of gonococci to long-chained antibacterial fatty acids. *Mol. Microbiol.* 33:839-845.

28. Rouquette-Loughlin, C. E., J. T. Balthazar, and W. M. Shafer. 2005. Characterization of the MacA-MacB efflux system in *Neisseria gonorrhoeae*. *J. Antimicrob. Chemother.* 56:856-860.

29. Blattner, F. R., G. Plunkette, 3rd, C. A. Block, N. T. Perna, V. Burland, M. Riley, J. Collado-Vides, J. D. Glasner, C. K. Rode, G. F. Mayhew, J. Gregor, N. W. Davis, H. A. Kirkpatrick, M. A. Goeden, D. J. Rose, B. Mau, and Y. Shao. 1997. The complete genome sequence of *Escherichia coli* K-12. *Science* 277:1453-1474.

30. Yang, S., S. R. Clayton, and E. L. Zechiedrich. 2003. Relative contributions of the AcrAB, MdfA and NorE efflux pumps to quinolone resistance in *Escherichia coli*. *J. Antimicrob. Chemother.* 51:545-556.

31. Yu, E. W., J. R. Aires, and H. Nikaido. 2003. AcrB multidrug efflux pump of *Escherichia coli*: composite substrate-binding cavity of exceptional flexibility generates its extremely wide substrate specificity. *J. Bacteriol.* 185:5657-5664.

32. Saier, M. H., Jr. 2000. A functional phylogenetic classification system for transmembrane solute transporters. *Microbiol. Mol. Bio. Rev.* 64:354-411.

33. Zgurskaya, H. I., and H. Nikaido. 2000. Multidrug resistance mechanisms: drug efflux across two membranes. *Mol. Microbiol.* 37:219-225.

34. Zgurskaya, H., and H. Nikaido. 1999. Bypassing the periplasm: Reconstitution of the AcrAB multidrug efflux pump of *Escherichia coli*. *Proc. Natl. Acad. Sci. U.S.A.* 96:7190-7195.

35. Murakami, S., R. Nakashima, E. Yamashita, and A. Yamaguchi. 2002. Crystal structure of bacterial multidrug efflux transporter AcrB. *Nature* 419:587-593.

36. Yu, E. W., G. McDermott, H. I. Zgruskaya, H. Nikaido, and D. E. Koshland, Jr. 2003. Structural basis of multiple drug binding capacity of the AcrB multidrug efflux pump. *Science* 300:976-980.

37. Yu, E. W., J. R. Aires, G. McDermott, and H. Nikaido. 2005. A periplasmic drug-binding site of the AcrB multidrug efflux pump: a crystallographic and site-directed mutagenesis study. *J. Bacteriol.* 187:6804-6815.

38. Murakami, S., R. Nakashima, E. Yamashita, T. Matsumoto, and A. Yamaguchi. 2006. Crystal structures of a multidrug transporter reveal a functionally rotating mechanism. *Nature* 443:173-179.

39. Seeger, M. A., A. Schiefner, T. Eicher, F. Verrey, K. Dietrichs, and K. M. Pos. 2006. Structural asymmetry of AcrB trimer suggests a peristaltic pump mechanism. *Science* 313:1295-1298.

40. Sennhauser, G., P. Amstutz, C. Briand, O. Storchenegger, and M. G. Grutter. 2006. Drug export pathway of multidrug exporter AcrB revealed by DARPin inhibitors. *PLos Biol.* 5:e7.

41. Su, C.-C., Li, M., Gu, R., Takatsuka, Y., Mcdermott, G., Nikaido, H., and Yu, E. W. 2006. Conformation of the AcrB multidrug efflux pump in mutants of the putative proton relay pathway. *J. Bacteriol.* 188:7290-7296.

42. Aires, J. R., and H. Nikaido. 2005. Aminoglycosides are captured from both periplasm and cytoplasm by the AcrD multidrug efflux transporter of *Escherichia coli*. *J. Bacteriol.* 187:1923-1929.

43. Lau, S. Y., and H. I. Zgurskaya. 2005. Cell division defects in *Escherichia coli* deficient in the multidrug efflux transporter AcrEF-TolC. *J. Bacteriol.* 187:7815-7825.

44. Baranova, N., and H. Nikaido. 2002. The BaeSR two-component regulatory system activates transcription of *yegMNOB* (*mdtABCD*) transporter gene cluster in *Escherichia coli* and increases its resistance to novobiocin and deoxycholate. *J. Bacteriol.* 184:4168-4176.

45. Nagakubo, S., K. Nishino, T. Hirata, and A. Yamaguchi. 2002. The putative response regulator BaeR stimulates multidrug resistance of *Escherichia coli* via a novel multidrug exporter system, MdtABC. *J. Bacteriol.* 184:4161-4167.

46. Nishino, K., and A. Yamaguchi. 2001. Analysis of a complete library of putative drug transporter genes in *Escherichia coli*. *J. Bacteriol.* 183:5803-5812.

47. Elkins, C. A., and L. B. Mullis. 2006. Mammalian steroid hormones are substrates for the major RND- and MFS-type tripartite multidrug efflux pumps of *Escherichia coli*. J. *Bacteriol.* 188:1191-1195.

48. Franke, S., G. Grass, and D. H. Nies. 2001. The product of the *ybdE* gene of the *Escherichia coli* chromosome is involved in detoxification of silver ions. *Microbiol.* 147:965-972.

49. Franke, S., G. Grass, C. Rensing, and D. H. Nies. 2003. Molecular analysis of the copper-transporting efflux system CusCFBA of *Escherichia coli*. *J. Bacteriol.* 185:3804-3812.

50. Sennhauser, G., M. A. Bukowska, C. Briand, and M. G. Grutter. 2009. Crystal structure of the multidrug exporter MexB from *Pseudomonas aeruginosa*. *J. Mol. Biol.* 389: 134-145

51. Saier, M. H., Jr., I. T. Paulsen, M. K. Sliwinski, S. S. Pao, R. A. Skurray, and H. Nikaido. 1998. Evolutionary origins of multidrug and drug-specific efflux pumps in

bacteria. *FASEB* 12: 265-274.

52. Eswaran, J., E. Koronakis, M. K. Higgins, C. Hughes, and V. Koronakis. 2004. Three's company: component structures bring a closer view of tripartite drug efflux pumps. *Curr. Opin. Struct. Biol.* 14: 741-747.
53. Koronakis, V., A. Sharff, E. Koronakis, B. Luisi, and C. Hughes. 2000. Crystal structure of the bacterial membrane protein TolC central to multidrug efflux and protein export. *Nature* 405: 914-919.
54. Mikolosko, J., K. Bobyk, H. I. Zgurskaya, and P. Ghosh. 2006. Conformational flexibility in the multidrug efflux system protein AcrA. *Structure* 14: 577-587.
55. Higgins, M. K., E. Bokma, E. Koronakis, C. Hughes, and V. Koronakis. 2004. Structure of the periplasmic component of a bacterial drug efflux pump. *Proc. Natl. Acad. Sci. USA* 101:9994-9999.
56. Symmons, M. F., E. Bokma, E. Koronakis, C. Hughes, and V. Koronakis. 2009. The assembled structure of a complete tripartite bacterial multidrug efflux pump. *Proc. Natl. Acad. Sci. USA* 106: 7173-7178.
57. Nies, D. H. 1999. Microbial heavy metal resistance. *Appl. Microbiol. Biotechnol.* 51: 730-750.
58. Stout, J. E., and V. L. Yu. 2003. Experiences of the first 16 hospitals using copper-silver ionization for *Legionella* control: implications for the evaluation of other disinfection modalities. *Infect. Control Hosp. Epidermio.* 24: 563-568.
59. Chopra, I. 2007. The increase use of silver-based products as antimicrobial agents: a useful development or a cause for concern? *J. Antimicrob. Chemother.* 59: 587-590.
60. Silver, S. 2003. Bacterial silver resistance: molecular biology and uses and misuses of

silver compounds. *FEMS Microbiol Rev.* 27: 341-353.

61. Lok, C. N., C. M. Ho, R. Chen, P. K. Tam, J. F. Chiu, C. M. Che. 2008. Proteomic identification of the Cus system as a major determinant of constitutive *Escherichia coli* silver resistance of chromosal origin. *J Proteome Res.* 7: 2351-2356
62. Munson, G. P., D. L. Lam, F. W. Outten, and T. V. O'Halloran. 2000. Identification of a copper-responsive two-component system on the chromosome of *Escherichia coli* K-12. *J. Bacteriol.* 182: 5864-5871.
63. Loftin, I. R., S. Franke, S. A. Roberts, A. Weichsel, A. Hérouxé, W. R. Montfort, C. Rensing, and M. M. McEvoy. 2005. A novel copper-binding fold for the periplasmic copper resistance protein CusF. *Biochemistry* 44: 10533-10540.
64. Xue, Y., A. V. Davis, G. Balakrishnan, J. P. Stasser, B.M. Staehlin, P. Focia, T. G. Spiro, J. E. Penner-Hahn, T. V. O'Halloran. 2008. Cu(I) recognition via cation-pi and methionine interactions in CusF. *Nat. Chem. Biol.* 4: 107-9.
65. Kittleson, J. T., I.R. Loftin, A. C. Hausrath, K. P. Engelhardt, C. Rensing, M. M. McEvoy. 2006. Periplasmic metal-resistance protein CusF exhibits high affinity and specificity for both CuI and AgI. *Biochemistry* 45(37): 11096-102.
66. Su, CC, F Yang, F Long, D Reyon, MD Routh, DW Kuo, AK Mokhtari, JD Van Ornam, KL Rabe, JA Hoy, YJ Lee, KR rajashankar, EW Yu. 2009. Crystal structure of the membrane fusion protein CusB from *Escherichi coli*. *J Mol Biol.* 393(2):342-55.

# CHAPTER 2. Functional cloning and characterization of the multidrug efflux pumps NorM from *Neisseria gonorrhoeae* and YdhE from *Escherichia coli*

A paper published in *Antimicrobial Agents and Chemotherapy*, 2008, 52: 3052-3060

**Feng Long,[1] Corinne Rouquette-Loughlin,[2] William M. Shafer,[2,3] and Edward W. Yu[1,4*]**

[1]Molecular, Cellular and Developmental Biology Interdepartmental Graduate Program, Iowa State University, Ames, IA 50011.

[2]Department of Microbiology and Immunology, Emory University School of Medicine, Atlanta, Georgia 30322.

[3]Laboratories of Microbial Pathogenesis, VA Medical Center, Decatur, Georgia 30033.

[4]Department of Physics and Astronomy, Iowa State University, Ames, IA 50011.

Running title: MATE efflux pumps

* corresponding author

## Abstract

Active efflux of antimicrobial agents is one of the most important adapted strategies that bacteria use to defend against antimicrobial factors that are present in their environment. The NorM protein of *Neisseria gonorrhoeae* and YdhE of *Escherichia coli* have been proposed to be multidrug efflux pumps that belong to the multidrug and toxic compound extrusion (MATE) family. In order to determine their antimicrobial export capability, we cloned, expressed, and purified these two efflux proteins, and characterized their functions both *in vivo* and *in vitro*. *E. coli* expressing *norM* or *ydhE* showed elevated (two-fold or greater) resistance to several antimicrobial agents, including fluoroquinolones, ethidium bromide, rhodamine 6G, acriflavin, crystal violet, barberine, doxorubicin, novobiocin, enoxacin, and tetraphenylphosphonium chloride. When expressed in *E. coli*, both transporters reduced ethidum bromide and norfloxacin accumulation through a mechanism requiring the proton motive force and direct measurements of efflux confirmed that NorM behaves as a $Na^+$-dependent transporter. The capacity of NorM and YdhE to recognize structurally divergent compounds was confirmed using steady-state fluorescence polarization assays, and the results revealed that these transporters bind antimicrobials with dissociation constants ($K_D$) in the micromolar region.

## Introduction

*Neisseria gonorrhoeae* is a gram-negative diplococcus, which is only found in humans and causes the sexually transmitted disease gonorrhea. Since it is a strictly human pathogen and can colonize male and female genital mucosal surfaces and other sites, it has developed mechanisms to overcome host antimicrobial systems that are important in innate host defense. One important mechanism that *N. gonorrhoeae* uses to subvert antimicrobial agents is the expression of multidrug efflux pumps that recognize and actively export a wide variety of toxic (often structurally unrelated) compounds, including antibacterial peptides, long-chain fatty acids, and several clinically useful antibiotics, from the bacterial cell (17, 34, 36, 37).

Recently, four efflux pumps have been identified in *N. gonorrhoeae*. One such pump is the MtrD inner membrane protein (21) that exists as a component of the tripartite resistance nodulation cell division (RND) transporter (42). MtrD interacts with a periplasmic membrane fusion protein, MtrC, and an outer membrane channel, MtrE, to mediate the export of hydrophobic antimicrobial agents, including antibiotics, nonionic detergents, certain antibacterial peptides, bile salts, and gonadal steroidal hormones (7, 9, 10, 37). The FarB efflux pump (17), belonging to the major facilitator (MF) family (8, 22), recognizes antibacterial long-chain fatty acids and exports them out of the cell in conjunction with a membrane fusion protein FarA and the MtrE outer membrane protein channel (17). The MacB transporter was recently described (33) and it belongs to the ATP binding cassette (ABC) transporter family (13). It is poorly expressed in wild type gonococci due to a natural mutation in its promoter, but can recognize and export certain macrolide antibiotics. Finally,

*N. gonorrhoeae* contains the NorM efflux pump (34), which is a member of the multidrug and toxic compound extrusion (MATE) family of efflux transporters (5, 25, 34). The *N. gonorrhoeae* NorM transporter is homologous to the NorM efflux pump of *Vibrio parahaemolyticus* (25), the YdhE protein of *Escherichia coli* (2, 25, 43), VmrA of *V. parahaemolyticus* (6), and *Vibrio cholerae* VcrM (1, 27). As a multidrug efflux pump, the gonococcal NorM appears to recognize a number of cationic toxic compounds, such as ethidium bromide, acriflavin, 2-N-methylellipticinium, and ciprofloxacin (34). The capacity of NorM to export ciprofloxacin was suggested to be of clinical relevance in the development of fluoroquinolone resistance in *N. gonorrhoeae* especially when isolates have other mutations that raise the minimal inhibitory concentration (MIC) to a level near that seen in treatment failures.

The MATE family transporters characteristically possess 12 putative transmembrane domains, and have been reported in all three kingdoms of life (Eukarya, Archaea, and Eubacteria) (5). Phylogenetic tree analysis suggests that this family possesses three distinct clusters: (i) the bacterial multidrug efflux pumps, including *N. gonorrhoeae* NorM and *E. coli* YdhE; (ii) the eukaryotic efflux proteins found in fungi and plants, such as Erc1; and (iii) a branch containing *E. coli* DinF (5). Among these three clusters, the putative NorM branch exhibits overall minimal identity and similarity of 26 and 47%.

In order to directly test the capacity of the *N. gonorrhoeae* NorM pump to recognize putative substrates, including ciprofloxacin that was, until recently, widely used in the U.S. to treat gonococcal infections (15), we expressed the gonococcal *norM* gene in *E. coli* and investigated its function using drug susceptibility and transport assays. We also studied the homologous protein YdhE in *E. coli*, and compared its function with that of *N. gonorrhoeae*

NorM. Using a sensitive fluorescence polarization assay (12, 18), we characterized the interactions of these two transporters with various drugs. The results revealed that NorM and YdhE bind a variety of structurally dissimilar agents in the micromolar range.

## Materials and Methods

### Cloning of *norM* and *ydhE*

The *norM* ORF from genomic DNA of *N. gonorrhoeae* strain FA19 was amplified by PCR using the primers 5′-GAGGAATAATAAATGCTGCTCGACCTCGACCGC-3′ and 5′-GTTTAAACTCAATGGTGATGGTGATGATGGACGGCCTTGTGTGATTTGACC-3′ to generate a product that would encode a NorM recombinant protein with a 6xHis tag at the C-terminus (34). The corresponding PCR product was extracted from the agarose gel and cloned into pBAD-TOPO as described by the manufacturer (Invitrogen). To remove the V5 epitope and polyhistidine region of the vector, the plasmid was digested with PmeI and then self-ligated to form the expression vector, pBADΩ*norM*. The recombinant plasmid was transformed into DH5α cells and transformants were selected on LB agar plates containing 100 μg/ml ampicillin. The presence of the correct *norM* sequence in the plasmid construct was verified by DNA sequencing.

Similarly, the ORF of *ydhE* from *E. coli K12* genomic DNA was amplified by PCR and TA-cloned into pBAD-TOPO using the primers 5′-GAGGAATAATAAATGCAGAAGTATATCAGTG-3′ and 5′-GTTTAAACTCAATGGTGATGGTGATGATG GCGGGATGCTCGTTGCAGAATG-3′ to

generate a PCR product that would encode a recombinant protein containing a 6xHis tag at the C-terminus. The recombinant plasmid (pBADΩ*ydhE*) was transformed into DH5α cells as described above, and the presence of the correct insert in a representative plasmid transformant was verified by DNA sequencing.

**Drug susceptibility assays**

The MICs to various antimicrobial agents of *E. coli* strains (inoculum, 500 cells/ml) harboring pBADΩ*norM*, pBADΩ*ydhE*, or the pBAD vector were determined by the twofold dilution method using LB agar containing the desired antimicrobial agent (28). Bacterial growth was recorded after18 to 24 h of incubation at 37℃. Each assay was repeated at least four times to ensure the reproducibility of the results.

**Drug accumulation assays**

Assays of norfloxacin and ethidium bromide accumulations were performed as described previously (20, 24, 25). In brief, *E. coli* AG100AX carrying pBADΩ*norM*, pBADΩ*ydhE*, or pBAD were grown in LB broth with 0.01% L-arabinose at 37$^{o}$C to $OD_{600}$ of 1.0, harvested, washed with buffer containing 0.1 M Tris-HCl (pH 7.0) three times, and suspended in the same buffer to $OD_{600}$ of 1.0. Norfloxacin was then added to a final concentration of 100 μM. 1 ml samples were taken at intervals, centrifuged at 10,000 rpm for 30 s at 4$^{o}$C, and washed once with the same buffer. After 15 min, carbonyl cyanide *m*-

chlorophenylhydrazone (CCCP) was added to a final concentration of 100 μM to disrupt the proton gradient across the membrane. Then, 15 min later, CCCP was removed by centrifugation at 10,000 rpm for 30 s, and cells were resuspended with buffer containing 0.1 M Tris-HCl (pH 7.0) and 0.4% glucose. Each pellet was resuspended in 1 ml of 100 mM glycine-HCl (pH 3.0), shaken vigorously for 1 h at room temperature to release the fluorescent content, and then centrifuged at 15,000 rpm for 10 min at room temperature. The fluorescence of supernatants was measured at $\lambda_{ex}$ and $\lambda_{em}$ of 277 and 448 nm, respectively, using a PerkinElmer LS55 spectrofluorometer equipped with a Hamamatsu R928 photomultiplier. The amount of maximum fluorescence was normalized to 100%.

For ethidium bromide accumulation, cells were prepared similarly as above. A final concentration of 20 μg/ml of ethidium bromide was added to the cell suspension to initiate the assay. 1 ml samples were taken at different time points. After 15 min of incubation, CCCP was added to a final concentration of 100 μM. Then, 15 min later, CCCP was removed by centrifugation at 10,000 rpm for 30 s, and cells were resuspended with buffer containing 0.1 M Tris-HCl (pH 7.0) and 0.4% glucose. The fluorescence of samples was measured at $\lambda_{ex}$ and $\lambda_{em}$ of 500 and 580 nm, respectively (3). The amount of maximum fluorescence was normalized to 100%.

**Accumulation of ethidium bromide in the presence of $Na^+$**

*E. coli* AG100AX containing pBADΩ*norM* or pBAD were grown in LB broth with 0.01% L-arabinose at 37°C to $OD_{600}$ of 1.0, harvested by centrifugation, washed three times

with buffer containing 0.1 M Tris-HCl (pH 7.0), and suspended in the same buffer to $OD_{600}$ of 1.0. Ethidium bromide was added to a final concentration of 20 μg/ml to the cell suspension, followed by the addition of 100 mM NaCl or KCl. At each time point, a 1 ml sample was removed, centrifuged at 10,000 rpm for 30 s at 4°C, and washed once with the same buffer. The fluorescence signal was measured at $\lambda_{ex}$ and $\lambda_{em}$ of 500 and 580 nm, respectively.

**Efflux of norfloxacin in the presence of $Na^+$**

For determining norfloxacin efflux, cells were grown in LB broth with 0.01% L-arabinose at 37°C to $OD_{600}$ of 1.0, harvested, and washed twice with buffer containing 0.1 M Tris-HCl (pH 7.0). To load cells with norfloxacin, bacteria were incubated in the same buffer supplemented with 100 μM norfloxacin and 20 μM CCCP at 37°C for 30 min as described previously (31). Cells were then pelleted, washed twice, and resuspended with the same buffer to $OD_{600}$ of 2.0. 1 ml samples were taken at intervals, centrifuged at 10,000 rpm for 30 s at 4°C, and washed once with the same buffer. After 10 min, NaCl or KCl was added to a final concentration of 100 μM. Fluorescence measurement of norfloxacin was performed by a similar procedure as described above.

**Purification of the transporters**

The *N. gonorrhoeae* NorM protein containing a 6xHis tag at the C-terminus was overproduced in *E. coli* TOP10 cells (Invitrogen) possessing pBADΩ*norM*. Cells were grown in 12 L of LB medium with 100 μg/ml ampicillin at 37°C. When the $OD_{600}$ reached 0.5, the culture was treated with 0.2% L-arabinose to induce *norM* expression and harvested within 3 h. The collected bacteria were resuspended as described (44) in low salt buffer containing 100 mM sodium phosphate (pH 7.2), 10 % glycerol, 1 mM EDTA and 1 mM phenylmethanesulfonyl fluoride (PMSF), and then disrupted with a French pressure cell. The membrane fraction was collected and washed twice with high salt buffer containing 20 mM sodium phosphate (pH 7.2), 2 M KCl, 10 % glycerol, 1 mM EDTA and 1 mM phenylmethanesulfonyl fluoride (PMSF), and once with 20 mM HEPES-NaOH buffer (pH 7.5) containing 1 mM PMSF. The membrane protein was then solubilized in 1 % (w/v) *n*-dodecyl-β-D-maltoside (DDM). Insoluble material was removed by ultracentrifugation at 370,000 x g. The extracted protein was loaded into a $Ni^{2+}$-affinity column, washed with buffer containing 20 mM HEPES-NaOH (pH 7.5), 50 mM imidazole and 0.02% DDM, and eluted with buffer consisting of 20 mM HEPES-NaOH (pH 7.5), 400 mM imidazole and 0.02% DDM. The eluted protein was then concentrated to 5 mg/ml and loaded into a G-200 sizing columns pre-incubated with 20 mM HEPES-NaOH (pH 7.5) and 0.02% DDM for further purification. The YdhE protein that contains a 6xHis tag at the C-terminus was overproduced in *E. coli* TOP10 pBADΩ*ydhE* and purified as described above for NorM. The purity (>90%) of the NorM and YdhE proteins were judged using 10% SDS-PAGE stained with Coomassie Brilliant Blue.

**Fluorescence polarization assays**

Fluorescence polarization assays (12, 18) were used to determine the drug binding affinities of NorM and YdhE, respectively. The experiments were done using a ligand binding solution containing 20 mM HEPES-NaOH (pH 7.5), 0.02% DDM, and 1 μM ligand (rhodamine 6G, ethidium, proflavin, ciprofloxacin, or norfloxacin). The protein solution consisting of NorM or YdhE in 20 mM HEPES-NaOH (pH 7.5), 0.02% DDM, and 1 μM ligand was titrated into the ligand binding solution until the polarization (P) was unchanged. As this is a steady-state approach, fluorescence polarization measurement was taken after a 5 min incubation for each corresponding concentration of the protein and drug to ensure that the binding has reached equilibrium. It should be noted that the detergent concentration was kept constant at all times to eliminate the change in polarization generated by drug-DDM micelle interaction. All measurements were performed at 25$^{o}$C using a PerkinElmer LS55 spectrofluorometer equipped with a Hamamatsu R928 photomultiplier. The excitation wavelengths were 527, 483, 447, 330, and 277 nm, respectively, for rhodamine 6G, ethidium, proflavin, ciprofloxacin, and norfloxacin. Fluorescence polarization signals (in ΔP) were measured at emission wavelengths of 550, 620, 508, 415, and 448 nm, respectively, for these ligands. Each titration point recorded was an average of 15 measurements. Data were analyzed using the equation, $P = \{(P_{bound} - P_{free})[protein]/(K_D + [protein])\} + P_{free}$, where P is the polarization measured at a given total protein concentration, $P_{free}$ is the initial polarization of free ligand, $P_{bound}$ is the maximum polarization of specifically bound ligand, and [protein] is the protein concentration. The titration experiments were repeated for three times to obtain the average $K_D$ value. Curve fitting was accomplished using the program ORIGIN (30).

## Results and Discussion

### Drug specificity of NorM and YdhE *in vivo*

To determine if the *N. gonorrhoeae* NorM multidrug transporter is functionally expressed in *E. coli*, and to compare its activity to a second member (YdhE) of the MATE family of efflux pumps, we transformed the *E. coli* AG100AX, an AcrAB-deficient strain (29) with the empty pBAD vector, pBADΩ*norM*, or pBADΩ*ydhE*. We then tested the susceptibility of the representative transformants bearing these plasmids to a panel of 24 structurally divergent antimicrobials (Table 1). These antimicrobials were selected based on whether or not they are putative substrates of MATE family exporters in the NorM subclass. It is important to stress that in many instances expression of drug efflux pumps, including members of the MATE superfamily (5), can have only modest changes (two-fold) in bacterial susceptibility to certain antimicrobials while more significant changes in susceptibility to other agents can be observed in the same system. Indeed, in our drug testing experiments we detected a range of changes in the susceptibility of *E. coli* cells producing either NorM or YdhE.

Of the 24 antimicrobials tested, the AG100AX cells expressing the *N. gonorrhoeae* NorM were less sensitive (two- to eight-fold) than AG100AX cells containing pBAD to a subset of antibiotics (norfloxacin, doxurubicin, novobiocin, lomefloxacin, enoxacin and ciprofloxacin), dyes (rhodamine 6G, ethidium bromide, acriflavine and crystal violet) and quartenary ammonium compounds (berberine, benzalkonium and tetraphenylphosphonium chloride). The YdhE-producing cells displayed a similar drug susceptibility profile (with the

exception of lomefloxacin) as that of the NorM-producing *E. coli* cells, suggesting that these two MATE transporters are functionally similar *in vivo*.

Like YdhE of *E. coli*, our drug susceptibility experiments showed that NorM functions as a multidrug efflux pump when expressed in *E.coli*. The MICs to 14 of the 24 antimicrobials (Table 1) were observed to increase by two- to eight-fold in NorM-producing AG100AX bacteria, which lacks the AcrB efflux pump. Similar differences (data not presented) in antimicrobial susceptibility were obtained in $AcrB^+$ *E. coli* TOP10 cells that were used to obtain recombinant NorM. In that the MICs of norfloxacin, ciprofloxacin, enoxacin, lomefloxacin were raised in cells expressing NorM or YdhE, our results suggest that like other MATE transporters, such as BexA of *B. thetaiotaomicron* (23), VcmA of *Vibrio cholerae* (16), NorM of *Vibrio cholerae* (38) and AbeM of *Acinetobacter baumannii* (41), fluoroquinolones might be a common substrate for MATE transporters in the NorM cluster.

**NorM and YdhE reduce drug accumulation in bacteria**

The observed (Table 1) capacity of NorM and YdhE to reduce the susceptibility of *E. coli* to norfloxacin, ciprofloxacin and ethidium bromide is consistent with the drug recognition profile of other members of the MATE efflux transporter family. To confirm the drug susceptibility testing results, we measured the accumulation of norfloxacin and ethidum bromide in AG100AX cells that carried pBADΩ*norM*, pBADΩ*ydhE*, or pBAD. The results showed lower levels of norfloxacin (Figure 1a) or ethidum bromide (Figure 1b) accumulation

in AG100AX cells producing NorM or YdhE compared to control cells harboring the empty pBAD vector.

Members of the MATE family use energy from the proton motive force (PMF) during export and loss of the PMF inactivates pump activity resulting in enhanced accumulation of substrates, which translates to increased susceptibility to the agents normally recognized by the transporter. Accordingly, we also measured norfloxacin and ethidium bromide accumulation after addition of CCCP, a de-coupler of the membrane proton gradient. After the addition of CCCP into the assay solution, the accumulation of norfloxacin (Figure 1a) and ethidum bromide (Figure 1b) increased drastically in the NorM- and YdhE- expressing cells, with the levels of accumulation being nearly the same in the three different strains within 5 min. It should be noted that the effect of CCCP is reversible simply by removing CCCP and adding glucose to re-energize AG100AX cells. The experiments were performed at least three times. Statistical comparisons were assessed by Student's *t* test, and *P* values of $< 0.05$ were considered statistically significant differences (Figure 1a and b).

**NorM expressed in *E. coli* behaves as a $Na^+$ ion-dependent transporter**

It has been suggested but not proven that NorM of *N. gonorrhoeae* is a $Na^+$-drug antiporter (34). Thus, we investigated the accumulation of ethidium bromide in isogenic strains AG100AX/pBADΩ*norM* and AG100AX/pBAD in the presence of $Na^+$ or $K^+$. In AG100AX/pBADΩ*norM* cells, a lower level of ethidum bromide accumulation was observed in the presence of 100 mM NaCl when compared to that in the presence of 100 mM

KCl (Figure 2a). In contrast, we did not observe a difference in ethidum bromide accumulation in AG100AX/pBAD regardless of the presence of NaCl or KCl (Figure 2b). Furthermore, in the presence of NaCl the accumulation level of ethidium bromide in the NorM-producing strain was lower than that in AG100AX/pBAD.

We next measured the efflux of norfloxacin that had accumulated in strains AG100AX/pBADΩ*norM* or AG100AX/pBAD, respectively, in the presence of $Na^+$ or $K^+$. Cells were first loaded with norfloxacin, thereafter, 100 mM of either NaCl or KCl was added to test the effect on drug efflux. As shown in Figure 3a, the addition of 100 mM NaCl to AG100AX/pBADΩ*norM* cells resulted in greater efflux of the drug from cells compared to that observed in the presence of KCl or without added salt. This effect was NorM-dependent because the addition of either NaCl (100 mM) or KCl (100 mM) to AG100AX/pBAD cells did not impact norfloxacin efflux (Figure 3b). Taken together with the ethidum bromide accumulation results, our observations support the earlier proposal (34) that the gonococcal NorM protein is a $Na^+$-dependent transporter.

In order to directly test whether efflux of an antimicrobial by NorM is $Na^+$-dependent, we then studied the extrusion of norfloxacin that has been accumulated in AG100AX/pBADΩ*norM* in the presence of CCCP. Cells were first loaded with norfloxacin. Thereafter, different concentrations of NaCl (50-200 mM) were added to test the effect on drug efflux. All these tests were done in the presence of 20 μM CCCP. If NorM requires proton ion as a coupler, then the accumulated level of norfloxacin in cell should not be reduced under these conditions. However, if the coupling ion is $Na^+$, we should be able to observe norfloxacin efflux in a [$Na^+$]-dependent manner. Figure 4 depicts the effect of $Na^+$

on the extrusion of norfloxacin. The experiment suggests that efflux activity was stimulated by $Na^+$ ion. The addition of NaCl resulted in a significant change in norfloxacin efflux. Previous study in *Pseudomonas aeruginosa* PmpM, an $H^+$-dependent transporter in the MATE family, indicated that $Na^+$ ion has no effect on drug transport (11). Thus, it is highly likely that $Na^+$ is the coupling cation for NorM.

Our drug accumulation and efflux assays confirm the earlier report which suggested that NorM of *N. gonorrhoeae* is a $Na^+$/drug antiporter (34). First, $Na^+$ was found to enhance the ability of *E. coli* producing NorM to maintain a lower accumulation level of ethidium bromide as compared to those cells not producing NorM, even in the presence of $Na^+$ (Figure 2). Hence, drug export mediated by NorM of *N. gonorrhoeae* is driven by $Na^+$ gradient. This export mechanism is also influenced by the integrity of the PMF of the cytoplasmic membrane since CCCP, a proton conductor, could significantly enhance the accumulation level of ethidium bromide in NorM-producing bacteria. These accumulation assays provide, however, indirect evidence for efflux. Accordingly, direct support for efflux was obtained in experiments that measured norfloxacin export by NorM-producing *E. coli*. The observed $Na^+$-dependent capacity of NorM to mediate export of norfloxacin (Figures 3 and 4) provides direct evidence for this model.

**Binding affinities of different drugs *in vitro***

The *in vivo* antimicrobial susceptibility testing (Table 1) and accumulation/efflux studies (Figures 1-4) suggested that NorM and YdhE recognize and export structurally

diverse compounds. There is, however, little known about the detail of substrate binding by these MATE transporters. In order to directly test the capacity of these proteins to bind such diverse compounds, we used a fluorescence polarization assay to quantify the binding affinities of several compounds to NorM and YdhE *in vitro.* This technique has been found to be sensitive and precise enough, and allow us for the first time, to detect ligand binding of the *E. coli* AcrB multidrug efflux pump (an RND transporter) in a detergent environment (40). As an example of the results obtained by this protocol, Figure 5a illustrates the binding isotherm of NorM in the presence of rhodamine 6G. As presented in the figure, a simple hyperbolic curve was observed for the binding of rhodamine 6G with a dissociation constant, $K_D$, of 3.4 ± 0.2 μM. A Hill plot of the data yielded a Hill coefficient of 1.01 ± 0.03 (Figure 5b), suggesting a simple drug binding process with a stoichiometry of one NorM monomer per rhodamine 6G ligand. When the data were presented as a Scatchard plot (not shown), it indicated a similar $K_D$ of 3.6 ± 0.1 μM with no sign of heterogeneity in binding sites. In addition, the titration experiments indicated that YdhE binds rhodamine 6G with a $K_D$ of 3.0 ± 0.2 μM (Figure 6a). This value is comparable with that of NorM, suggesting that these two transporters share similar affinity for this ligand. The Hill (Figure 6b) and Scatchard (not shown) plots of the data indicated that the transporter employs a simple binding stoichiometry of 1:1 monomeric YdhE-to-rhodamine 6G molar ratio.

Fluorescence polarization assays were also employed to elucidate the interaction of a variety of drugs with the NorM and YdhE transporters. The titration experiments indicated that NorM binds ethidium bromide, proflavin, ciprofloxacin, and norfloxacin with dissociation constants of 12.3 ± 1.3 μM, 33.6 ± 1.9 μM, 121.3 ± 15.7 μM, and 105.6 ± 9.8

μM, respectively (Table 2). These values are in the same range with those of YdhE, which binds ethidium bromide, proflavin, ciprofloxacin and norfloxacin with $K_D$ values of 9.8 ± 0.9 μM, 22.1 ± 0.9 μM, 90.9 ± 12.4 μM, and 98.4 ± 16.2 μM, respectively (Table 2). This binding was not impacted by detergent since similar dissociation constants for the rhodamine 6G-YdhE complex were obtained in reaction mixtures that included 0.2%, 0.02% and 0.0075% DDM.

To verify the validity of the fluorescence polarization assay, we studied the binding affinity of rhodamine 6G with the purified, detergent-solubilized YdhE efflux pump using equilibrium dialysis. The dialysis data suggest a $K_D$ of 3.0 ± 0.1 μM, with a stoichiometry of 1:1 monomeric YdhE-to-ligand molar ratio, for the binding of YdhE with rhodamine 6G (see Suppl. Fig. S1). This result is in good agreement with that observed from fluorescence polarization in which the $K_D$ of YdhE-rhodamine 6G is 3.0 μM with a 1:1 binding stoichiometry. Apparently, NorM and YdhE bind these drugs with similar affinities. These values are similar to the $K_D$ values for tetraphenylphosphonium binding in MdfA, a MF transporter, and EmrE, a SMR transporter, determined by radiolabeled binding assays (19, 26), as well as the most recently determined dissociation constants for AcrB, an RND transporter, with four different ligands using fluorescence polarization assays (40).

The results from fluorescence polarization and equilibrium dialysis assays suggest that NorM and YdhE use a binding stoichiometry of 1:1 monomeric transporter-to-ligand ratio. Thus, it is very likely that these transporters employ a simple drug binding process with no cooperativity. There is, however, a possibility that drug molecules may bind to more than one site in the proteins, with similar affinities, that may not be able to be distinguished

using these techniques. Further experiments utilizing different approaches may need to confirm this drug binding stoichiometry.

**pH dependence of drug binding to NorM**

We performed fluorescence polarization experiments to determine the binding of rhodamine 6G to NorM at different pH values. Figure 7 illustrates the decrease in $K_D$ values for rhodamine 6G as the pH increases from 5.8 to 8.5. Within this pH range, the $K_D$ value decreases by about 2.6 μM. This change is quite modest when compared with the effect of proton on the PMF-dependent efflux pumps, *E. coli* AcrB (40) and EmrE (26). The binding affinities for drugs in these two transporters were strikingly dependent on pH. In the case of AcrB, within the range of pH from 5.5 to 8.4, fluorescence polarization assay suggests that the change in $K_D$ for AcrB-rhodamine 6G reached 10.3 μM. As NorM shows a very different pH-dependent profile compared with those of the PMF-dependent pumps AcrB and EmrE, it is very likely that NorM does not use $H^+$ as an energy-coupling ion. Since NorM tends to bind positively charged drugs, we expect that its drug-binding pocket should consist of at least one acidic residue. Indeed, the protein sequence of NorM suggests that this transporter consists of two negatively charged residues, Glu 261 and Asp 377, in the transmembrane region. These acidic residues potentially could form the multidrug binding site. Thus, the modest pH effect on NorM could be accounted for the protonation state of the acid residue(s) in the binding pocket.

**$Na^+$ dependence of drug binding to NorM**

As *in vivo* studies of drug accumulation and efflux suggest, NorM is a $Na^+$-dependent transporter, the presence of $Na^+$ ions may affect the drug binding affinity *in vitro*. We therefore investigated the $Na^+$ dependence of drug binding using fluorescence polarization. As shown in Figure 8, the $K_D$ for rhodamine 6G is $Na^+$ dependent when the concentration of $Na^+$ is in the sub-micromolar range. In this region, the dissociation constant for rhodamine 6G was a simple hyperbolic function of the $Na^+$ concentration. The curve showed saturability over 0.01 to 100 mM. Like the pH effect, the change in $K_D$ for rhodamine 6G due to the presence of $Na^+$ ion is quite small. Within 0 to 100 mM $Na^+$, the change in $K_D$ only reached 2.5 μM (Figure 8). We also added various concentrations of NaCl ranging from 100 to 400 mM (data not shown) and observed no significant change in the $K_D$.

**Competition binding of different drugs in YdhE**

To confirm that the drug molecules bind specifically in these transporters, we performed competition experiments in which tetraphenylphosphonium chloride (TPP) was titrated into a solution containing the preformed YdhE-rhodamine 6G complex. In this case, TPP was chosen as a second ligand to knock off the bound rhodamine 6G from YdhE. The absorption spectra of TPP (from 200 to 600 nm) showed that this molecule absorbs light at the wavelengths of 224.9, 268.0 and 275.9 nm. At $\lambda$ = 527 nm, which is the excitation wavelength for rhodamine 6G, the energy is too low to excite TPP. Thus, TPP was treated as a non-fluorescent ligand in the "knock off" experiments. The data revealed that TPP was

able to bind YdhE and replace the bound rhodamine 6G molecule from the protein as demonstrated by the release of rhodamine 6G observed from the reduction of polarization (Figure 9). This binding assay provides direct evidence that TPP interferes with the binding of rhodamine 6G, possibly by a direct competitive binding process for the same binding site. Alternatively, the release of rhodamine 6G by TPP may be due to an allosteric interaction between distinct binding sites of these two ligands. Regardless, the titrations demonstrate that rhodamine 6G is bound specifically in the YdhE transporter.

We have determined the binding affinities of five different drugs to the purified, detergent-solubilized NorM and YdhE proteins, respectively, using fluorescence polarization assays. We note that fluorescence polarization has been widely used for studying protein-DNA interaction (12, 14, 18), and protein-ligand interaction in transcriptional regulators (4, 35, 39). To our knowledge, this is the first attempt using this methodology to investigate interaction between MATE proteins and their transported substrates. This approach also allows us, for the first time, to quantify the strength of transporter-drug interaction among the MATE family of transporters.

**Acknowledgments.** We thank Dr. Hiroshi Nikaido for providing us the *E. coli* AG100AX strain. This work was supported by PHS grants AI-21150 (W.M.S.) and GM-074027 (E.W.Y.) from the NIH. W. Shafer is the recipient of a Senior Research Career Scientist Award from the VA Medical Research Service.

## References


1. Begum, A., M. Rahaman, W. Ogawa, T. Mizushima, T. Kuroda, and T. Tsuchiya. 2005. Gene cloning and characterization of four MATE family multidrug efflux pumps from *Vibrio cholerae* non-O1. *Microbiol. Immunol*. **49**:949-957.
2. Blattner, F. R., G. Plunkette, 3rd, C. A. Block, N. T. Perna, V. Burland, M. Riley, J. Collado-Vides, J. D. Glasner, C. K. Rode, G. F. Mayhew, J. Gregor, N. W. Davis, H. A. Kirkpatrick, M. A. Goeden, D. J. Rose, B. Mau, and Y. Shao. 1997. The complete genome sequence of *Escherichia coli* K-12. *Science* **277**:1453-1474.
3. Bolhuis, H., D. Molenaar, G. Polarends, H. W. van Veen, B. Poolman, A. J. M. Driessen, and W. N. Konings. 1994. Proton motive force-driven and ATP-dependent drug extrusion systems in multidrug-resistant *Lactococcus lactis*. *J. Bacteriol.* **176**:6957-6964.
4. Brooks, B. E., K. M. Piro, and R. G. Brennan. 2007. Multidrug-binding transcription factor QacR binds the bivalent aromatic diamidines DB75 and DB359 in multiple positions. *J. Am. Chem. Soc.* **129**:8389-8395.
5. Brown, M. H., I. T. Paulsen, and R. A. Skurray. 1999. The multidrug efflux protein NorM is a prototype of a new family of transporters. *Mol. Microbiol.* **31**:394-395.
6. Chen, J., Y. Morita, M. N. Huda, T. Kuroda, T. Mizushima, and T. Tsuchiya. 2002. VmrA, a member of a novel class of $Na^+$-coupled multidrug efflux pumps from *Vibrio parahaemolyticus*. *J. Bacteriol.* **184**:572-576.
7. Delahay, R. M., B. D. Robertson, J. T. Balthazar, and C. A. Ison. 1997. Involvement of the gonococcal MtrE protein in the resistance of *Neisseria gonorrhoeae* to toxic hydrophobic agents. *Microbiology* **143**:2127-2133.

8. Griffith, J. K., M. E. Baker, D. A. Rouch, M. G. Page, R. A. Skurray, I. T. Paulsen, K. F. Chater, S. A. Baldwin, and P. J. Henderson. 1992. Membrane transport proteins: Implications of sequence comparisons. *Curr. Opin. Cell Biol.* **4**:684-695.
9. Hagman, K. E., W. Pan, B. G. Spratt, J. T. Balthazar, R. C. Judd, and W. M. Shafer. 1995. Resistance of *Neisseria gonorrhoeae* to anitmicrobial hydrophobic agents is modulated by the *mtrRCDE* efflux system. *Microbiology* **141**:611-622.
10. Hagman, K. E., C. E. Lucas, J. T. Balthazar, L. A. Snyder, M. Nilles, R. C. Judd, and W. M. Shafer. 1997. The MtrD protein of *Neisseria gonorrhoeae* is a member of resistance/nodulation/division protein family constituting part of an efflux system. *Microbiology* **143**:2117-2125.
11. He, G.-X., T. Kuroda, T. Mima, Y. Morita, T. Mizushima, and T. Tsuchiya. 2004. An $H^+$-coupled multidrug efflux pump, PmpM, a member of the MATE family of transporters, from *Pseudomonas aeruginosa*. *J. Bacteriol.* **186**:262-265.
12. Heyduk, T., and J. C. Lee. 1990. Application of fluorescence energy transfer and polarization to monitor *Escherichia coli* camp receptor protein *lac* promoter interaction. *Proc. Natl. Acad. Sci. USA* **87**:1744-1748.
13. Higgins, C. F. 1992. ABC transporters: from microorganisms to man. *Annu. Rev. Cell Biol.* **8**:67-113.
14. Hoffmann, K. M., D. Williams, W. M. Shafer, and R. G. Brennan. 2005. Characterization of the multiple transferable resistance repressor, MtrR, from *Neisseria gonorrhoeae. J. Bacteriol.* **187**:5008-5012.
15. Hooper, D. C. 2000. New uses for new and old quinolones and the challenge of resistance. *Clin. Infect. Dis.* **30**: 243-254.

16. Huda M. N., Y. Morita, T. Kuroda, T. Mizushima, and T. Tsuchiya. 2001. $Na^+$-driven multidrug efflux pump VcmA from *Vibrio cholerae* non-O1, a non-halophilic bacterium. *FEMS Microbiol. Letters* **203**:235-239.

17. Lee, E.-H., and W. M. Shafer. 1999. The *far*AB-encoded efflux pump mediates resistance of gonococci to long-chained antibacterial fatty acids. *Mol. Microbiol.* **33**:839-845.

18. LeTilly, V, and C. A. Royer. 1993. Fluorescence anisotropy assays implicate protein-protein interactions in regulating *trp* repressor DNA binding. *Biochemistry* **32**:7753-7758.

19. Lewinson, O., and E. Bibi. 2001. Evidence for simultaneous binding of dissimilar substrates by the *Escherichia coli* multidrug transporter MdfA. *Biochemistry* **40**:12612-12618.

20. Li, L., Z. He, G. K. Pandey, T. Tsuchiya, and S. Luan. 2002. Functional cloning and characterization of a plant efflux carrier for multidrug and heavy metal detoxification. *J. Biol. Chem.* **277**:5360-5368.

21. Maness, M. J., and P. F. Sparling. 1973. Multiple antibiotic resistance due to a single mutation in *Neisseria gonorrhoeae*. *J. Infect. Dis.* **128**:321-330.

22. Marger, M. D., and M. H. Saier, Jr. 1993. A major superfamily of transmembrane facilitators that catalyse uniporter, symporter and antiporter. *Trends Biochem. Sci.* **18**:13-20.

23. Miyamae, S., O. Ueda, F. Yoshimura, J. Hwang, Y. Tanaka, and H. Nikaido. 2001. A MATE family multidrug efflux transporter pumps out fluoroquinolones in *Bacteroides thetaiotaomicron*. *Antimicrob. Agents Chemother.* **45**:3341-3346.

24. Morita, Y, A. Kataoka, S. Shiota, T. Mizushima, and T. Tsuchiya. 2000. NorM of *Vibrio parahaemolyticus* is an $Na^+$-driven multidrug effux pump. *J. Bacteriol.* **182**:6694-6697.

25. Morita, Y., K. Kodama, S. Shiota, T. Mine, A. Kataoka, T. Mizushima, and T. Tsuchiya. 1998. NorM, a putative multidrug efflux protein, of *Vibrio parahaemolyticus* and its homolog in *Escherichia coli*. *Antimicrob. Agents Chemother.* **42**:1778-1782.

26. Muth, T. R., and S. Schuldiner. 2000. A membrane-embedded glutamate is required for ligand binding to the multidrug transporter EmrE. *EMBO J.* **19**:234-240.

27. Nazmul Huda, N., J. Chen, Y. Morita, T. Kuroda, T. Mizushima, and T. Tsuchiya. 2003. Gene cloning and characterization of VcrM, a $Na^+$-coupled multidrug efflux pump from *Vibrio cholerae* non-O1. *Microbiol. Immunol.* **47**:419-427.

28. Nishino, K., and A. Yamaguchi. 2001. Analysis of a complete library of putative drug transporter genes in *Escherichia coli. J. Bacteriol.* **183**:5803-5812.

29. Okusu, H., D. Ma, and H. Nikaido. 1996. AcrAB efflux pump plays a major role in the antibiotic resistance phenotype of *Escherichia coli* multiple-antibiotic-resistance (Mar) mutants. *J. Bacteriol.* **178**:306-308.

30. ORIGIN Ver. 7.5. OriginLab Corporation, Northampton, Massachusetts, USA.

31. Otsuka, M., M. Yasuda, Y. Morita, C. Ostuka, T. Tsuchiya, H. Omote, and Y. Moriyama. 2005. Identification of essential amino acid residues of the NorM $Na^+$/multidrug antiporter in *Vibrio parahaemolyticus*. *J. Bacteriol.* **187**:1552-1558.

32. Pao, S. S., I. T. Paulsen, and M. H. Saier, Jr. 1998. Major facilitator superfamily. *Microbiol. Mol. Biol. Rev.* **62**:1-34.

33. Rouquette-Loughlin, C. E., J. T. Balthazar, and W. M. Shafer. 2005. Characterization of the MacA-MacB efflux system in *Neisseria gonorrhoeae*. *J. Antimicrob. Chemother.* **56**:856-860.

34. Rouquette-Loughlin, C., S. A. Dunham, M. Kuhn, J. T. Balthazar, and W. M. Shafer. 2003. The NorM efflux pump of by *Neisseria gonorrhoeae* and *Neisseria meningitides* recognizes antimicrobial cationic compounds. *J. Bacteriol.* **185**:1101-1106.

35. Schumacher, M. A., M. C. Miller, and R. G. Brennan. 2004. Structural mechanism of the simultaneous binding of two drugs to a multidrug-binding protein. *EMBO J.* **23**:2923-2930.

36. Shafer, W. M., W. L. Veal, E.-H. Lee, L. Zarentonelli, J. T. Balthazar, and C. Rouquette. 2001. Genetic organization and regulation of antimicrobial efflux systems possessed by *Neisseria gonorrhoeae* and *Neisseria meningitides*. *J. Mol. Microbiol. Biotechnol.* **3**:219-225.

37. Shafer, W. M., X.-D. Qu, A. J. Waring, and R. I. Lehrer. 1998. Modulation of *Neisseria gonorrhoeae* susceptibility to vertebrate antibacterial peptides due to a member of the resistance/nodulation/division efflux pump family. *Proc. Natl. Acad. Sci. USA* **95**:1829-1833.

38. Singh, A. K., R. Halder, D. Mandal, and M. Kundu. 2006. Analysis of the topology of *Vibrio cholerae* NorM and identification of amino acid residues involved in norfloxacin resistance. *Antimicrob. Agents Chemother.* **50**:3717-3723.

39. Su, C.-C., D. J. Rutherford, and E. W. Yu. 2007. Characterization of the multidrug efflux regulator AcrR from *Escherichia coli*. *Biochem. Biophys. Res. Comm.* **361**:85-90.

40. Su, C.-C., H. Nikaido, and E. W. Yu. 2007. Ligand-transporter interaction in the AcrB multidrug efflux pump determined by fluorescence polarization assay. *FEBS Lett.* **581**:4972-4976.

41. Su, X.-Z., J. Chen, T. Mizushima, T. Kuroda, and T. Tsuchiya. 2005. AbeM, an $H^+$-coupled *acinetobacter baumannii* multidrug efflux pump belonging to the MATE family of transporters. *Antimicrob. Agents Chemother.* **49**:4362-4364.

42. Tseng, T. T., K. S. Gratwick, J. Kollman, D. Park, D. H. Nies, A. Goffeau, and M. H. Saier, Jr. 1999. The RND permease superfamily: an ancient, ubiquitous and diverse family that includes human disease and development proteins. *J. Mol. Microbiol. Biotechnol.* **1**:107-125.

43. Yang, S., S. R. Clayton, and E. L. Zechiedrich. 2003. Relative contributions of the AcrAB, MdfA and NorE efflux pumps to quinolone resistance in *Escherichia coli*. *J. Antimicrob. Chemother.* **51**:545-556.

44. Yu, E. W., G. McDermott. H. I. Zgurskaya, H. Nikaido, and D. E. Koshland, Jr. 2003. Structural basis of multiple drug-binding capacity of the AcrB multidrug efflux pump. *Science* **300**:976-980.

## Tables

Table 1. Drug susceptibility.

| Drug | MIC (μg/ml) | | |
|---|---|---|---|
| | AG100AX/ pBADΩ*norM* | AG100AX/ pBADΩ*ydhE* | AG100AX/pBAD |
| Ethidium bromide | 15.63 | 15.63 | 7.81 |
| Ciprofloxacin | 0.006 | 0.006 | 0.003 |
| Rhodamine 6 G | 12.5 | 12.5 | 3.125 |
| Chloramphenicol | 0.625 | 0.625 | 0.625 |
| Tetraphenyl-phosphonium chloride | 25 | 25 | 12.5 |
| Norfloxacin | 0.032 | 0.016 | 0.008 |
| Ofloxacin | 0.013 | 0.013 | 0.013 |
| Lomefloxacin | 0.032 | 0.016 | 0.016 |
| Tetracycline | 1.25 | 1.25 | 1.25 |
| Enoxacin | 0.063 | 0.063 | 0.031 |
| Doxorubicin | 6.25 | 6.25 | 1.56 |
| Benzalkonium | 0.625 | 0.312 | 0.156 |
| Novobiocin | 3.125 | 3.125 | 1.56 |
| Nalidixic acid | 0.625 | 0.625 | 0.625 |
| Crystal violet | 2.5 | 2.5 | 0.625 |
| Carbonyl cyanide *m*-chlorophenylhydrazone | 6.25 | 6.25 | 6.25 |
| Rifampin | 6.25 | 6.25 | 6.25 |
| Streptomycin | >50,000 | >50,000 | >50,000 |
| Methyl viologen | 156.3 | 156.3 | 156.3 |
| Vancomycin | 250 | 250 | 250 |
| Minocycline | 0.625 | 0.625 | 0.625 |
| Berberine | 250 | 250 | 31.25 |
| Acriflavine | 7.82 | 7.82 | 3.91 |
| Proflavin | 12.5 | 12.5 | 6.25 |
| Gentamicin | 2.5 | 2.5 | 2.5 |

Table 2. Dissociation constants and Hill coefficients of NorM and YdhE with five different transported drugs.

| Drug | NorM | | YdhE | |
|---|---|---|---|---|
| | $K_D$ (μM) | Hill coefficient | $K_D$ (μM) | Hill coefficient |
| Rhodamine 6G | 3.4 ± 0.2 | 1.01 ± 0.03 | 3.0 ± 0.2 | 1.00 ± 0.04 |
| Ethidium | 12.3 ± 1.3 | 0.96 ± 0.05 | 9.8 ± 0.9 | 0.97 ± 0.05 |
| Profloxacin | 33.6 ± 1.9 | 0.94 ± 0.03 | 22.1 ± 0.9 | 1.02 ± 0.01 |
| Ciprofloxacin | 121.3 ± 15.7 | 1.08 ± 0.06 | 90.9 ± 12.4 | 1.09 ± 0.06 |
| Norfloxacin | 126.3 ± 11.3 | 1.06 ± 0.03 | 98.4 ± 16.2 | 1.14 ± 0.05 |

## Figures and Captions

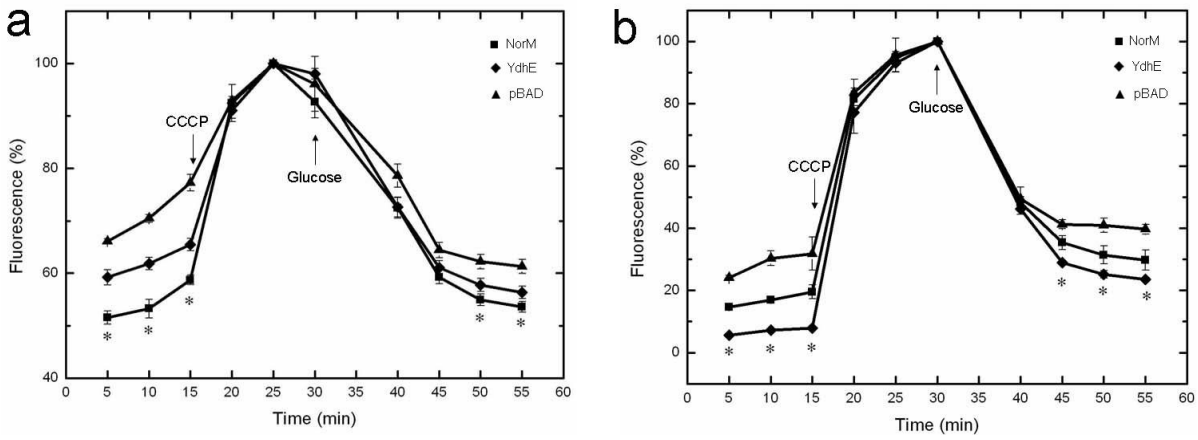


Figure 1. NorM and YdhE reduce accumulation of norfloxacin and ethidium bromide in *E. coli* cells. (a) Accumulation of norfloxacin in cells transformed by NorM (AG100AX/pBADΩ*norM*), YdhE (AG100AX/pBADΩ*ydhE*), or empty vector (AG100AX/pBAD). CCCP was added to the suspensions (first arrow) at a final concentration of 100 μM. After 15 min, glucose was added (second arrow) at a final concentration of 0.4%. (b) Accumulation of ethidium bromide in the same strains. CCCP was added to the suspensions (first arrow) at a final concentration of 100 μM. After 15 min, glucose was added (second arrow) at a final concentration of 0.4%. "*" indicates values of AG100AX/pBADΩ*norM* and AG100AX/pBADΩ*ydhE* cells that are significantly different from the control (AG100AX/pBAD) values ($P < 0.05$).

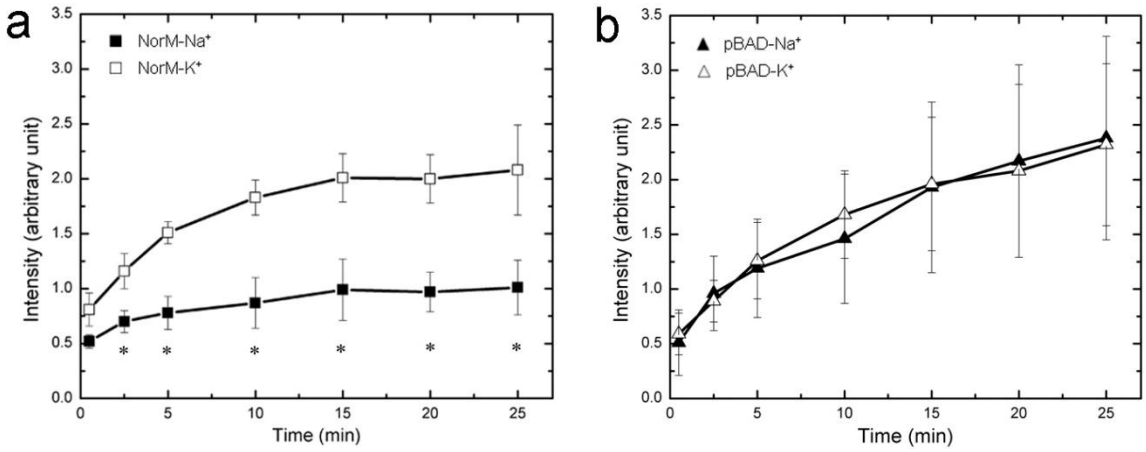


Figure 2. Sodium ion reduces accumulation of ethidium bromide in cells transformed by NorM. (a) Accumulation of ethidium bromide in AG100AX/pBADΩ*norM* after the addition of 100 mM NaCl or KCl. (b) Accumulation of ethidium bromide in AG100AX/pBAD (carrying the empty vector) after the addition of 100 mM NaCl or KCl. "*" indicates values of ethidium fluorescence intensity in the presence of 100 mM NaCl that are significantly different from those in the presence of 100 mM KCl ($P < 0.01$).

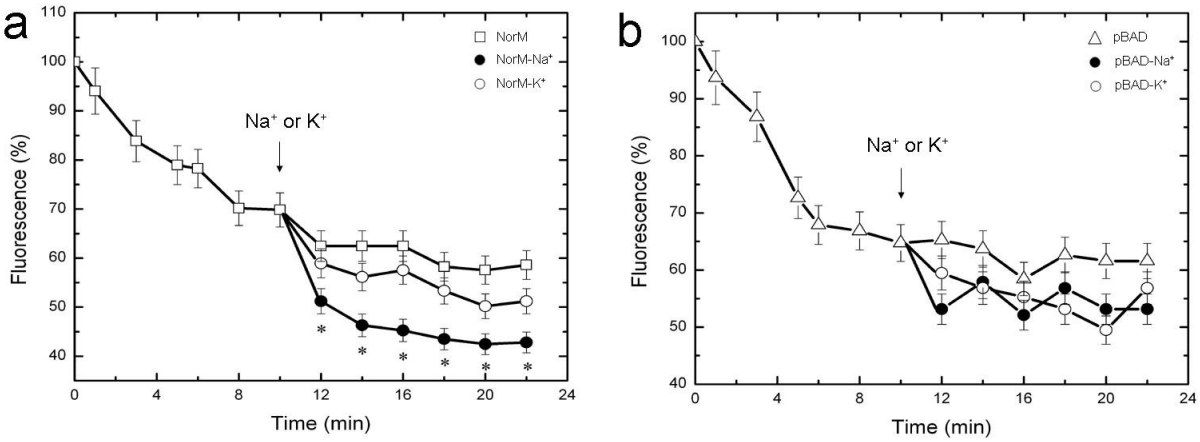


Figure 3. Sodium ion enhances norfloxacin efflux via NorM. (a) Norfloxacin efflux from AG100AX/pBADΩ*norM* cells carrying the *norM* gene from *N. gonorrhoeae*. (b) Norfloxacin efflux from AG100AX/pBAD cells carrying the empty vector. NaCl or KCl was added to the suspensions (arrow) at a final concentration of 100 mM. "*" indicates values of norfloxacin fluorescence in the presence of 100 mM NaCl that are significantly different from those in the presence of 100 mM KCl ($P < 0.05$).

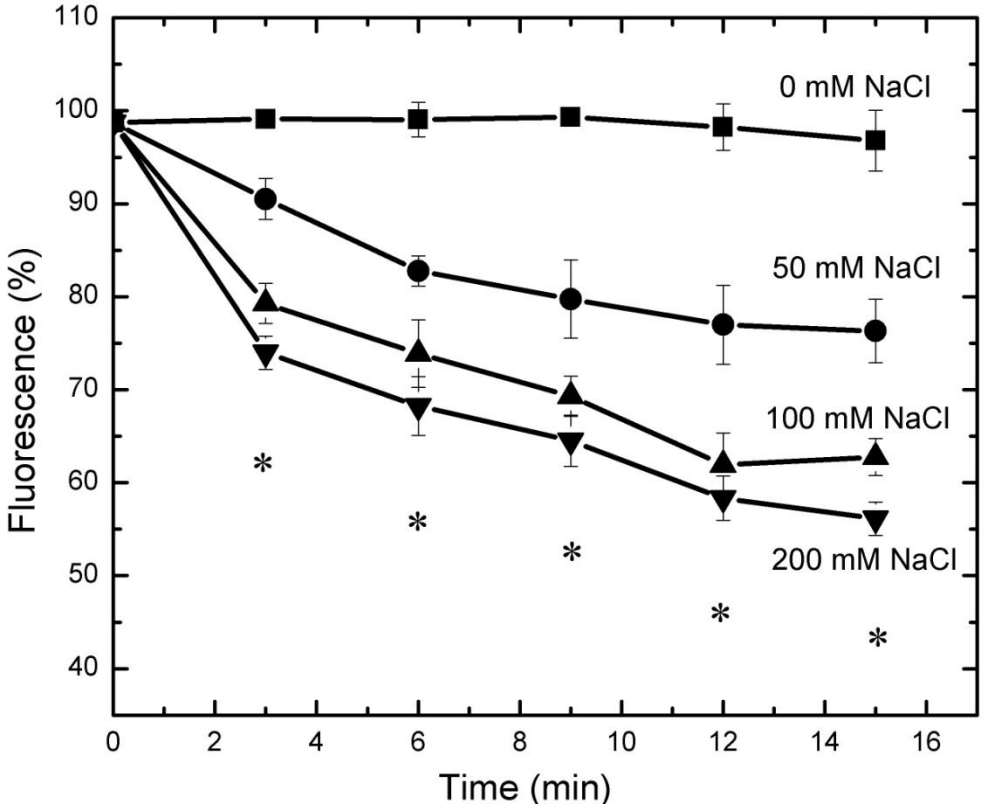


Figure 4. Effect of $Na^+$ concentration on norfloxacin extrusion via NorM. Norfloxacin efflux from AG100AX/pBADΩ*norM* cells carrying the *norM* gene in the presence of 0 to 200 mM NaCl. "*" indicates values of norfloxacin fluorescence in the presence of 50, 100 or 200 mM NaCl that are significantly different from those without NaCl ($P < 0.003$), as well as values of norfloxacin fluorescence in the presence of 100 or 200 mM NaCl that are significantly different from those in the presence of 50 mM NaCl ($P < 0.01$).

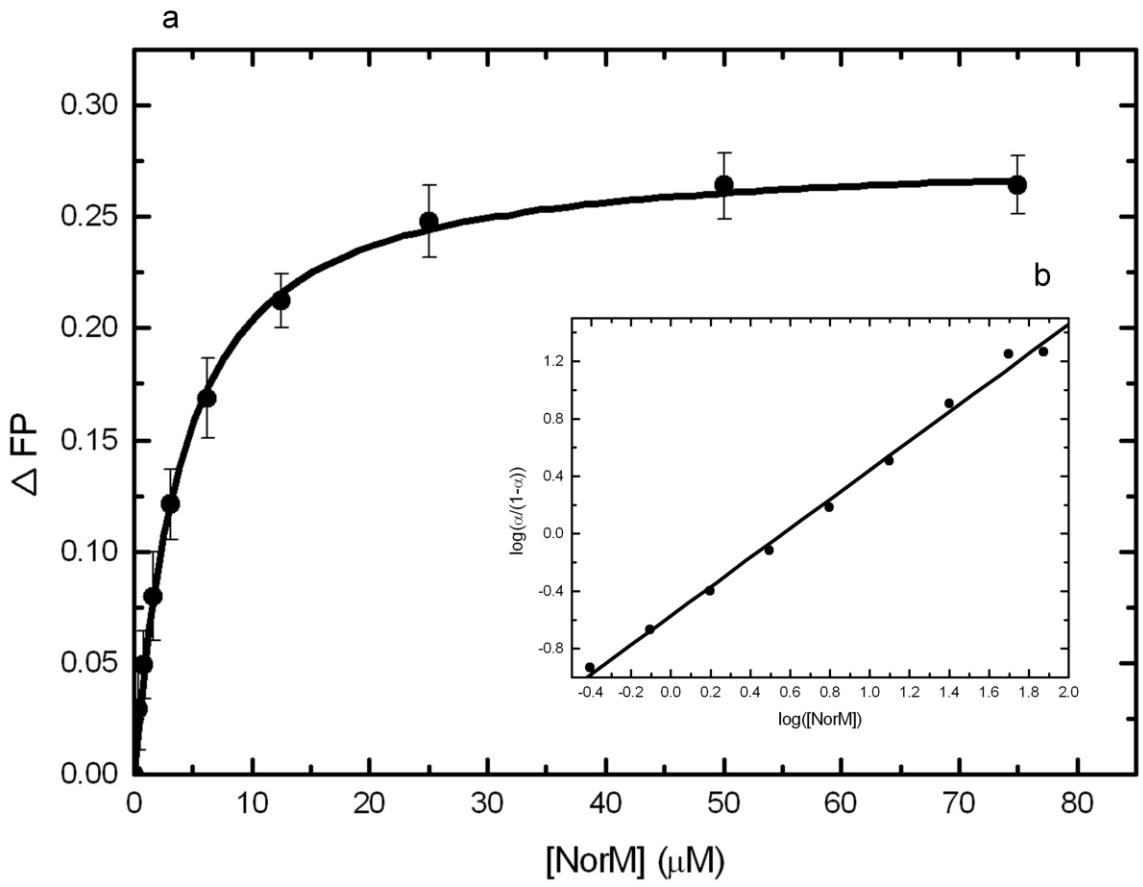


Figure 5. Representative fluorescence polarization of NorM in 0.02% DDM with rhodamine 6G. (a) Binding isotherm of NorM with rhodamine 6G, showing a $K_D$ of 3.4 ± 0.2 μM, in buffer containing 20 mM Tris (pH 7.5) and 0.02% DDM. (b) Hill plot of the data obtained for rhodamine 6G binding to NorM. α corresponds to the fraction of bound rhodamine 6G. The plot gives a slope of 1.01 ± 0.03, indicating a simple binding process with no cooperativity. The interception of the plot provides a $K_D$ of 3.6 ± 0.1 μM for the rhodamine 6G binding.

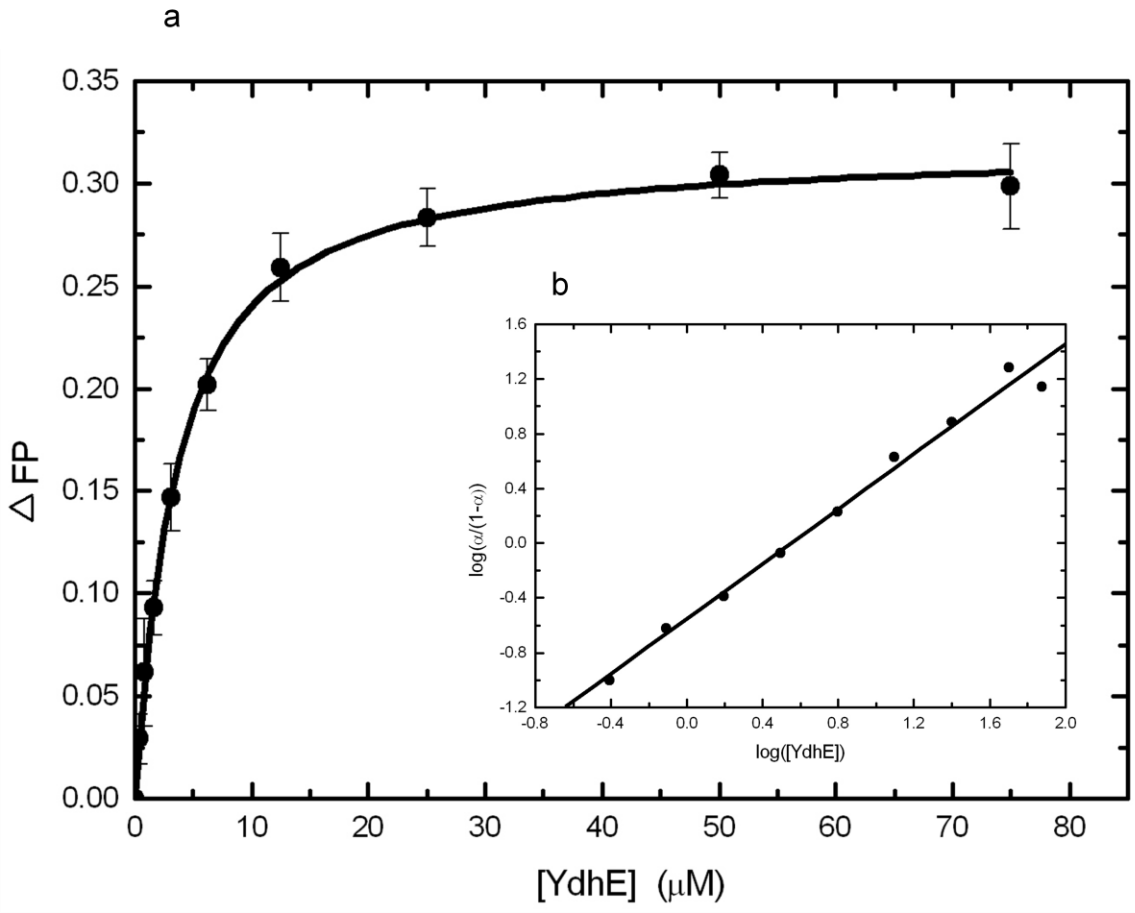


Figure 6. Representative fluorescence polarization of YdhE in 0.02% DDM with rhodamine 6G. (a) Binding isotherm of YdhE with rhodamine 6G, showing a $K_D$ of 3.0 ± 0.2 μM, in buffer containing 20 mM Tris (pH 7.5) and 0.02% DDM. (b) Hill plot of the data obtained for rhodamine 6G binding to YdhE. α corresponds to the fraction of bound rhodamine 6G. The plot gives a slope of 1.00 ± 0.04, indicating a simple binding process with no cooperativity. The interception of the plot provides a $K_D$ of 3.6 ± 0.2 μM for the rhodamine 6G binding.

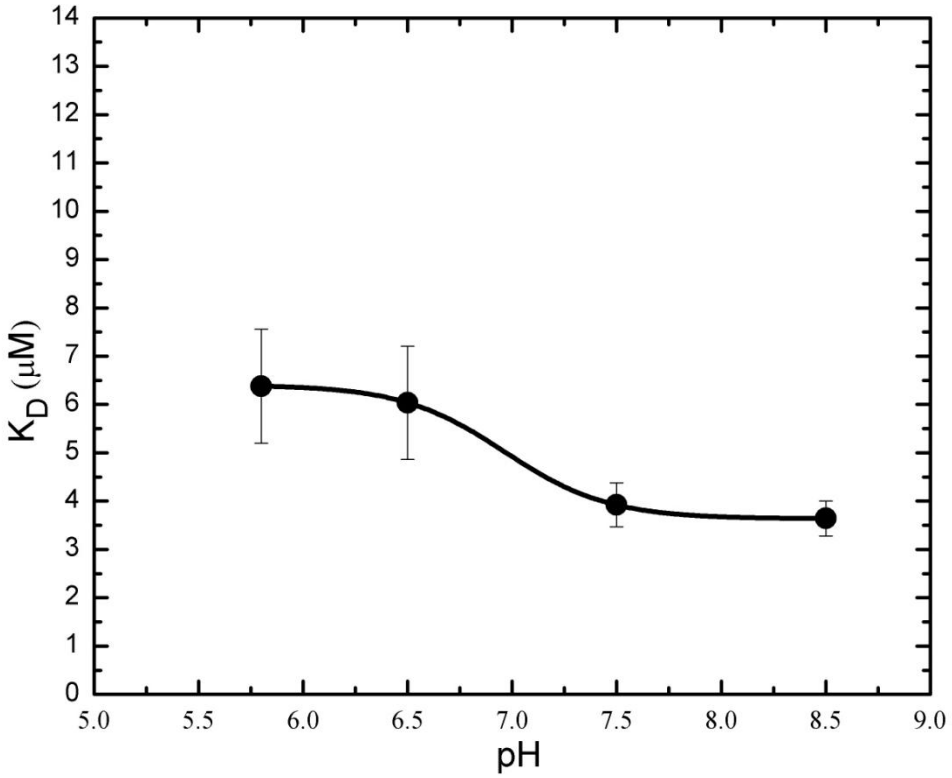


Figure 7. Effect of pH on the $K_D$ of rhodamine 6G binding to NorM. The resulting $K_D$s were plotted against pH.

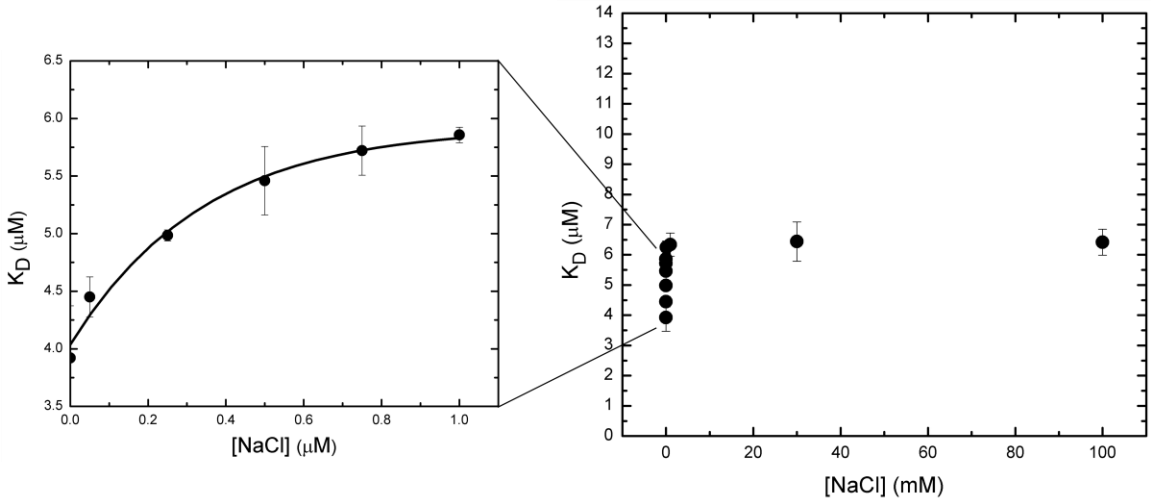


Figure 8. Effect of $Na^+$ concentration on the $K_D$ of rhodamine 6G binding to NorM. The resulting $K_D$s were plotted against NaCl concentration.

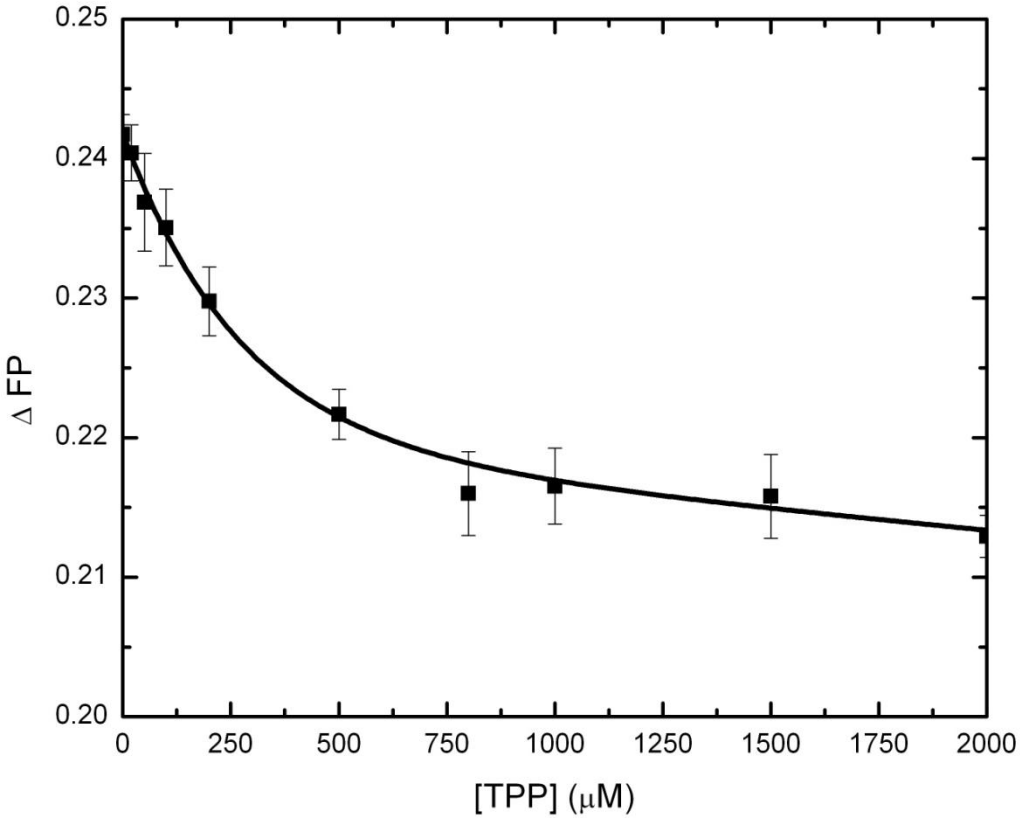


Figure 9. YdhE binding competition experiment between rhodamine 6G and tetraphenylphosphonium chloride (TPP). YdhE (5 μM) was pre-incubated with rhodamine 6G (1 μM) for two hours before titration. The change in fluorescence polarization signals (ΔFP) of rhodamine 6G was measured at an emission wavelength of 550 nm. TPP was non-fluorescent in the experimental conditions. The decrease in ΔFP showed that the bound rhodamine 6G was knocked off by TPP.

**Supplemental material**

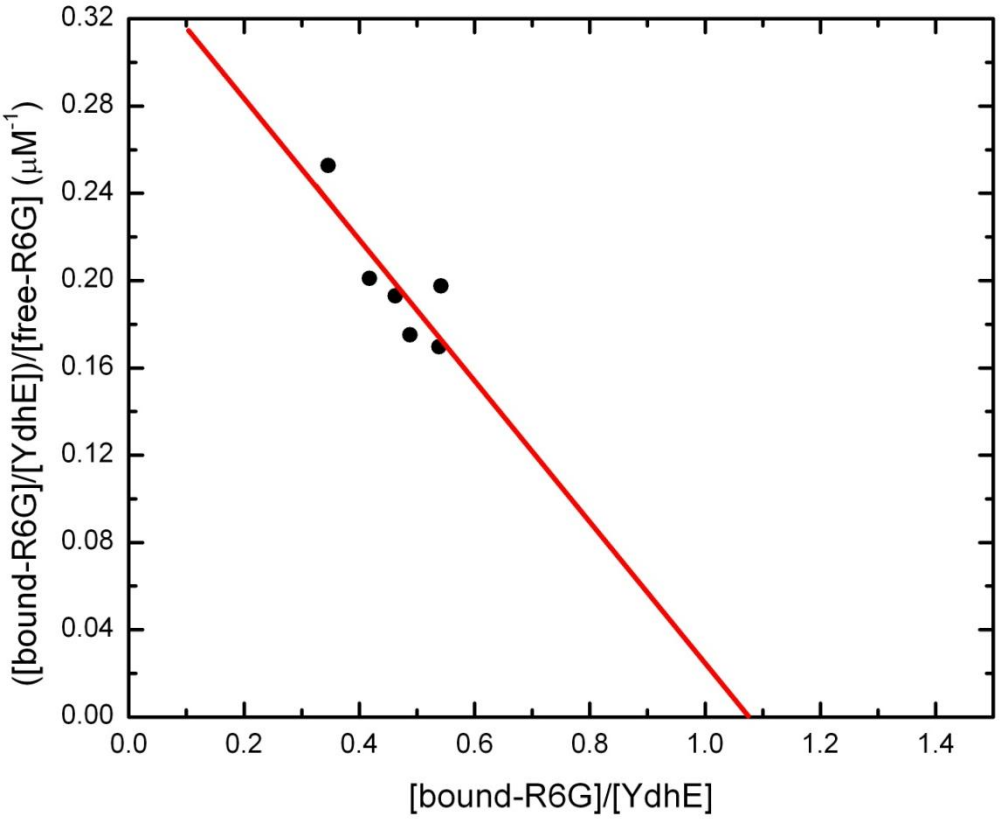


Figure S1. Scatchard plot of equilibrium dialysis data for YdhE binding to rhodamine 6G. The YdhE-rhodamine 6G dialysis experiments were carried out with 2-5 μM monomeric YdhE dialyzed against 3-5 μM rhodamine 6G. The slope of the plot provides a $K_D$ of 3.0 ± 0.1, and the interception (1.0 ± 0.2) gives a stoichiometry of 1:1 monomeric YdhE-to-R6G molar ratio.

# CHAPTER 3. Crystal structures of the CusA heavy-metal efflux pump suggest a methionine-mediated transport mechanism

A manuscript submitted to *Nature*

**Feng Long[1,ψ], Chih-Chia Su[2,ψ], Michael T. Zimmermann[3], Scott E. Boyken[3], Wei Wang[4], Mathew D. Routh[1], Kanagalaghatta R. Rajashankar[5], Robert L. Jernigan[3,4] and Edward W. Yu[1,2,3,4,6*]**

[1]Molecular, Cellular and Developmental Biology Interdepartmental Graduate Program, Iowa State University, IA 50011, USA

[2]Department of Chemistry, Iowa State University, Ames, IA 50011, USA

[3]Bioinformatics and Computational Biology Interdepartmental Graduate Program, Iowa State University, Ames, IA 50011, USA

[4]Department of Biochemistry, Biophysics and Molecular Biology, Iowa State University, Ames, IA 50011, USA

[5]NE-CAT and Department of Chemistry and Chemical Biology, Cornell University, Bldg. 436E, Argonne National Laboratory, 9700 S. Cass Avenue, Argonne. IL 60439, USA

[6]Department of Physics and Astronomy, Iowa State University, Ames, IA 50011, USA

[ψ]F.L. and C.S. contributed equally to this work.

* To whom correspondence should be addressed. E-mail: ewyu@iastate.edu

**Gram-negative bacteria, such as *Escherichia coli*, frequently utilize tripartite efflux complexes in the resistance-nodulation-division (RND) family to expel diverse toxic compounds from the cell.[1,2] One such efflux system CusCBA is responsible for extruding biocidal Cu(I) and Ag(I) ions.[3,4] As no structural information is available for the heavy-metal efflux (HME) subfamily of the RND efflux pumps, we here describe the crystal structures of the inner membrane transporter CusA in the absence and presence of bound Cu(I) or Ag(I). The CusA structures reported here provide important new structural information about the HME subfamily of RND efflux pumps. The structures suggest that the metal binding sites, formed by a three-methionine cluster, are located within the cleft region of the periplasmic domain. Intriguingly, this cleft is closed in the apo-CusA form but open in the CusA-Cu(I) and CusA-Ag(I) structures, which directly suggests a plausible pathway for ion export. The binding of Cu(I) and Ag(I) triggers significant conformational changes in both the periplasmic and transmembrane domains. The crystal structure indicates that CusA has, in addition to the three-methionine metal binding site, five methionine pairs - three located in the transmembrane region and two in the periplasmic domain. Genetic analysis and transport assays suggest that CusA is capable of actively picking up metal ions from the cytosol, utilizing five of these methionine pairs/clusters to bind and export metal ions. We propose a stepwise shuttle mechanism for transport between these sites.**

Silver is a heavy metal with a relatively high toxicity in prokaryotes. Ionic silver exhibits antimicrobial activity against a broad range of microorganisms, and has long been used as an effective broad antimicrobial agent against pathogens.[5,6] Copper, although

required in trace amounts for bacterial growth, is highly toxic even at low concentrations.[7] Thus, both silver and copper are well-known bactericides, and their biocidal effects have been used for centuries. In Gram-negative bacteria, efflux systems of the resistance-nodulation-division (RND) superfamily play major roles in the intrinsic and acquired tolerance of antibiotics and toxic compounds, including silver and copper ions.[1,2] The Gram-negative bacterium *Escherichia coli* harbors seven different RND efflux transporters. These transporters can be categorized into two distinct sub-families, the hydrophobic and amphiphilic efflux RND (HAE-RND) and heavy-metal efflux RND (HME-RND) families.[1,2] Six of these transporters, such as AcrB, AcrD, AcrF, MdtB, MdtC and YhiV, are multidrug efflux pumps, which belong to the HAE-RND protein family.[1] In addition to these multidrug efflux pumps, *E. coli* contains one HME-RND efflux transporter, CusA, which specifically recognizes and confers resistance to Ag(I) and Cu(I) ions.[3,4] The two sub-families of these RND transporters share relatively low protein sequence homology. For example, sequence alignment shows that CusA and AcrB have only 19% identity.

As a RND transporter, CusA works in conjunction with a periplasmic component, belonging to the membrane fusion protein family, and an outer membrane channel to form a functional protein complex. CusA is a large proton motive force-dependent inner membrane efflux pump comprised of 1,047 amino acids.[3,4] CusC, however, is a 457 amino acid protein that forms an outer membrane channel.[3,4] The membrane fusion protein CusB (379 amino acids) contacts both the inner membrane CusA and outer membrane CusC proteins.[3,4] Presumably, the three components of this HME-RND system form a tripartite efflux complex CusCBA, which spans both the inner and outer membranes of *E. coli* to export Ag(I) and

Cu(I) directly out of the cell. Heavy-metal efflux by the CusCBA complex is driven by proton import, and this process is catalyzed through the inner membrane transporter CusA.

At present, only two crystal structures of RND-type efflux pumps are available. These efflux pumps, belonging to the HAE-RND subfamily, are the *E. coli* AcrB[8-12] and *Pseudomonas aeruginosa* MexB[13] multidrug transporters. Their structures suggest that both AcrB and MexB span the entire width of the inner membrane and protrude approximately 70Å into the periplasm. Along with the models of these two HAE-RND transporters, the crystal structures of the other components of these tripartite complex systems have also been determined. These include the outer membrane channels, *E. coli* TolC[14] and *P. aeruginosa* OprM,[15] as well as the periplasmic membrane fusion proteins, *E. coli* AcrA[16] and *P. aeruginosa* MexA.[17-19]

Currently, no structural information has yet been available for any HME-RND type efflux pump. Several attempts at crystallizing the CusA efflux pump have not succeeded, probably because of the flexible nature of this pump.[20,21] Presumably, the three components of this HME-RND system form a tripartite complex that resembles the AcrAB-TolC complex. Different from the HAE-RND family, members of the HME-RND family are highly substrate-specific, with the ability to differentiate between monovalent and divalent ions. To elucidate the mechanism used by the CusCBA efflux system for Cu(I)/Ag(I) recognition and extrusion, we have previously reported the crystal structure of the full-length CusB membrane fusion protein.[22] Now we describe the crystal structure of the HME-RND transporter CusA, both in the absence and presence of Cu(I) or Ag(I). The structures

strongly suggest that CusA relies upon methionine residues to bind and export the metal ions, as has been proposed.[4]

We cloned, expressed and purified the full-length CusA protein containing a 6xHis tag at the N-terminus. We obtained crystals of the *E. coli* CusA heavy-metal efflux pump following an extensive screening for crystallization conditions with different detergents. We then used multiple-isomorphous replacement with anomalous scattering (MIRAS) to determine the three-dimensional structure. The diffraction data can be indexed to the space group *R*32. Data collection and refinement statistics are summarized in Tables S1 and S2. The resulting experimental electron density maps (Fig. S1) reveal that the asymmetric unit consists of one protomer. The native crystal structure of CusA has been determined to a resolution of 3.52 Å (Table S1). Currently, 97.9% of the residues (residues 5-504 and 516-1040) are included in our final model. The final structure is refined to $R_{work}$ and $R_{free}$ of 23.7% and 27.9%, respectively.

Overall, the crystal structure of CusA is quite distinct from those of the HAE-RND pumps, AcrB and MexB. Superimposition of the structure of CusA with the structure of AcrB (pdb code:1IWG)[8] results in a high RMSD of 11.4 Å for 1,003 $C^{\alpha}$ atoms, suggesting highly significant differences between these two transporters. CusA exists as a homotrimer, and each subunit of CusA consists of 12 transmembrane helices (TM1-TM12) and a large periplasmic domain formed by two periplasmic loops between TM1 and TM2, and TM7 and TM8, respectively (Fig. 1 and Fig. S2). In the transmembrane region, the relative locations of TM1-TM6 are related to those of TM7-TM12 by pseudo-twofold symmetry. These TM helices are arranged in such a way that TM4 and TM10 form the center of the core and are

surrounded by the other TM helices. Differently from AcrB and MexB, four helices, TM4, TM5, TM10 and TM11, extend into the cytoplasm, forming the cytoplasmic domain of the pump. Two other helices, TM2 and TM8, protrude into the periplasm and contribute part of the periplasmic domain. It is important to note that TM2, TM4 and TM5 of the N-terminal half correspond to TM8, TM10 and TM11 of the C-terminal half, respectively, in the pseudo-twofold symmetry.

Like AcrB and MexB, the periplasmic domain of CusA can be divided into six sub-domains, PN1, PN2, PC1, PC2, DN and DC (Fig. 1). Sub-domains PN1, PN2, PC1 and PC2 form the pore domain, with PN1 making up the central pore and stabilizing the trimeric organization. Sub-domains DN and DC, however, contribute to form the docking domain, presumed to be interacting with the outer membrane channel CusC. The trimeric CusA structure suggests that sub-domains PN2, PC1 and PC2 are located at the outermost core of the periplasmic domain, facing the periplasm. In AcrB, sub-domains PC1 and PC2 form a large external cleft and are presumed to create the entrance for drugs from the periplasm. However, the apo-CusA structure shows that the gap between PC1 and PC2 is completely closed (Fig. 1b). *In vitro* cross-linking coupled with mass spectrometry suggested that sub-domain PN2 of CusA should interact with the N-terminus of the CusB membrane fusion protein.[22] This result agrees with the cross-linking experimentwhere the N and C-termini of AcrA was found to contact PN2 and PC1 of AcrB.[19] Thus, sub-domains PN2 and PC1 of CusA most likely form the binding surface for the membrane fusion protein CusB.

Perhaps the most interesting secondary structural feature appears in the cleft region of the periplasmic domain. Residues located on the left side of the wall (Fig. 2), formed by one

α-helix (residues 690-706) and three β-sheets (residues 681-687, 711-716 and 821-827), appear to tilt into the cleft to close the opening. Surprisingly, residues 665-675, located at the bottom of the cleft, form an α-helix. This structural feature, not found in AcrB and MexB, likely governs the specificity of the CusA pump. The α-helix orients horizontally and roughly divides the transmembrane and periplasmic domains into two compartments. Located just above this horizontal helix, we find three proximal methionine residues, M573, M623 and M672, presumably creating a three-methionine specific binding site for Cu(I) and Ag(I) ions.[23,24] Notably M672 is also one of the residues within the horizontal helix. Site-directed mutagenesis had suggested that these three methionine residues are essential for mediating copper resistance.[4] Indeed, a strong peak at the copper edge was observed at the center of these three methionines in our CusA-Cu(I) crystal derivative, indicating the binding of a Cu(I) ion in a three-sulfur binding site (see below). The location of this Cu(I) binding site is coincident with the multidrug binding site in AcrB at the periplasmic cleft.[25,26]

Intriguingly, the overall structure of the CusA-Cu(I) complex is quite distinct from that of apo-CusA (Fig. 2). Superimposition of these two structures gives an overall RMSD of 3.9 Å (for 1,006 $C^{\alpha}$ atoms). As mentioned above, the bound Cu(I) ion was found to coordinate residues M573, M623 and M672. These three methionines specifically form a typical three-methionine coordination site for binding Cu(I)/Ag(I).[23,24] The signal for this bound copper is strong with a large peak height of 44 σ. Binding of Cu(I) initiates significant conformational changes in the periplasmic as well as transmembrane domains of CusA. Perhaps, the most noticeable difference between the apo and ion-bound structures appears in the PC2 region (Fig. 2 and Fig. S3). Cu(I) binding leads to a $30^{o}$ swing of the

entire PC2 sub-domain. This motion shifts PC2 away from the PC1 sub-domain. The hinge for this rotational movement appears to be at the junction between sub-domains PC2 and DC with residues G721 and P810 forming the hinge. As a consequence, the gap between PC1 and PC2 appears to open up after binding this metal ion. This gap presumably creates an entrance for metal ions from the periplasmic space. The horizontal helix, residues 665-675, located inside the cleft also makes a substantial movement. The C-terminal end of this helix is found to tilt upward by $21^{o}$ in the Cu(I)-bound structure with respect to the apo form (Fig. 2c). This tilting motion allows M672 to move closer to M573 and M623 to complete the three-methionine coordination site. Coupled with this movement, TM8 also shifts in position to a more vertical orientation while retaining its α-helical structure. Overall, the N-terminal end of TM8 is found to shift away from the core by 10 Å after Cu(I) binding.

For the CusA-Ag(I) complex, an anomalous difference Fourier peak (38 σ) was found at the center of residues M573, M623 and M672, indicating that the bound $Ag^{+}$ ion is coordinated by these three methionines (Fig. 2d). The overall conformational changes triggered by Cu(I) and by Ag(I) binding are nearly identical. Superimposition of the CusA-Cu(I) and CusA-Ag(I) structures gives an overall RMSD of 1.0 Å (for 1,021 $C^{\alpha}$s). Based on the crystal structures, the horizontal helix in the cleft directly interacts with the N-terminal end of TM8. The movement of TM8 may relate directly to transmembrane signaling and could initiate the translocation of a proton across the membrane. Indeed, in the AcrB pump, there is evidence that proton translocation is coupled to the conformational change in TM8.[12,27] The change in conformation takes place in TM8 by reeling in some random coil residues to extend the helix.[12] In addition, when individual residues of the proton-relay

network was changed to alanine, disrupting the hydrogen bonds in the system, it was reported that TM8 of AcrB becomes longer and extends into the periplasmic domain.[27] In contrast to AcrB, the helical structure of the N-terminus of TM8 in CusA is retained after metal binding. Instead, the N-terminal end of TM8 moves outward, together with the movement of the PC2 sub-domain. According to the crystal structures of the apo and bound-CusA, we confirm prior speculation that the structure of apo-AcrB is actually the detergent-bound form.[13]

Intriguingly, it appears that the binding of Cu(I) or Ag(I) also triggers significant conformational changes in the other transmembrane helices of the pump. In addition to the movement of TM8, all other transmembrane helices except TM2 shift horizontally by as much as 4 Å, mimicking the motion of TM8. Further, TM1, TM3 and TM6 readjust in an approximately 3 Å upward shift with respect to the inner membrane surface. The net result is that all three of these transmembrane helices move towards the periplasm by one turn. Mutagenesis studies of the transmembrane domain of CusA indicated the conserved charged residue D405 of TM4 to be essential for transporter function.[4] Based on the crystal structure, this acidic residue interacts with E939 and K984 (Fig. S4). It is possible that these three charged residues participate in forming the proton-relay network in the transmembrane region of the pump.

Coupled with the above conformational changes, the sub-domain PN1 at the periplasmic domain was also found to undergo substantial movement. Overall, PN1 also shifts upward by 3 Å. This moves the central pore helix upward by one turn upon metal binding. It should be noted that the binding of metal ions does not significantly affect the conformation of the sub-domains DN, DC, PN2 or the transmembrane helix TM2. PN2 has

been found to interact with the N-terminus of the CusB membrane fusion protein. Thus, we expect that PN2 and TM2 could move in the presence of CusB, to accommodate the binding of this membrane fusion protein. If TM8 were responsible for signaling the binding of metal ions, it would suggest that TM2 is important for detecting the presence of the membrane fusion component CusB.

Flexible docking was then carried out, where flexibility between the domains of CusB was accounted for by docking Domains 1 and 2 of CusB separately to the structure of apo-CusA using 3-D dock,[28] followed by energy minimization with the CHARMM27 force field[29] and steered molecular dynamics to restrain CusB to fit the docked fragments. The resulting CusBA structure suggests that Domains 1 and 2 of the CusB membrane fusion protein contact CusA at the interface between PN2 and PC1 (Fig. S5).

The full-length CusA includes 34 methionine residues with 18 of them located in the transmembrane domain. Of the 18 methionines, six are paired up to form three distinct methionine pairs (Fig. S1b). These methionine pairs are M410 of TM4 and M501 of TM6; M403 of TM4 and M486 of TM6; and M391 of TM4 and M1009 of TM12 (Fig. 3, Fig. S6 and Fig. S7). Copper tolerance proteins, such as CusF,[30,31] CueR[32] and Atx1,[33] have been found to utilize two-methionine or two-cysteine binding pockets to carry their Cu(I)/Ag(I) cargos. Thus, these methionine pairs could potentially form binding sites for Ag(I) and Cu(I) in the transmembrane region of the pump. If this is the case, then CusA could transport these metal ions from the cytoplasm along these methionine pairs. In the periplasmic domain of CusA, we have also found two pairs of methionines (M271-M755, and M738-M792) in addition to the three-methionine metal binding site (Fig. 3). In view of the crystal structures,

these six methionine pairs/clusters are deemed to be important for binding and transport of metal ions.

We then determined whether the CusA protomer forms a channel by using the program CAVER (http://loschmidt.chemi.muni.cz/caver) and found that each protomer of CusA forms a channel spanning the entire transmembrane region up to the bottom of the periplasmic funnel (Fig. S8). Intriguingly, the channel includes four methionine pairs, three (M410-M501, M403-M486, M391-M1009) from the transmembrane region and one (M271-M755) from the periplasmic domain, as well as the three-methionine binding site formed by M573, M623 and M672 (Fig. 3). Taken together these five methionine pairs/clusters are likely to form a relay network facilitating metal ion transport. Remarkably, this channel spans almost the entire length of each protomer, from the transmembrane domain through to the bottom of the periplasmic funnel region, and is likely to represent a real path for transporting the metal ion from both the cytoplasm and periplasm to the periplasmic funnel for extrusion. It should be noted that the pair M738-M792, located at the top of the funnel, is not located directly within this channel.

We made an *E. coli* knock-out strain BL21(DE3)Δ*cueO*Δ*cusA* that lacks both the *cueO* and *cusA* genes. We mutated M573, M623 and M672, which are members of the binding site triad inside the cleft of the periplasmic domain, into isoleucines (M573I, M623I and M672I). We then expressed these three mutant transporters in BL21(DE3)Δ*cueO*Δ*cusA*, and tested their ability to confer copper and silver resistance *in vivo*. We found that the CusA mutants, M573I, M623I and M672I are unable to relieve the copper or silver sensitivity of strain BL21(DE3)Δ*cueO*Δ*cusA* (Tables S3 and S4), thus agreeing well with the work of

Franke et al.[4] in which M573, M623 and M672 were shown to be essential for the function of CusA.

We mutated M410 into an isoleucine (M410I) to disrupt the pair formed by M410 and M501 at the bottom of the transmembrane and also replaced M486 and M391, which pair with M403 and M1009, with isoleucines (M486I and M391I). Expression of these three mutants in BL21(DE3)Δ*cueO*Δ*cusA* showed a significant decrease in the level of copper and silver tolerances when compared with cells expressing wild-type CusA. In addition, we introduced M755I in the periplasmic domain. Again, when expressed in BL21(DE3)Δ*cueO*Δ*cusA*, this mutant transporter (M755I) showed a decrease in copper/silver tolerance in comparison with cells harboring the wild-type transporter. We then made two mutant transporters, M738I and M792I, in which these two methionines form a pair at the top of the periplasmic funnel. Unlike the other mutations, cells expressing these mutant transporters do not elevate the sensitivity level for copper or silver compared with cells expressing the wild-type pump (Tables S3 and S4). Together, these results strongly support five of these methionine pairs/clusters engaging in the methionine-residue ion relay channel.

Based on the crystal structure of CusA, it is expected that the charged residues D405, E939 and K984 are important for the proton-relay network of the pump, and these in turn were replaced with alanines (D405A, E939A and K984A) to disrupt the hydrogen-bonded network. Indeed, cells expressing this mutant were unable to tolerate copper and silver, demonstrating that these three charged residues are essential for the transporter's functioning.

To investigate whether CusA can transport metal ions from the cytoplasm, we reconstituted the purified CusA protein into liposomes containing the fluorescent indicator

Phen Green SK (PGSK) in the intravesicular space (Fig. S9). The intravesicular and extravesicular pHs of these proteoliposomes were 6.6 and 7.0, respectively. We then determined whether these proteoliposomes can capture metal ions from the extravesicular medium with a stopped-flow transport assay. (The charged metal ions are unlikely to diffuse spontaneously across membrane bilayers.) When $Ag^+$ ions were added into the extravesicular medium, we detected the quenching of the fluorescence signal, suggesting the uptake of $Ag^+$ into the intravesicular space (Fig. 4a). The uptake into proteoliposomes is presumably due to the CusA active transport activity. It should be noted that no decrease in fluorescence signal was detected in the absence of a pH gradient (i.e. no differential pH) between the inside and outside of the proteoliposomes, or if the intravesicular pH is higher than the extravesicular pH (i.e. reverse pH gradient) (Fig. S10).

In addition to the above experiment, we investigated the methionine residues that were shown to be important for copper and silver tolerances with the above transport assay. We expressed, purified and reconstituted the CusA mutants, M573I, M623I and M672I, into liposomes encapsulated with the same fluorescence indicator. Surprisingly, these mutant transporters do not take up $Ag^+$ from the extravesicular medium of the proteoliposomes (Fig. 4a). It is clear that even single point mutations M573I, M623I or M672I abolish the process of metal transport across the membrane. Thus, it is expected that this three-methionine site is requisite for both metal binding and export.

We then purified the mutants, M391I, M486I and M755I, and reconstituted them into liposomes. In these three cases, the fluorescence signals did not attenuate as indicated by the stopped-flow assay (Fig. 4a). When compared with the result from the wild-type CusA, this

suggests that the M391I, M486I and M755I mutant transporters are unable to actively transport $Ag^+$ across the membrane.

Although all of the above experimental results strongly suggest that these five methionine pairs/clusters (Fig. 3) are important for metal transport, we cannot definitively rule out the possibility that these mutations may affect the structure of the pump and in that way impair metal binding. Nonetheless, our collective experiments provide direct compelling evidence that CusA is capable of taking up $Ag^+$ from the cytoplasm.

The crystal structure of CusA suggests that the charged residues D405, E939 and K984 in the transmembrane domain may be important for proton translocation. When reconstituted into liposomes, mutant transporters (D405A, E939A and K984A) do not take up $Ag^+$ into the intravesicular space (Fig. 4b), thus confirming the importance of D405, E939 and K984 for the function of the pump.

It is likely that CusA operates through an alternating-access mechanism.[10-12] Thus we superimposed a protomer of apo-CusA onto each protomer of the "asymmetric" AcrB (pdb code: 2DHH).[10] Likewise, we also superimposed a protomer of CusA-Cu(I) onto those of the AcrB pump. These superpositions gave high overall RMSDs, each RMSD exceeding 11 Å. However, when the portion of the apo-CusA protomer that contains only sub-domains PC1, PC2, PN1 and PN2 was supimposed onto those of the "extrusion", "binding" and "access" conformers of AcrB (2DHH),[10] we obtained much smaller RMSDs of 4.7 Å, 5.6 Å and 5.5 Å. Similarly, superpositions of the periplasmic domain (only containing PC1, PC2, PN1 and PN2) of a protomer of CusA-Cu(I) onto those of the "extrusion", "binding" and "access" conformers of AcrB (2DHH)[10] gave RMSDs of 6.2 Å, 5.0 Å and 5.3 Å, respectively. These

superpositions suggest that the conformation of the apo-CusA protomer may correspond to the "extrusion" state, and that the CusA-Cu(I) protomer structure may represent the "binding" conformation of the pump. If this is the case, CusA may go through a cyclic conformational change, from the "access", through to the "binding" and finally to the "extrusion" conformer, as suggested for the AcrB pump,[10-12] to export copper/silver.

We also calculated the dynamics of the trimeric CusA pump using the elastic network model.[34] The result indeed suggests that CusA functions through three coupled motions in which the periplasmic cleft formed by sub-domains PC1 and PC2, presumably acting as the periplasmic metal entry site, alternately open and close (Figs. S11 and S12).

There is strong evidence that the CusCBA system captures Cu(I) and Ag(I) ions from the periplasm. The periplasmic membrane fusion protein CusB is known to specifically bind Cu(I).[35] It has also been demonstrated that the periplasmic chaperone protein CusF can directly transfer these metals to CusB.[36] Indeed, the crystal structure of CusB indicates that this membrane fusion protein consists of multiple Cu(I) and Ag(I) binding sites.[22] Thus, in addition to capturing metal ions from the periplasm, the CusA pump may also be able to take up these metals from the cytoplasm. In fact, it has been demonstrated that the divalent cation efflux pump CzcA is capable of catalyzing the transport of divalent cations, such as $Zn^{2+}$, from the cytosol.[37] Further, the AcrD multidrug efflux pump has also been observed to capture aminoglycosides from both the periplasm and cytoplasm.[38]

We hypothesize that CusA can pick up metal ions from both the cytoplasm and periplasm. We propose that this transporter utilizes methionine pairs/clusters to export Cu(I) and Ag(I). The periplasmic cleft of CusA presumably remains closed when there is no

Cu(I)/Ag(I). In the presence of Cu(I) or Ag(I) ions, the periplasmic cleft opens. Metal ions could enter the three-methionine binding site inside the cleft directly through the periplasmic cleft or via the methionine pairs within the transmembrane region (Fig. 3). Thus, transport of a metal ion within the membrane is likely to involve a stepwise process that shuttles the metal ion from one methionine pair to another along the pathway. The locations of these methionine pairs/clusters allow us to depict a direct pathway for metal transport and extrusion. The metal ion bound at the three-methionine binding site of the periplasmic cleft could then be released to the nearest methionine pair, formed by M277 and M755, following which the metal ion could then be released into the central funnel to reach the CusC channel for final extrusion. Interestingly, the proposed metal export pathway in the periplasmic domain, based on the location of the methionine pairs/clusters, is similar to the proposed drug export pathway in AcrB.[12] Nonetheless, our mechanism for export of metal ions intermediated by binding to sequential methionine pairs/clusters is fully consistent with the body of evidence in all of the structural and mutagenesis studies reported here.

**Methods Summary**

Crystals were grown by sitting-drop vapor diffusion. Phasing, refinement methods and statistics are provided in the Methods.

**Author Information**

Atomic coordinates and structure factors have been deposited with the Protein Data Bank as codes 3KO7 (apo-CusA), 3KSS (CusA-Cu(I)) and 3KSO (CusA-Ag(I)).

**Acknowledgements.** This work is supported by NIH Grants GM 074027 (E.W.Y.), GM 086431 (E.W.Y.), GM 081680 (R.L.J.) and GM 072014 (R.L.J.). This work is based upon research conducted at the Northeastern Collaborative Access Team beamlines of the Advanced Photon Source, supported by award RR-15301 from the National Center for Research Resources at the National Institutes of Health. Use of the Advanced Photon Source is supported by the U.S. Department of Energy, Office of Basic Energy Sciences, under Contract No. DE-AC02-06CH11357.

## References

1. Tseng, T. T., Gratwick, K. S., Kollman, J., Park, D., Nies, D. H., Goffeau, A. & Saier, M. H. Jr. The RND permease superfamily: an ancient, ubiquitous and diverse family that includes human disease and development protein. *J. Mol. Microbiol. Biotechnol.* **1,** 107-125 (1999).

2. Nies, D. H. Efflux-mediated heavy metal resistance in prokaryotes. *FEMS Microbiol. Rev.* **27,** 313-339 (2003).

3. Franke, S., Grass, G. & Nies, D. H. The product of the *ybdE* gene of the *Escherichia coli* chromosome is involved in detoxification of silver ions. *Microbiol.* **147,** 965-972 (2001).

4. Franke, S., Grass, G., Rensing, C. & Nies, D. H. Molecular analysis of the copper-transporting efflux system CusCFBA of *Escherichia coli*. *J. Bacteriol.* **185,** 3804-3812 (2003).

5. Silver, S. Bacterial silver resistance: molecular biology and uses and misuses of silver compounds. *FEMS Microbiol. Rev.* **27,** 341-353 (2003).

6. Percival, S. L., Bowler, P. G. & Russell, D. Bacterial resistance to silver in wound care. *J. Hosp. Infect.* **60,** 1-7 (2005).

7. Ercal, N., Gurer-Orhan, H. & Aykin-Burns, N. Toxic metals and oxidative stress part I: mechanisms involved in metal induced oxidative damage. *Curr. Topics Med. Chem.* **1,** 529-539 (2001).

8. Murakami, S., Nakashima, R., Yamashita, E. & Yamaguchi, A. Crystal structure of bacterial multidrug efflux transporter AcrB. *Nature* **419,** 587-593 (2002).

9. Yu, E. W., McDermott, G., Zgruskaya, H. I., Nikaido, H. & Koshland, D. E., Jr. Structural basis of multiple drug binding capacity of the AcrB multidrug efflux pump. *Science* **300,** 976-980 (2003).

10. Murakami, S., Nakashima, R., Yamashita, E., Matsumoto, T. & Yamaguchi, A. Crystal structures of a multidrug transporter reveal a functionally rotating mechanism. *Nature* **443,** 173-179 (2006).

11. Seeger, M. A., Schiefner, A., Eicher, T., Verrey, F., Dietrichs, K. & Pos, K. M. Structural asymmetry of AcrB trimer suggests a peristaltic pump mechanism. *Science* **313,** 1295-1298 (2006).

12. Sennhauser, G., Amstutz, P., Briand, C., Storchengegger, O., Grütter, M. G. Drug export pathway of multidrug exporter AcrB revealed by DARPin inhibitors. *PLoS Biol.* **5**, e7 (2007).

13. Sennhauser, G., Bukowska, M. A., Briand, C. & Grütter, M. G. Crystal structure of the multidrug exporter MexB from *Pseudomonas aeruginosa*. *J. Mol. Biol.* **389,** 134-145 (2009).

14. Koronakis, V., Sharff, A., Koronakis, E., Luisi, B. & Hughes, C. Crystal structure of the bacterial membrane protein TolC central to multidrug efflux and protein export. *Nature* **405,** 914-919 (2000).

15. Akama, H., Kanemaki, M., Yoshimura, M., Tsukihara, T., Kashiwag, T., Yoneyama, H., Narita, S., Nakagawa, A. & Nakae, T. Crystal structure of the drug discharge outer membrane protein, OprM, of *Pseudomonas aeruginosa*. *J. Biol. Chem.* **279,** 52816-52819 (2004).

16. Mikolosko, J., Bobyk, K., Zgurskaya, H. I. & Ghosh, P. Conformational flexibility in the multidrug efflux system protein AcrA. *Structure* **14,** 577-587 (2006).

17. Higgins, M. K., Bokma, E., Koronakis, E., Hughes, C. & Koronakis, V. Structure of the periplasmic component of a bacterial drug efflux pump. *Proc. Natl. Acad. Sci. USA* **101,** 9994-9999 (2004).

18. Akama, H., Matsuura, T., Kashiwag, S., Yoneyama, H., Narita, S., Tsukihara, T., Nakagawa, A. & Nakae, T. Crystal structure of the membrane fusion protein, MexA, of

the multidrug transporter in *Pseudomonas aeruginosa*. *J. Biol. Chem.* **279,** 25939-25942 (2004).

19. Symmons, M., Bokma, E., Koronakis, E., Hughes, C. & Koronakis, V. The assembled structure of a complete tripartite bacterial multidrug efflux pump. *Proc. Natl. Acad. Sci.* USA **106,** 7173-7178 (2009).

20. Stroebel, D., Sendra, V., Cannella, D., Helbig, K., Nies, D. H. & Covès, J. Oligomeric behavior of the RND transporters CusA and AcrB in micellar solution of detergent. *Biochim. Biophys. Acta* **1768**, 1567-1573 (2007).

21. Deniaud, A., Goulielmakis, A., Covès, J. & Pebay-Peyroula, E. Differences between CusA and AcrB crystallization highlighted by protein flexibility. *PLoS One* **4**, e6214 (2009).

22. Su, C.-C., Yang, F., Long, F., Reyon, D., Routh, M. D., Kuo, D. W., Mokhtari, A. K., Van Ornam, J. D., Rabe, K. L., Hoy, J. A., Lee, Y. J., Rajashankar, K. R. & Yu, E. W. Crystal structure of the membrane fusion protein CusB from *Escherichia coli*. *J. Mol. Biol.* **393,** 342-355 (2009).

23. Zhou, H. & Thiele, D. J. Identification of a novel high affinity copper transport complex in the fission yeast *Schizosaccharomyces pombe*. *J. Biol. Chem.* **276,** 20529-20535 (2001).

24. Jiang, J., Nadas, I. A., Kim, M. A. & Franz, K. J. A Mets motif peptide found in copper transport proteins selectively binds Cu(I) with methionine-only coordination. *Inorg. Chem.* **44,** 9787-9794 (2005).

25. Drew, D., Klepsch, M. M., Newstead, S., Flaig, R., De Gier, J. W., Iwata, S. & Beis, K. The structure of the efflux pump AcrB in complex with bile acid. *Mol. Membr. Biol.* **25**, 677-682 (2008).

26. Yu, E. W., Aires, J. R., McDermott, G. & Nikaido, H. A periplasmic-drug binding site of the AcrB multidrug efflux pump: a crystallographic and site-directed mutagenesis study. *J. Bacteriol.* **187**, 6804-6815 (2005).

27. Su, C.-C., Li, M., Gu, R., Takatsuka, Y., McDermott, G., Nikaido, H. & Yu, E. W. Conformation of the AcrB multidrug efflux pump in mutants of the putative proton relay pathway. *J. Bacteriol.* **188**, 7290-7296 (2006).

28. Gabb, H. A., Jackson, R. M. & Sternberg, M. J. E. Modelling protein docking using shape complementarity, electrostatics, and biochemical information. *J Mol Biol.* **272,** 106-120 (1997).

29. Feller, S. E. & MacKerell, A. D., Jr. An improved empirical potential energy for molecular simulations of phospholipids. *J. Phys. Chem. B* **104,** 7510-7515 (2000).

30. Xue, Y., Davis, A. V., Balakrishnan, G., Stasser, J. P., Staehlin, B. M., Focia, P., Spiro, T. G., Penner-Hahn, J. E. & O′Halloran, T. V. (2008). Cu(I) recognition via cation-π and methionine interactions in CusF. *Nature Chem. Biol.* **4**, 107-109.

31. Loftin, I. R., Franke, S., Blackburn, N. J. & McEvoy, M. M. (2007). Unusual Cu(I)/Ag(I) coordination of *Escherichia coli* CusF as revealed by atomic resolution crystallography and x-ray absorption spectroscopy. *Protein Sci.* **16**, 2287-2293.

32. Changela, A., Chen, K., Xue, Y., Holschen, J., Outten, C. E., O′Halloran, T. V. & Mondragón, A. (2003). Molecular basis of metal-ion selectivity and zeptomolar sensitivity by CueR. *Science* **301**, 1383-1387.

33. Arnesano, F., Banci, L., Bertini, I., Huffman, D. L. & O′Halloran, T. V. (2001). Solution structure of the Cu(I) and apo-forms of the yeast metallochaperone, Atx1. *Biochemistry* **40**, 1528-1539.

34. Atilgan, A. R., Durell, S. R., Jernigan, R. L., Demirel, M. C., Keskin, O. & Bahar I. Anisotropy of fluctuation dynamics of proteins with an elastic network model. *Biophys. J.* **80,** 505-515 (2001).

35. Bagai, I., Liu, W., Rensing, C., Blackburn, N. J. & McEvoy, M. M. Substrate-linked conformational change in the periplasmic component of a Cu(I)/Ag(I) efflux system. *J. Biol. Chem.* **282,** 35695-35702 (2007).

36. Bagai, I., Rensing, C., Blackburn, N. J. & McEvoy, M. M. Direct metal transfer between periplasmic proteins identifies a bacterial copper chaperone. *Biochemistry* **47**, 11408-11414 (2008).

37. Goldberg, M., Pribyl, T., Juhuke, S. & Nies, D. H. Energetics and topology of CzcA, a cation/proton antiporter of the resistance-nodulation-cell division protein family. *J. Biol. Chem.* **274**, 26065-26070 (1999).

38. Aires, J. R. & Nikaido, H. Aminoglycosides are captured from both periplasm and cytoplasm by the AcrD multidrug efflux transporter of *Escherichia coli*. *J. Bacteriol.* **187,** 1923-1929 (2005).

## Figures and Captions

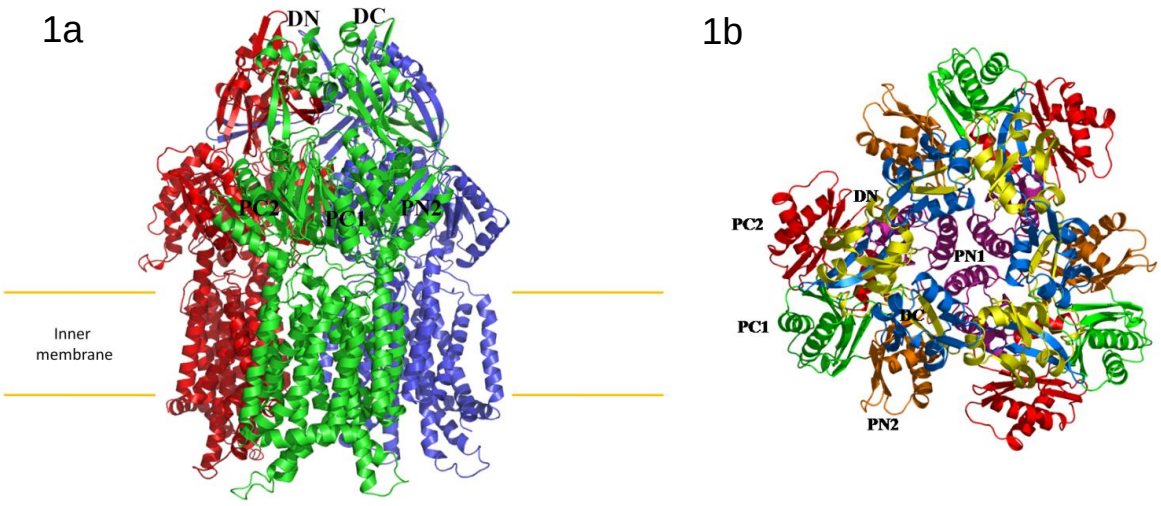


Fig. 1. Structure of the CusA efflux pump. (a) Ribbon diagram of the CusA homotrimer viewed in the membrane plane. Each subunit of CusA is labeled with a different color. Sub-domains DN, DC, PN2, PC1 and PC2 are labeled on the front protomer (green). The location of PN1 in this protomer is behind PN2, PC1 and PC2 (see text). (b) Top view of the CusA trimer. The six sub-domains are labeled yellow (DN), blue (DC), pink (PN1), orange (PN2), green (PC1) and red (PC2). In the apo-CusA structure, the cleft between PC1 and PC2 is closed.

2a

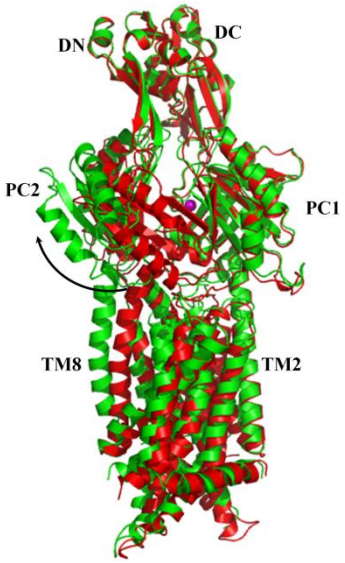
DN
DC
PC2
PC1
TM8
TM2

2b

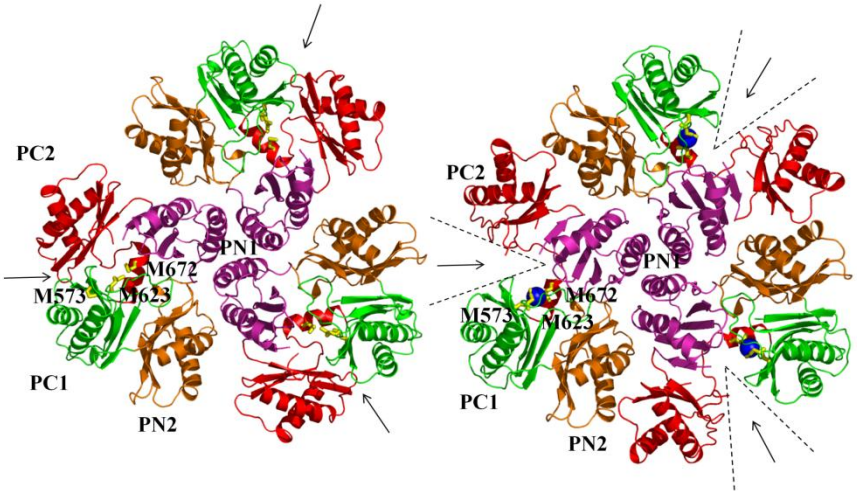
PC2
PN1
M672
M573
M623
PC1
PN2
PC2
PN1
M672
M573
M623
PC1
PN2

2c

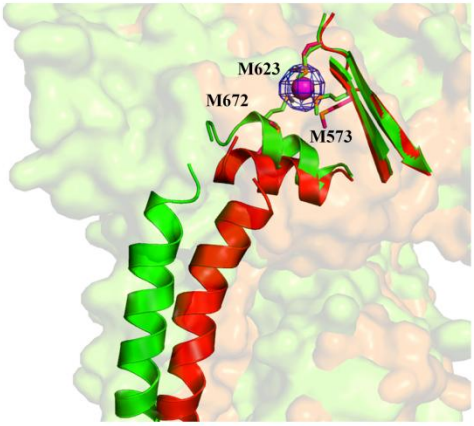
M623
M672
M573

2d

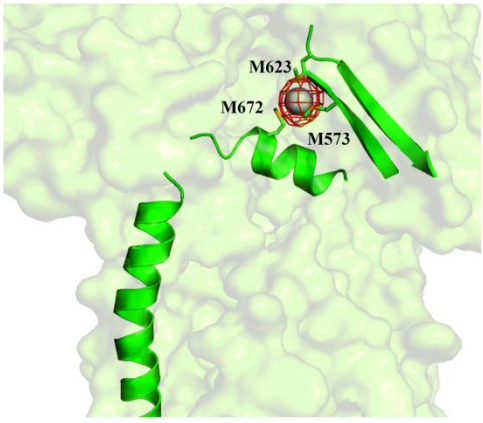
M623
M672
M573

Fig. 2. Comparison of the apo and metal bound structures of CusA. (a) Superposition of a monomer of apo-CusA (red) onto a monomer of Cu(I) bound-CusA (green). The bound Cu(I) is pink. The arrow represents a major swing of the PC2 sub-domain initiated by Cu(I) binding. (b) Conformational changes of the periplasmic domain of CusA. The conformation of each sub-domain of CusA before (left) and after (right) Cu(I) binding. The periplasmic cleft formed between PC1 and PC2 is opened after Cu(I) binding. The bound coppers in the CusA-Cu(I) structure are blue. M573, M623 and M672 forming a metal binding site at the periplasmic cleft are shown in stick form (yellow). (c) The changes in conformation of the horizontal helix and TM8, are shown in a superimposition of the structures of apo (red) and Cu(I)-bound (green) CusA. The bound Cu(I) is shown as a pink sphere. Anomalous map of the bound Cu(I), contoured at 8$\sigma$, is in blue. M573, M623 and M672 are shown as sticks. (d) The Ag(I) binding site. The bound Ag(I) is shown as a gray sphere. Anomalous map of the bound Ag(I) , contoured at 10$\sigma$, is in red.

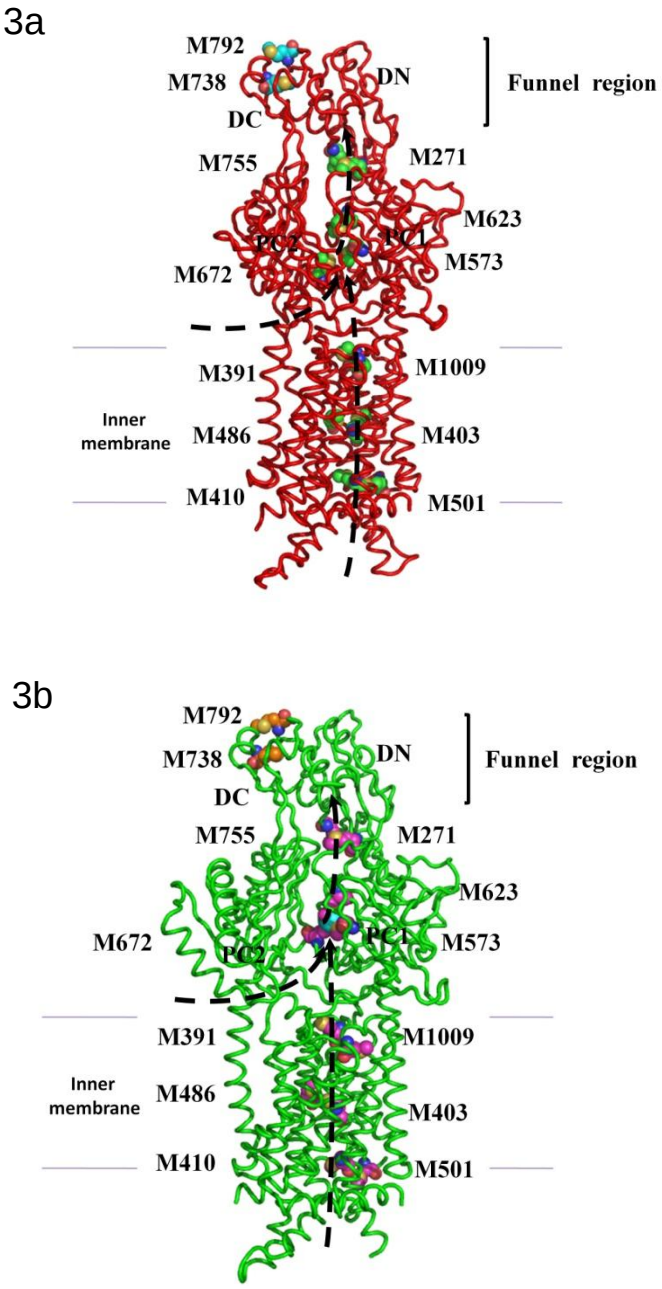


Fig. 3. Proposed metal transport pathway of the CusA efflux pump. (a) The five methionine pairs/clusters of the apo-CusA transporter form a pathway for metal export. These five methionines are shown as spheres (C, green; O, red; N, blue; S, orange). The carbon atoms

of the pair M738-M792, located at the top of the periplasmic funnel, are in blue. This pair does not engage directly in the methionine-residue relay network. (b) The five methionine pairs/clusters of the Cu(I) bound-CusA transporter form a pathway for metal export. These five methionines are given as spheres (C, pink; O, red; N, blue; S, orange). The carbon atoms of the pair M738-M792, located at the top of the periplasmic funnel, are in orange. This pair is not involved in the methionine-residue relay network. The pair M271-M755 is located at the bottom of the periplasmic funnel where the metal ion could then be released for final extrusion. The paths for metal transport through the periplasmic cleft and transmembrane region are illustrated with black curves.

4a

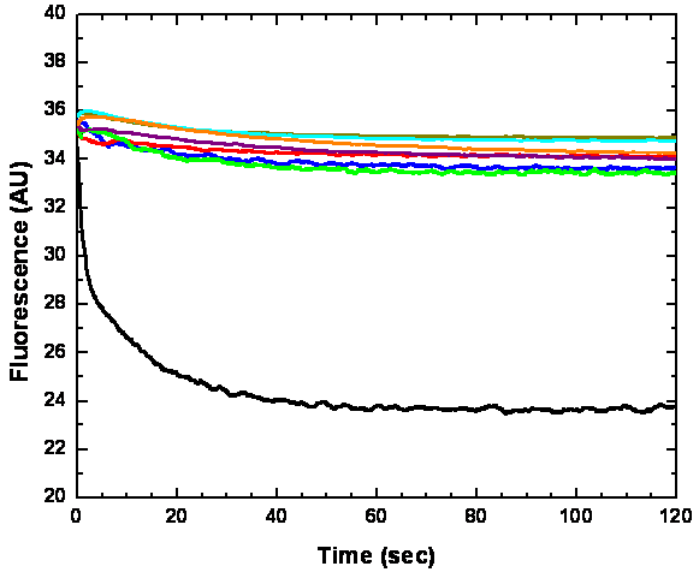


4b

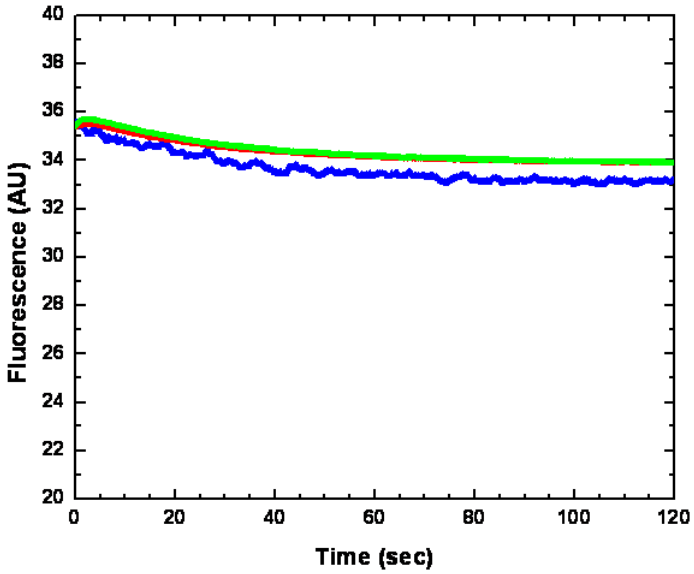


Fig. 4. Stopped-flow transport assay of reconstituted CusA with extravesicular $Ag^{+}$ ion. (a) Mutants of the methionine-residue relay network. The decrease in fluorescence signal of

PGSK mediated by proteoliposomes of wild-type CusA indicates the transport of $Ag^{+}$ across the membrane. The stopped-flow traces are the cumulative average of four successive recordings (wild-type CusA, black curve; M486I mutant, green curve; M391I mutant, brown curve; M573I mutant, red curve; M623I, purple curve; M672I, orange curve; M755I, cyan curve; control liposome, dark blue curve). (b) Mutants of the proton relay network. The stopped-flow traces are the cumulative average of four successive recordings (D405A mutant, dark blue curve; E939A mutant, red curve; K984A mutant, green curve). The wild-type CusA and control liposomes are shown in part (a).

## Supplemental Materials

### Methods

### Cloning, expression and purification of CusA

Briefly, the full-length CusA membrane protein containing a 6xHis tag at the N-terminus was overproduced in *E. coli* BL21(DE3)*ΔacrB* cells, which harbors a deletion in the chromosomal *acrB* gene, possessing pET15bΩ*cusA*. Cells were grown in 12 L of LB medium with 100 μg/ml ampicillin at 37$^{o}$C. When the $OD_{600}$ reached 0.5, the culture was treated with 1 mM IPTG to induce *cusA* expression, and cells were harvested within 3 h. The collected bacteria were resuspended in low salt buffer containing 100 mM sodium phosphate (pH 7.2), 10 % glycerol, 1 mM ethylenediaminetetraacetic acid (EDTA) and 1 mM phenylmethanesulfonyl fluoride (PMSF), and then disrupted with a French pressure cell. The membrane fraction was collected and washed twice with high salt buffer containing 20 mM sodium phosphate (pH 7.2), 2 M KCl, 10 % glycerol, 1 mM EDTA and 1 mM PMSF, and once with 20 mM HEPES-NaOH buffer (pH 7.5) containing 1 mM PMSF. The membrane protein was then solubilized in 1 % (w/v) Cymal-6. Insoluble material was removed by ultracentrifugation at 100,000 x g. The extracted protein was purified with a $Ni^{2+}$-affinity column. The purity of the CusA protein (>95%) was judged using 10% SDS-PAGE stained with Coomassie Brilliant Blue. The purified protein was then dialyzed and concentrated to 20 mg/ml in a buffer containing 20 mM Na-HEPES (pH 7.5) and 0.05% CYMAL-6.

For 6xHis SeMet-CusA protein expression, a 10 ml LB broth overnight culture containing *E. coli* BL21(DE3)*ΔacrB*/pET15bΩ*cusA* cells was transferred into 120 ml of LB

broth containing 100 μg/ml ampicillin and grown at 37°C. When the $OD_{600}$ value reached 1.2, cells were harvested by centrifugation at 6000 rev/min for 10 min, and then washed two times with 20 ml of M9 minimal salts solution. The cells were re-suspended in 120 ml of M9 media and then transferred into a 12 L pre-warmed M9 solution containing 100 μg/ml ampicillin. The cell culture was incubated at 37°C with shaking. When the $OD_{600}$ reached 0.4, 100 mg/l of lysine, phenylalanine and threonine, 50 mg/l isoleucine, leucine and valine, and 60 mg/l of L-selenomethionine were added. The culture was induced with 1 mM isopropyl-β-D-thiogalactopyranoside (IPTG) after 15 min. Cells were then harvested within 3 h after induction. The procedures for purifying the 6xHis SeMet-CusA were identical to those of the native protein.

**Crystallization of CusA**

Crystals of the 6xHis CusA were obtained using sitting-drop vapor diffusion. The CusA crystals were grown at room temperature in 24-well plates with the following procedures. A 2 μl protein solution containing 20 mg/ml CusA protein in 20 mM Na-HEPES (pH 7.5) and 0.05% (w/v) CYMAL-6 was mixed with a 2 μl of reservoir solution containing 10% PEG 3350, 0.1 M Na-MES (pH 6.5), 0.4 M $(NH_4)_2SO_4$, 1% JM 600 and 10% glycerol. The resultant mixture was equilibrated against 500 μl of the reservoir solution. The crystallization conditions for SeMet-CusA were the same as those for the native CusA protein. Crystals of CusA grew to a full size in the drops within a month. Typically, the dimensions of the crystals were 0.2 mm x 0.2 mm x 0.2 mm. Cryoprotection was achieved

by raising the glycerol concentration stepwise to 30% with a 5% increment in each step. Crystals of the gold or tantalum derivatives were prepared by incubating the crystals of apo-CusA in solution containing 10% PEG 3350, 0.1 M Na-MES (pH 6.5), 0.4 M $(NH_4)_2SO_4$, 1% JM 600, 10% glycerol, 0.05% (w/v) CYMAL-6, and 1 mM $KAuCl_4$ or 5 mM $Ta_6Br_{12}{\cdot}2Br$ for 1.5 hours at 25°C.

The CusA-Cu(I) complex crystals were prepared by incubating crystals of apo-CusA in solution containing 10% PEG 3350, 0.1 M Na-MES (pH 6.5), 0.4 M $(NH_4)_2SO_4$, 1% JM 600, 10% glycerol, 2 mM $[Cu(CH_3CN)_4]PF_6$, 2 mM tris(2-carboxyethyl)phosphine (TCEP) and 0.05% (w/v) CYMAL-6 for 1 hour at 25°C. Crystals of the CusA-Ag(I) complex were prepared using a similar method in solution containing 10% PEG 3350, 0.1 M Na-MES (pH 6.5), 0.4 M $(NH_4)_2SO_4$, 10% glycerol, 1 mM $AgNO_3$ and 0.05% (w/v) CYMAL-6 for 1 hour at 25°C.

**Data collection, structural determination and refinement**

All diffraction data were collected at 100K at beamline 24ID-C located at the Advanced Photon Source, using an ADSC Quantum 315 CCD-based detector. Diffraction data were processed using DENZO and scaled using SCALEPACK.[39] The crystals belong to space group *R*32 (Tables S1 and S2). Based on the molecular weight of CusA (115.72 kDa), a single molecule per asymmetric unit with a solvent content of 67.5% is expected. Two heavy-atom derivatives (gold and $Ta_6Br_{12}$ cluster) and the selenomethionyl-substituted (SeMet) crystal were isomorphous with the native crystal (Table S1). Ten heavy-atom sites

for the gold derivative were identified using SHELXC and SHELXD[40] as implemented in the HKL2MAP package.[41] These heavy-atom sites were refined using the program MLPHARE.[42,43] The resulting phases were subjected to density modification by RESOLVE[44] using the native structure factor amplitudes. Density modified phases were good enough to allow us to visualize the secondary structural features of the molecule. These phases were then used to locate three $Ta_6$ clusters and 31 selenium sites using the corresponding data sets. The final experimental phases were generated using 10 Au, three $Ta_6$ and 33 Se sites. The $Ta_6$ sites were treated as super-atoms containing all six tantalum atoms at a given site. These phases were then subjected to density modification and phase extension to 3.52 Å-resolution using the program RESOLVE.[44] The resulting phases were of excellent quality that enabled tracing of most of the molecule. The full-length CusA protein consists of 34 methionine residues. The SeMet data not only augmented the experimental phases, but also helped in tracing the molecules by anomalous difference Fourier maps where we could ascertain the proper registry of SeMet residues. After tracing the initial model manually using the program Coot,[45] the model was refined against the native data at 3.52 Å-resolution using TLS refinement techniques adopting a single TLS body as implemented in PHENIX[46] leaving 5% of reflections in Free-R set. Iterations of refinement using PHENIX[46] and CNS[47] and model building in Coot[45] lead to the current model, which consists of 1,025 residues with excellent geometrical characteristics (Table S1).

While the structure of CusA-Cu(I) complex could be determined using molecular replacement, the structure resulted in a relatively high refinement R-factor of 48.7%. Upon inspection of the electron density maps, it was found that several regions, especially the PC2

sub-domain, of CusA-Cu(I) have undergone significant conformational changes as discussed in the main text. To aid modeling of these conformational changes in the least biased manner, SAD phasing using the program PHASER[48] was employed to obtain experimental phases in addition to the phases from the structural model of apo-CusA that has sub-domains PC2 and PN1 removed. Phases were then improved using RESOLVE.[44] Even though the data resolution is low (4.10 Å), the phases were of sufficient quality that allowed for modeling of the conformational change (Fig. S3) using the program COOT.[45] At a later stage, higher resolution (3.88 Å) data of the CusA-Cu(I) were collected (Table S2). To reduce radiation damage, the data was collected away from the copper absorption edge, at 1.033 Å, where Cu still has ~2.4 anomalous electrons. The model was refined using PHENIX[46] and CNS.[47]

Since the X-ray absorption edge of Ag was not reachable at the synchrotron beamline (L-edges below 4 KeV and K-edge above 25 KeV), the data were collected at the copper edge where Ag has an anomalous contribution of ~3.5$e^-$. The structure of the CusA-Ag(I) complex was phased using molecular replacement by using CusA-Cu(I) as the search model. Structural refinement was then performed using PHENIX[46] and CNS[47] by refining the model against the 4.35 Å-resolution data from the CusA-Ag(I) crystal (Table S2).

**Docking structures of CusB onto CusA**

Initial rigid-body docking of the crystal structures of CusA and CusB did not reveal any feasible complexes that satisfied the CusA-K150/CusB-K95 crosslinking constraint,[22] indicating that docking may likely require a conformational change in one or both molecules.

As previously mentioned in this paper it has been hypothesized that the PN2 and PC1 sub-domains may move to accommodate CusB. For CusA, the normal modes from the Anisotropic-Network-Models (ANMs)[34] were calculated, but did not reveal any appropriate structures. For CusB, ANM revealed significant hinge motions between Domains 1 and 2. And, following this lead these two domains were docked individually onto CusA. Steered molecular dynamics simulations were then used to drive the CusB into a docked form agreeing with the individually docked fragments, thus allowing for the flexibility of the PC1, PN2 and TM2 domains of CusA.

**Data-driven docking of Domains 1 and 2 of CusB**

Rigid-body docking was performed using the 3D-dock software suite,[28] which utilizes the Katchalski-Katzir algorithm.[49] For all runs, 10,000 conformations were generated and filtered using the following data-driven constraints: transmembrane helices were masked from docking interactions; and side-chain amines of CusA-K150 and CusB-K95 were within 25 Å[22]; CusB was oriented so that its domains were free to interact with CusC and its N-terminus was directed towards the inner membrane.

**Steered Molecular Dynamics and Energy minimization**

An initial conformation was calculated by aligning CusB with the two individually docked fragments. To relax CusB from this conformation, we utilized steered molecular dynamics to guide the center of mass of domains 1 and 2 into the corresponding docked

position. Energy minimization was employed to alleviate steric clashes. During the simulation CusA was kept rigid with the exception of TM2, PN2, and PC1, which make up most of the CusB binding region. All calculations were performed using NAMD[50] and the CHARMM27 force field.[29]

**Double knocked-out strain and susceptibility assays**

The double knocked-out *E. coli* strain BL21(DE3)Δ*cueO*Δ*cusA* was produced from the BL21(DE3) strain using an RED disruption system as described by Datsenko and Wanner.[51] The Δ*cueO::kan* cassette, which was used to replace the chromosomal *cueO* gene, was produced by PCR, and then introduced into pKD46/BL21(DE3) by electroporation. The knocked-out BL21(DE3)Δ*cueO::kan* strain was selected on LB plate containing 30 μg/ml kanamycin, and verified by PCR. The kanamycin resistant gene was then released to generate the BL21(DE3)Δ*cueO* knocked-out strain. The deletion of *cusA* from BL21(DE3)Δ*cueO* was done using similar procedures as described above to generate the final BL21(DE3)Δ*cueO*Δ*cusA* double knocked-out strain.

The susceptibility to copper of *E. coli* BL21(DE3)Δ*cueO*Δ*cusA* harboring pET15bΩ*cusA* expressing the wild-type or mutant transporters, or the pET15b empty vector was tested on agar plates. Cells were grown in Luria Broth (LB) medium with 100 μg/ml ampicillin at 37 $^{o}$C. When the $OD_{600}$ reached 0.5, the cultures were induced with 0.5 mM IPTG and harvested in two hours after induction. The minimum growth inhibitory concentrations (MICs) to copper of *E. coli* BL21(DE3)Δ*cueO*Δ*cusA* (incoculum, 500 cells/ml)

harboring these vectors were then determined using LB agar containing 50 μg/ml ampicillin, 0.1 mM IPTG and different concentrations of $CuSO_4$ (0.25 to 2.75 mM in steps of 0.25 mM).

For the susceptibility to silver of *E. coli* BL21(DE3)Δ*cueO*Δ*cusA* harboring these vectors, cells were grown in Mueller Hinton (MH) medium containing 100 μg/ml ampicillin with the same procedures. The MICs to silver of *E. coli* BL21(DE3)Δ*cueO*Δ*cusA* (incoculum, 500 cells/ml) harboring these vectors were then performed in MH agar containing 50 μg/ml ampicillin, 0.1 mM IPTG and different concentrations of $AgNO_3$ (5.0 to 50.0 μM in steps of 2.5 μM). The expression level of each mutant in BL21(DE3)Δ*cueO*Δ*cusA* is similar to that of the wild-type transporter as indicated by Western blot analysis (Fig. S13). Bacterial growth in the LB or MH agar was recorded after 24 h of incubation at 37$^{o}$C. Each assay was repeated at least four times to ensure the reproducibility of the results.

**Reconstitution and stop-flow transport assay**

The purified wild-type CusA, M391I, M486I, M573I, M623I, M672I, M722I, D405A, E939A or K984A was reconstituted into liposomes made of *E. coli* polar lipid and egg-yolk phosphatidylcholine (Avanti Polar Lipids) in a molar ratio of 3:1. Briefly, 50 μg of the purified protein (wild-type CusA or its mutant) was added to 4.5 mg of lipids dispersed in the reconstitution buffer containing 20 mM HEPES-KOH, pH 6.6. The protein samples were completely incorporated into liposomes as judged using 10% SDS-PAGE stained with Coomassie Brilliant Blue. Control liposomes were prepared following the same procedure

without adding protein. 200 μM fluorescence indicator Phen Green SK (PGSK) (Invitrogen) was encapsulated by two freeze-thaw cycles, followed by gel filtration to remove the untrapped dye. Transport experiments were performed at 25$^{o}$C on a stopped-flow apparatus (Hi-Tech Scientific) connected to a spectrofluorometer (PerkinElmer LS55). Proteoliposomes and a transport assay buffer (20 mM HEPES-KOH pH 7.0 and 1 mM $AgNO_3$) were loaded into a two separate syringes of equal volume. Transport reactions were initiated by pushing 400 μl fresh reactants at a 1:1 ratio through the 90 μl mixing cell at a flow rate of 2 ml/s. Stopped-flow traces were the cumulative average of four successive recordings at 530 nm with the excitation wavelength at 480 nm.

**Dynamics Simulations**

The observed conformational changes between the Cu(I) bound and the apo forms, displayed in Fig. 2, are shown to be intrinsically favored by the new structure through the use of normal mode analysis (Fig. S11). A coarse-grained elastic network model[34] was investigated that is composed of the $C^{\alpha}$ atom coordinates and a portion of coarse-grained lipid bilayer between the trans-membrane domains. The opening and closing of the space between PC1 and PC2 coupled with a shift of TM8 is reproduced by this simple model (Fig. S12). The model does not show simultaneous opening and closing of all three periplasmic heavy metal entrance sites, but rather has a more complex opening/closing motion in which each pair of two adjacent is alternately open and closed. All three combinations of these coupled motions are obtained by using just two low energy motions.

**References**


39. Otwinowski, Z. & Minor, M. Processing of X-ray diffraction data collected in oscillation mode. *Methods Enzymol.* **276,** 307-326 (1997).

40. Schneider T. R. & Sheldrick G. M. Substructure solution with SHELXD. *Acta Crystallogr.* **D58,** 1772–1779 (2002).

41. Pape T. & Schneider T. R. HKL2MAP: a graphical user interface for macromolecular phasing with SHELX programs. *J Appl Crystallogr* **37,** 843–844 (2004).

42. Otwinowski, Z. MLPHARE, CCP4 Proc. 80 (Daresbury Laboratory, Warrington, UK, 1991).

43. Collaborative Computational Project No. 4. The CCP4 suite: programs for protein crystallography. *Acta Crystallogr.* **D50,** 760-763 (1994).

44. Terwilliger, T. C. Maximum-likelihood density modification using pattern recognition of structural motifs. *Acta Cryst.* **D57**, 1755-1762 (2001).

45. Emsley, P. & Cowtan, K. Coot: model-building tools for molecular graphics. *Acta Crystallogr.* **D60**, 2126 (2004).

46. Adams, P. D., Grosse-Kunstleve, R. W., Hung, L. W., Ioerger, T. R., McCroy, A. J., Moriarty, N. W. *et al.* PHENIX: building new software for automated crystallographic structure determination. *Acta Crystallogr.* **58**, 1948-1954 (2002).

47. Brünger, A. T., Adams, P. D., Clore, G. M., DeLano, W. L., Gros, P., Grosse-Kunstleve, R. W., Jiang, J. S., Kuszewski, J., Nilges, M., Pannu, N. S., Read, R. J., Rice, L. M.,

Simonson, T. & Warren, G. L. Crystallography & NMR system: A new software suite for macromolecular structure determination. *Acta Cryst.* **D54,** 905-921 (1998).

48. McCoy, A. J., Grosse-Kunstleve, R. W., Adams, P. D., Winn, M. D., Storoni, L. C. & Read, R. J. *Phaser* crystallographic software. *J. Appl. Crystallogr.* 40, 658-674 (2007).

49. Katchalski-Katzir, E., Shariv, I., Eisenstein, M., Friesem, A. A., Aalo, C. & Wodak, S. J. Molecular surface recognition: Determination of geometric fit between proteins and their ligands by correlation techniques. *Proc. Nat. Acad. Sci.* **89,** 2195-2199 (1992).

50. Phillips, J. C., Braun, R., Wang, W., Gumbart, J., Tajkhorshid, E., Villa, E., Chipot, C., Skeel, R. D., Kale, L. & Schulten, K. Scalable molecular dynamics with NAMD. *J. Comp. Chem.* **26,** 1781-1802 (2005).

51. Datsenko, K. A. & Wanner, B. L. One-step inactivation of chromosomal genes in *Escherichia coli* K-12 using PCR products. *Proc. Nat. Acad. Sci.* **97,** 6640-6645 (2000).

**Supplemental Tables**

Table S1. Data collection, phasing and structural refinement statistics of apo-CusA.

| | Native CusA | Derivatives | | |
|---|---|---|---|---|
| | | Au(III) | $Ta_6Br_{12}^{2+}$ | Se (peak) |
| **Data Collection** | | | | |
| Detector type/source | ADSC Q315 APS-24IDC | ADSC Q315 APS-24IDC | ADSC Q315 APS-24IDC | ADSC Q315 APS-24IDC |
| Wavelength (Å) | 0.9791 | 1.0398 | 1.0089 | 0.9791 |
| Space group | *R*32 | *R*32 | *R*32 | *R*32 |
| Cell constants (Å) | a = b = 178.42, c = 285.75 | a = b = 179.31, c = 287.10 | a = b = 178.34, c = 284.23 | a = b = 178.21, c = 285.57 |
| Resolution (Å) | 50-3.52 (3.67-3.52) | 50-4.31 (4.50-4.31) | 50-3.52 (3.66-3.52) | 50-3.68 (3.81-3.68) |
| Total reflections | 432,346 | 759,214 | 604,127 | 509,675 |
| Unique reflections | 21,820 | 14,948 | 24,417 | 19,264 |
| Redundancy | 6.9 (6.9) | 3.2 (2.8) | 3.8 (3.9) | 3.9 (3.9) |
| Completeness (%) | 94.2 (95.8) | 100 (100) | 99.9 (100) | 100 (100) |
| $R_{sym}$(%) | 5.7 (43.5) | 10.2 (35.9) | 6.2 (37.7) | 7.5 (46.9) |
| Average I/σ(I) | 32.5 (4.0) | 17.3 (5.3) | 21.7 (3.4) | 19.7 (2.6) |
| **MIR Phasing** | | | | |
| Number of sites | | 10 | 3 | 33 |
| Phasing power (acentric/centric) | | 1.51/1.10 | 1.09/1.23 | 2.51/1.51 |
| $R_{cullis}$ (acentric/centric) | | 0.58/0.80 | 0.76/0.71 | 0.84/1.23 |
| Figure of merit (acentric/centric) | | | 0.29/0.36 | |
| **Refinement** | CusA | | | |
| Resolution (Å) | 50-3.52 | | | |
| $R_{work}$ (%) | 23.8 | | | |
| $R_{free}$ (%) | 27.5 | | | |
| Protein residues built | 1,025 | | | |
| Protein atoms | 7,884 | | | |
| rms deviation from ideal | | | | |
| Bond lengths (Å) | 0.004 | | | |
| Bond angles (°) | 0.874 | | | |
| **Ramachandran** | | | | |
| most favored | 87.6 | | | |
| additional allowed | 11.4 | | | |
| generously allowed | 1.0 | | | |
| disallowed | 0.0 | | | |

Table S2. Data collection, phasing and structural refinement statistics of the CusA-Cu(I) and CusA-Ag(I) complexes.

| | Cu(I) (peak) | Cu(I) | Ag(I) |
|---|---|---|---|
| **Data Collection** | | | |
| Detector type/source | ADSQ Q315 APS-24IDC | ADSQ Q315 APS-24IDC | ADSQ Q315 APS-24IDC |
| Wavelength (Å) | 1.3779 | 1.0333 | 1.3779 |
| Space group | *R*32 | *R*32 | *R*32 |
| Cell constants (Å) | a = b = 178.21, c = 285.57 | a = b = 179.14, c = 286.12 | a = b = 179.99, c = 287.98 |
| Resolution (Å) | 50-4.10 (4.25-4.10) | 50-3.88 (4.03-3.88) | 50-4.35 (4.51-4.35) |
| Total reflections | 224,272 | 346,057 | 258,908 |
| Unique reflections | 14,211 | 17,119 | 15,666 |
| Redundancy | 2.5 (2.5) | 3.2 (3.1) | 3.3 (3.4) |
| Completeness (%) | 96.6 (98.7) | 99.5 (98.8) | 99.7 (99.9) |
| $R_{sym}$(%) | 8.9 (42.4) | 9.0 (42.6) | 9.2 (39.6) |
| Average I/σ(I) | 11.1 (1.8) | 10.5 (2.1) | 14.9 (2.0) |
| **Phasing** | | | |
| Figure of merit (acentric/centric) | 0.50/0.43 | | |
| **Refinement** | | CusA-Cu(I) | CusA-Ag(I) |
| Resolution (Å) | | 50-3.88 | 50-4.35 |
| $R_{work}$ (%) | | 26.1 | 27.1 |
| $R_{free}$ (%) | | 29.6 | 31.2 |
| Protein residues built | | 1,015 | 1,014 |
| Protein atoms | | 7,802 | 7,782 |
| rms deviation from ideal | | | |
| Bond lengths (Å) | | 0.005 | 0.006 |
| Bond angles ( °) | | 0.995 | 1.252 |
| **Ramachandran** | | | |
| most favored | | 85.1 | 84.5 |
| additional allowed | | 12.1 | 12.3 |
| generously allowed | | 1.5 | 1.8 |
| disallowed | | 1.2 | 1.4 |

Table S3. MICs of copper for different CusA mutants expressed in *E. coli* BL21(DE3)Δ*cueO*Δ*cusA*

| Gene in BL21(DE3)Δ*cueO*Δ*cusA* | MIC (mM) of $CuSO_4$ |
|---|---|
| Empty vector | 0.50 |
| *cusA* (wild-type) | 2.25 |
| *cusA* (M573I) | 0.50 |
| *cusA* (M623I) | 0.50 |
| *cusA* (M672I) | 0.50 |
| *cusA* (M391I) | 1.25 |
| *cusA* (M410I) | 1.75 |
| *cusA* (M486I) | 1.75 |
| *cusA* (M755I) | 1.75 |
| *cusA* (M738I) | 2.25 |
| *cusA* (M792I) | 2.25 |
| *cusA* (D405A) | 0.50 |
| *cusA* (E939A) | 0.50 |
| *cusA* (K984A) | 0.50 |
| *cusA* (E412A) | 1.00[a] |
| *cusA* (S453A) | 1.00[a] |
| *cusA* (C353A) | 2.25[b] |
| *cusA* (C375A) | 2.25[b] |

[a]Resdiues E412 and S453, located in the vicinity of the triad formed by D405, E939 and K984, may also involve in the proton-relay network.

[b]The CusA pump contains only two cysteine residues, C353 and C375, which may not involve in copper resistance.

Table S4. MICs of silver for different CusA mutants expressed in *E. coli* BL21(DE3)Δ*cueO*Δ*cusA*

| Gene in BL21(DE3)Δ*cueO*Δ*cusA* | MIC (μM) of $AgNO_3$ |
|---|---|
| Empty vector | 10.0 |
| *cusA* (wild-type) | 30.0 |
| *cusA* (M573I) | 12.5 |
| *cusA* (M623I) | 12.5 |
| *cusA* (M672I) | 12.5 |
| *cusA* (M391I) | 10.0 |
| *cusA* (M410I) | 17.5 |
| *cusA* (M486I) | 17.5 |
| *cusA* (M755I) | 12.5 |
| *cusA* (M738I) | 30.0 |
| *cusA* (M792I) | 30.0 |
| *cusA* (D405A) | 12.5 |
| *cusA* (E939A) | 12.5 |
| *cusA* (K984A) | 12.5 |
| *cusA* (E412A) | 12.5[a] |
| *cusA* (S453A) | 15.0[a] |

[a]Resdiues E412 and S453, located in the vicinity of the triad formed by D405, E939 and K984, may also involve in the proton-relay network.

**Supplemental Figures and Captions**

a

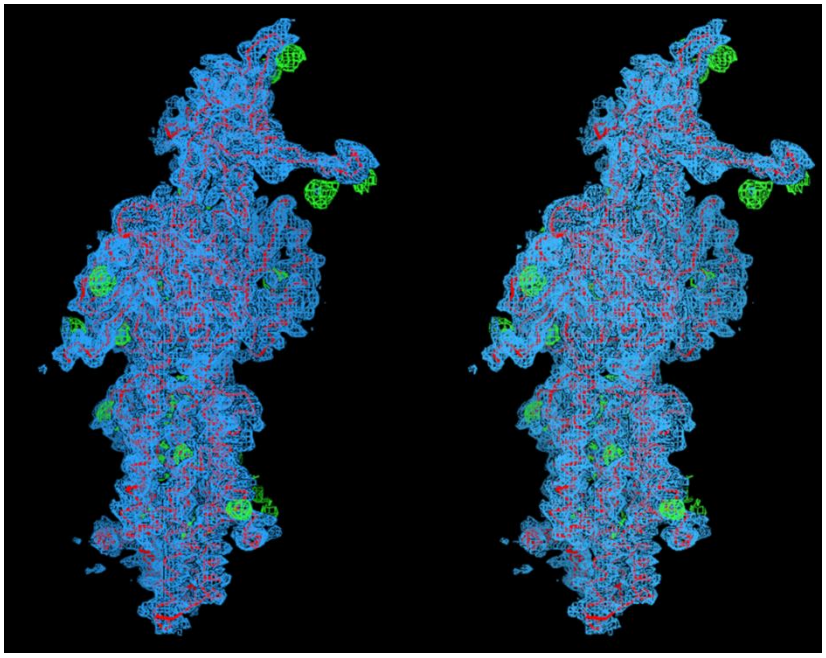

b

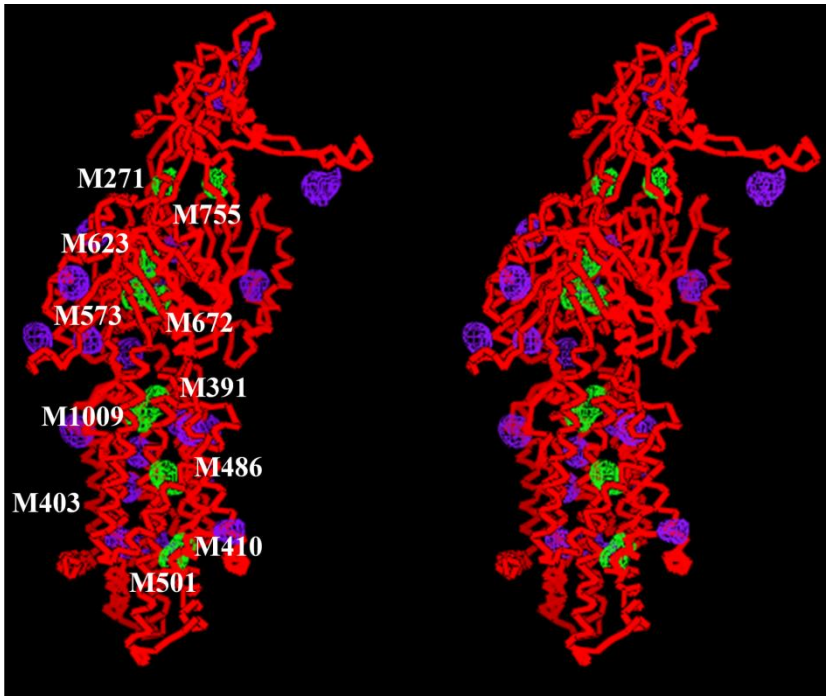

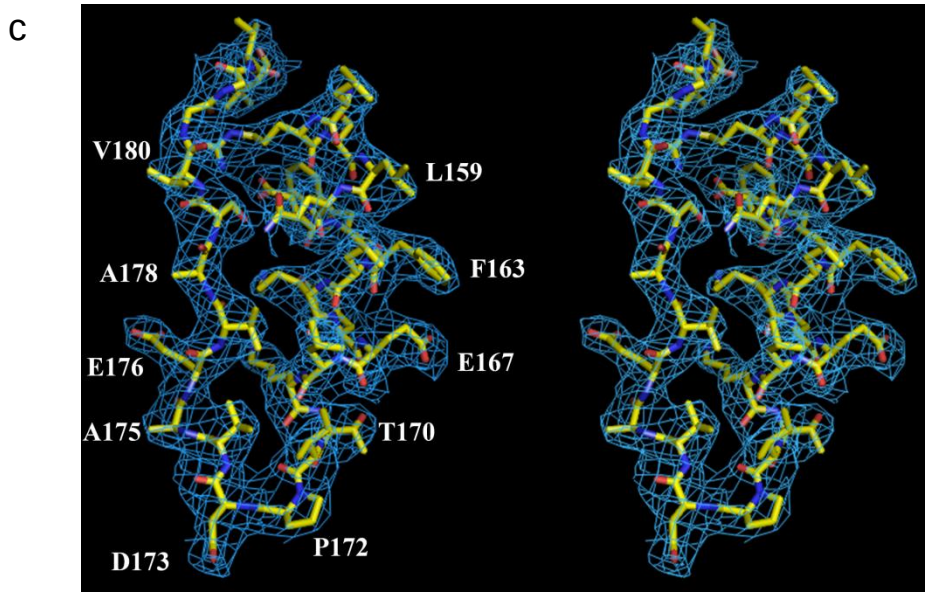


Fig. S1. Stereo view of the experimental electron density map at a resolution of 3.8 Å. (a) The electron density map contoured at 1.2 σ is in blue. Each subunit of CusA consists of 34 methionines. 33 selenium sites are found with a single SeMet crystal. The anomalous maps of the selenium sites contoured at 4 σ are in green. The Cα traces of CusA are in red. (b) Anomalous maps of the 33 selenium sites (contoured at 4 σ). The selenium sites corresponding to the 11 methionines forming the methionine-residue relay network are in green. The rest of the 22 selenium sites are in purple. The Cα traces of CusA are in red. (c) Representative section of the electron density in the second domain of CusA. The electron density (colored blue) is contoured at the 1.2 σ level and superimposed with the final refined model (yellow, carbon; red, oxygen; blue, nitrogen).

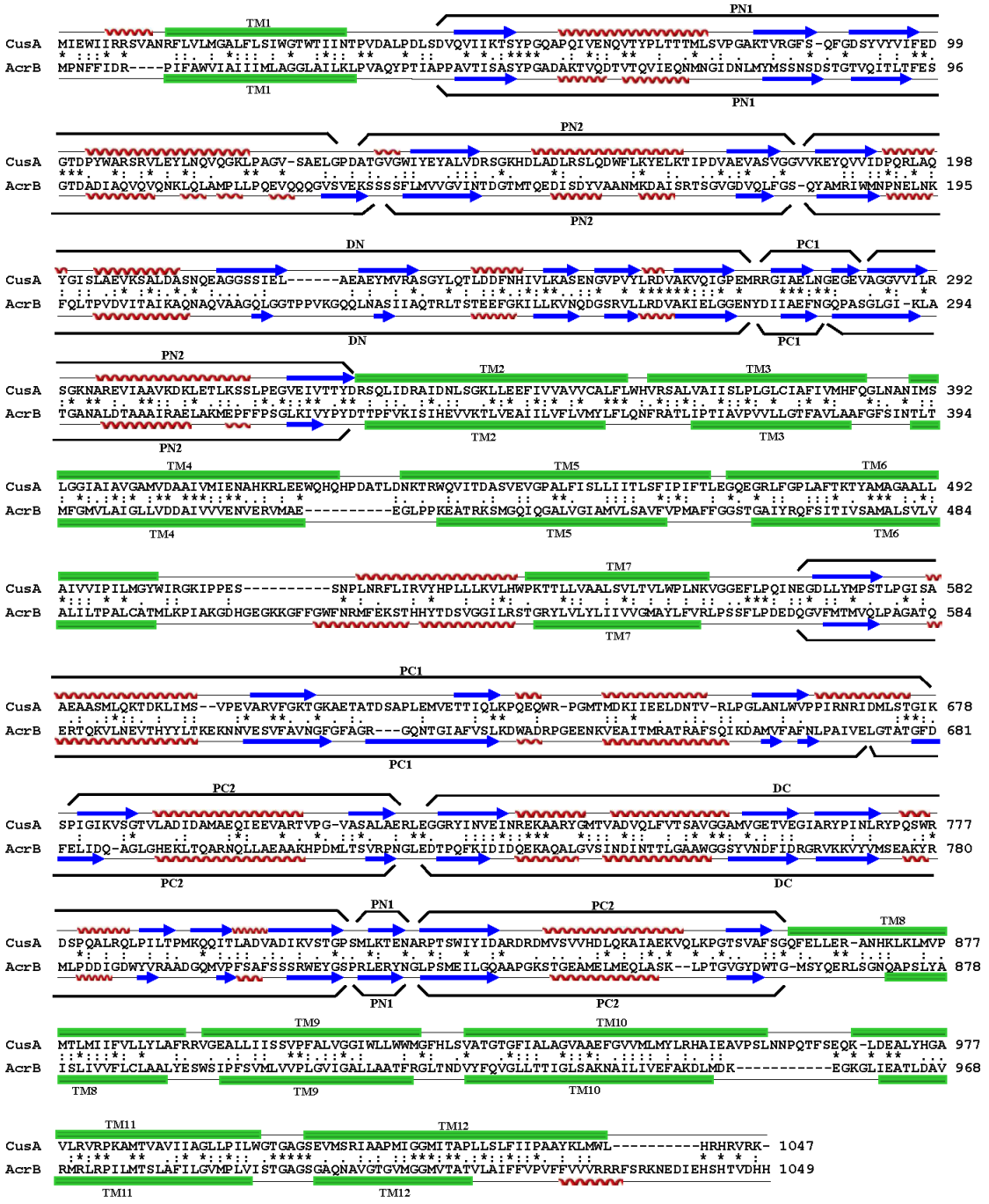


Fig. S2. Sequence and topology of CusA and AcrB. Alignment of the amino acid sequences of CusA and AcrB were done using CLUSTAL W. *, identical residues; :, >60% homologous residues. Secondary structural elements are indicated: TM, transmembrane

helix; Nα and Nβ, helix and strand, respectively, in the N-terminal half; Cα and Cβ, helix and strand, respectively, in the C-terminal half. The CusC or TolC docking domain is divided into two sub-domains, DN and DC; whereas the pore domain is divided into four sub-domains, PN1, PN2, PC1 and PC2. The sequence and topology of CusA are shown at the top, and those for the AcrB pump are shown at the bottom.

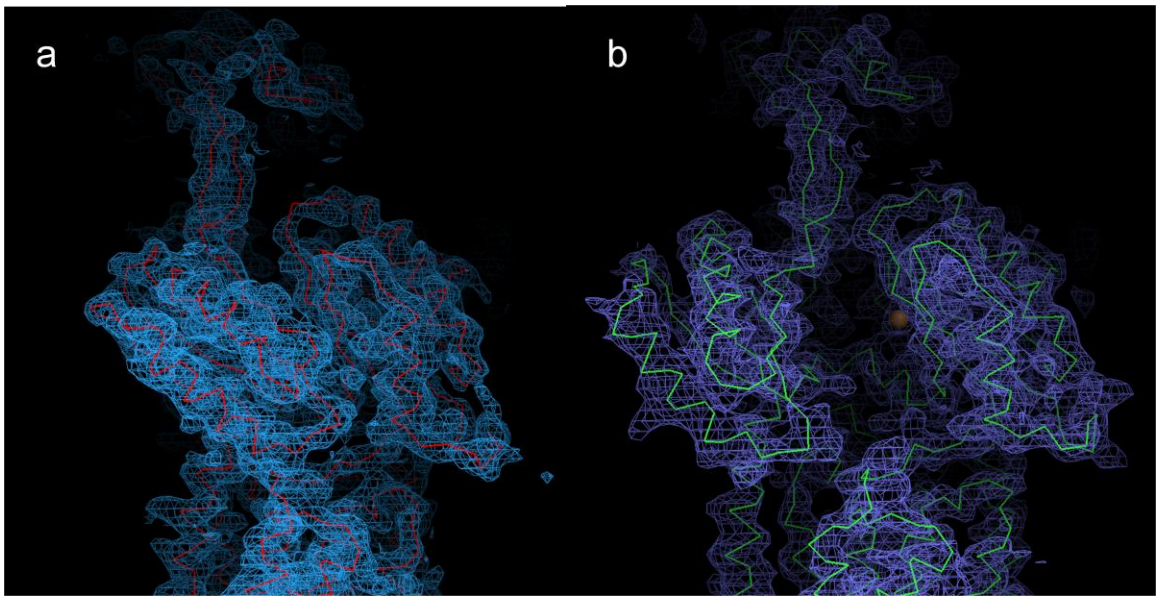


Fig. S3. Experimental electron density of the periplasmic domain of CusA. (a) The electron density map of apo-CusA (3.8 Å-resolution) contoured at 1.2 σ is in blue. The Cα traces of the periplasmic domain of apo-CusA are in red. (b) The electron density map of CusA-Cu(I) (4.1 Å-resolution) contoured at 1.2 σ is in purple. The Cα traces of the periplasmic domain of CusA-Cu(I) are in green. The bound copper is shown as a brown sphere.

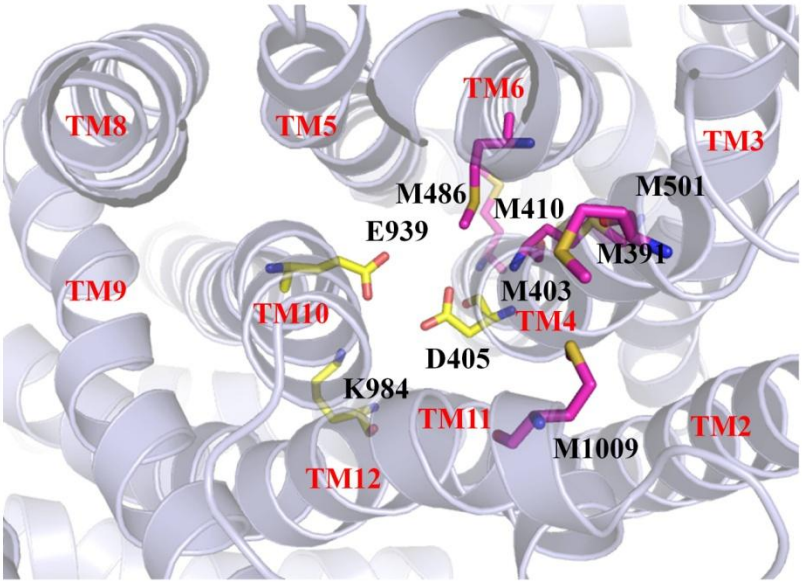


Fig. S4. Ion pairs in the transmembrane domain viewed from the cytoplasmic side. Residues D405 of TM4, E939 of TM10 and K984 of TM11 that form ion pairs, which may play an important role in proton translocation, are in yellow sticks. The six methionines, M391, M403, M410, M486, M501 and M1009, are shown as pink sticks.

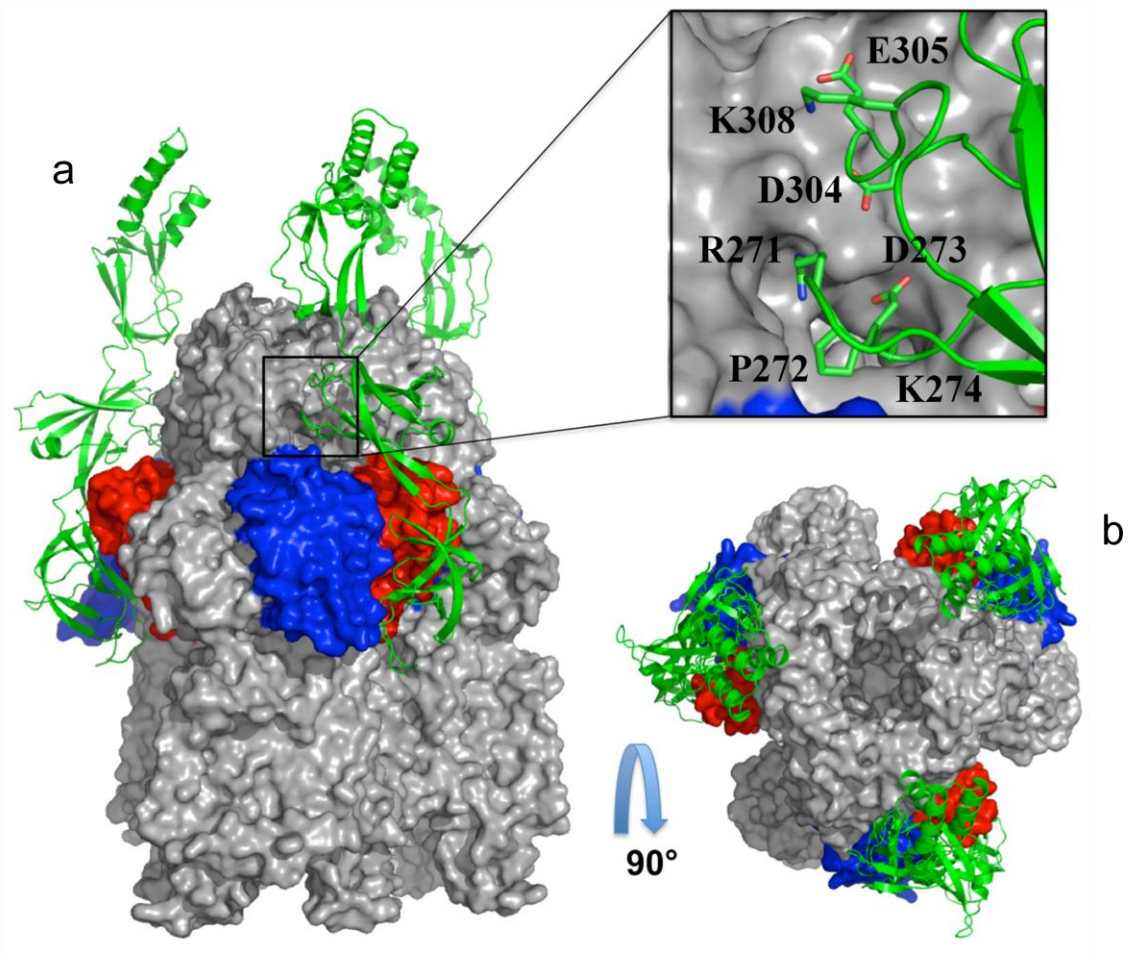


Fig. S5. Docking of CusB to CusA. (a) Side view of the docked complex of CusBA. The three CusB protomers are shown in green ribbons. The trimeric CusA is in gray surfaces. Sub-domains PN2 and PC1 of CusA are in red and blue, respectively. Specific interaction is found to occur between Domain 2 of CusB and the groove formed between DN and DC sub-domains of CusA to further stabilize the complex. (b) Top view of the docked complex of CusBA.

a

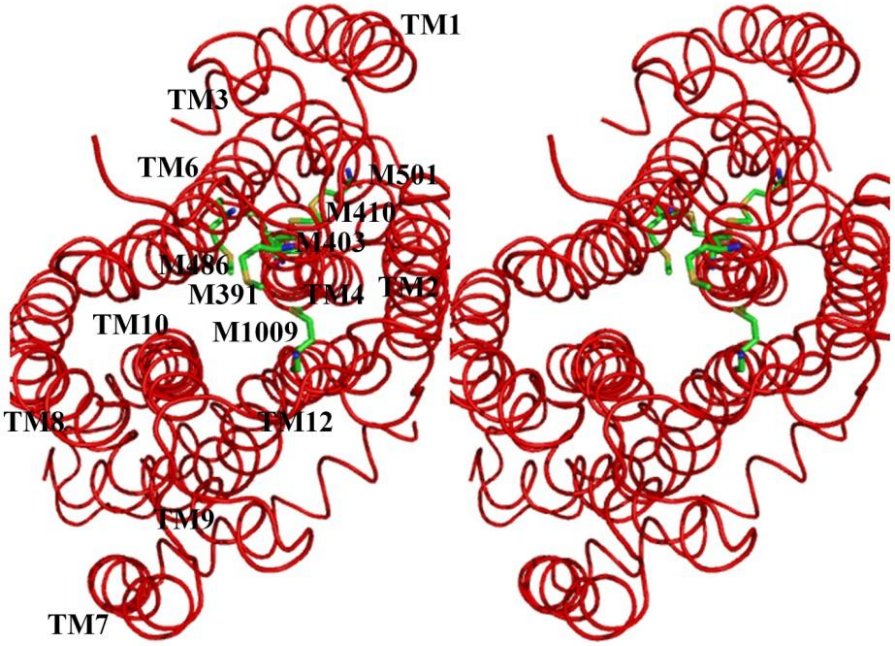
TM1
TM3
TM6
M501
M410
M403
M486
M391
TM4
TM2
TM10
M1009
TM8
TM12
TM9
TM7

b

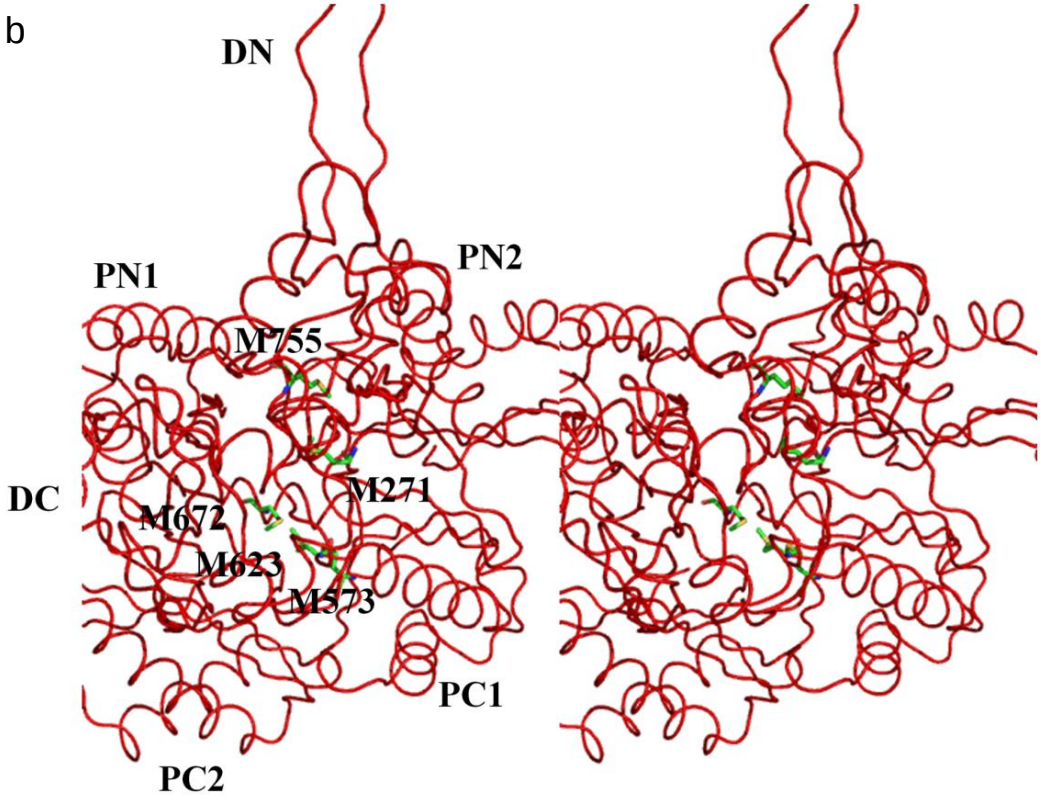
DN
PN1
PN2
M755
DC
M271
M672
M623
M573
PC1
PC2

Fig. S6. Stereo view of the methionine-residue relay network. (a) The transmembrane domain of a subunit of CusA viewed from the cytoplasmic side. The six methionines that form three pairs in the transmembrane region are in green sticks. (b) The periplasmic domain of a subunit of CusA viewed from the periplasmic side. The five methionines that form a triad and a pair in the periplasmic domain are in green sticks.

```
CusA_Escherichia coli K12                MIEWIIRRSVANRFLVLMGALFLSIWGTWTIINTPVDALPDLSDVQVIIKTSYPGQAPQIVENQVTYPLTTTMLSVPGAK 80
Putative_Shigella sonnei                 MIEWIIRRSVANRFLVLMGALFLSIWGTWTIINTPVDALPDLSDVQVIIKTSYPGQAPQIVENQVTYPLTTTMLSVPGAK
CzcA_Shewanella sp. ANA-3                MIEWIIRRSVANRFLVMMGALFLSIWGTWTIINTPVDALPDLSDVQVIIKTSYPGQAPQIVENQVTYPLTTTMLSVPGAK
SilA_Klebsiella pneumoniae               MIEWIIRRSVANRFLVMMGALFLSIWGTWTIINTPVDALPDLSDVQVIIKTSYPGQAPQIVENQVTYPLTTTMLSVPGAK
Putative_Serratia marcescens             MIEWIIRRSVANRFLVMMGALFLSIWGTWTIINTPVDALPDLSDVQVIIKTSYPGQAPQIVENQVTYPLTTTMLSVPGAK
SilA_Salmonella Typhimurium              MIEWIIRRSVANRFLVMMGALFLSIWGTWTIINTPVDALPDLSDVQVIIKTSYPGQAPQIVENQVTYPLTTTMLSVPGAK
CzcA_Erythrobacter sp. NAP1              MIARIIDASIANRFFIVLAAIAVTLAGFWAVRATPVDAIPDLSDVQVVVRSNYPGQAPRIVEDQVTYPLATTMLSVPGAE
CzcA_Sphingopyxis alaskensis RB2256      MIARLIHWSVQNRFFILLGALALVFAGLWAVRTTPIDALPDLSDTQVIIRTSYPGQAPRIVEDQVTYPLTTTMLSVPGAK
CzcA_Caulobacter sp. K31                 MIAAVIRWSLANRFFVLLGALALLAGGLVALRETPLDALPDLSDVQVVIRTPAQGQAPRLVEDQITYPLATTMLSVPGAK
CzcA_Phenylobacterium zucineum HLK1      MIAAIIRASVRARFFVLLAAAALLAAGLWAVRSTPVDALPDLSDVQVVIRTSYPGQAPQIVENQVTYPLTTTMLSVPGAK
CzcA_Asticcacaulis excentricus CB 48     MIAAVIRWSVRNRFFVILATLAIVAGGIFAIKATAVDALPDLSDVQVIIRTPYAGQAPQIVENQVTYPLATTMLSVPGAK
CzcA_Pseudomonas fluorescens Pf0-1       MIAALIRWSVANRFLVLLATLFVTGWGVWSVQNTPIDALPDLSDVQVIIRTPYPGQAPQIVENQVTYPLTTTMLSVPGAK
CzcA_Thiobacillus denitrificans          MIARLIRWSVANRFLVLLATLFTVAWGIWAVKTTPIDALPDLSDVQVIIRTAYPGQAPQIVENQVTYPLATTMLSVPGAK
CzcA_Stenotrophomonas sp. SKA14          MIAKLIRWSVANRFLVLLATAMLTAWGVWGVRSTPVDALPDLSDVQVIIRTNYPGQAPQIVENQVTYPLATTMLSVPGAK
CzcA_ Acidovorax sp. JS42                MIAKLIRWSVANRFLVLLATAMLTAWGVWGVRSTPVDALPDLSDVQVIIRTNYPGQAPQIVENQVTYPLATTMLSVPGAK
CzcA_Leptothrix cholodnii SP-6           MIARLIRWSVANRFLVLLATVLLTAWGVWGLRSTPIDALPDLSDVQVIIRTSYPGQAPQIVENQVTYPLATTMLSVPGAK
CusA_curvibacter                         MIARIIRWSVSNRFLVLLATVFLAGAGLWAVRSTPIDALPDLSDVQVIIRTSYPGQAPQIVENQVTYPLATTMLSVPGAK
CzcA_Ralstonia pickettii 12J             MIARLILASIRNRFLVLLATVMLTAWGLWAARSTPLDALPDLSDVQVIIRTPFPGQAPQIVENQVTYPLTTTMLSVPGAK
SilA_Ralstonia metallidurans CH34        MIASLILASIRNRFLVLLATVMLTAWGLWAVRSTPLDALPDLSDVQVIIRTPFPGQAPQIVENQVTYPLTTTMLSVPGAK
Putative_Methylibium petroleiphilum PM1  MIAELIRWSIVNRFLVLLATVIVTAWGLWAVQRTPLDALPDLSDVQVIIRTPYPGQAPRIVENQVTYPLTTTMLSVPGAK
CzcA_Delftia acidovorans SPH-1           MIAKLIRWSIANRFLVLLATVALSAWGIYAVQRTPLDALPDLSDVQVIIRTTYPGQAPRIVENQVTYPLTTTMLSVPGAK
CzcA_Yersinia kristensenii               ---------MRNRLLVLLGAVMMAAWGVWSLQQTPLDALPDLSDTQVIIRVSYPGKAPQVVEDQVTYPLTTTMLSVPGAK
CusA_Klebsiella pneumoniae               MIEWIIRRSVANRFLVMMGALFLSIWGTWTIVHTPVDALPDLSDVQVIIKTSYPGQAPQIVENQVTWPLTTTMLSVPGAK
CzcA_Polaromonas naphthalenivorans CJ2   MIARFIRWSIVNRFLVLLATLMLGAWGVYSVLRTPLDALPDLSDVQVIIRTSYPGQAPRIVENQVTYPLTTTMLSVPGAK
CusA_Edwardsiella ictaluri               MIEWIIRRAVANRFLVMMGVLFLGIWGAWTVANTPVDALPDLSDVQVIIKTSYPGQAPQLVEDQVTYPLTTTMLSVPGAK
CusA_Enhydrobacter aerosaccus SK60       MIARIIRFSITNRVFVLLAALVLAIWGTWAVKNTPVDALPDLSDVQVIVRTNFPGQAPQIVENQVTYPLTTTMLSVPGVK
CusA_Citrobacter sp. 30-2                MIEWIIRRSVANRFLVMMGALFLSVWGTWTIINTPVDALPDLSDVQVIVKTSYPGQAPQIVENQVTYPLTTTMLSVPGAK
CzcA_Acinetobacter junii SH205           MIARIIRFSILNRVFVLLAALILAAWGVWAVKNTPVDALPDLSDVQVIVRTNYPGQAPQIVENQVTYPLTTTMLSVPGVK
Putative_Pectobacterium  carotovorum     MIAYIIRWSLKNRLLVLLAALFMAAWGLLSLQKTPLDALPDLSDVQVIIRVSYPGKAPQVVENQVTYPLTTTMLSVPGAK
CusA_Providencia rettgeri DSM1131        MLEWIIRRSVANRFLVLMGVVFLVIAGIWSIRSTPVDALPDLSDVQVIIKTTYPGQAPQLVENQVTYPITTTMLSVPGAK
                                                 :  *.:::::..      *      *.:**:*****.**:::    *:**::**:*:*:*::********.:

CusA_Escherichia coli K12                TVRGFSQFGDSYVYVIFEDGTDPYWARSRVLEYLNQVQGKLPAGVSAELGPDATGVGWIYEYALVDR------------ 147
Putative_Shigella sonnei                 TVRGFSQFGDSYVYVIFEDGTDPYWARSRVLEYLNQVQGKLPAGVSAELGPDATGVGWIYEYALVDR------------
CzcA_Shewanella sp. ANA-3                TVRGFSQFGDSYVYVIFEDGTDLYWARSRVLEYLNQVQGKLPAGVSSEIGPDATGVGWIFEYALVDR------------
SilA_Klebsiella pneumoniae               TVRGFSQFGDSYVYVIFEDGTDLYWARSRVLEYLNQVQGKLPAGVSSEIGPDATGVGWIFEYALVDR------------
Putative_Serratia marcescens             TVRGFSQFGDSYVYVIFEDGTDLYWARSRVLEYLNQVQGKLPAGVSSEIGPDATGVGWIFEYALVDR------------
SilA_Salmonella Typhimurium              TVRGFSQFGDSYVYVIFEDGTDLYWARSRVLEYLNQVQGKLPAGVSSEIGPDATGVGWIFEYALVDR------------
CzcA_Erythrobacter sp. NAP1              TVRGYSMFGDSFVYVIFEDGTDLYWARSRVLEYLNQVQNELPEGVTSSLGPDATGVGWIYEYALVDR------------
CzcA_Sphingopyxis alaskensis RB2256      TVRGYSFFGDSFVYVIFEDGTDLYWARSRVLEYLNQVQGRLPETARSAIGPDATGVGWIYEYALVDR------------
CzcA_Caulobacter sp. K31                 TVRGYSFFGDSFVYVLFADGTDPYWARSRVLESLSQVQSRLPAGARPALGPDATGVGWIFEYALVDR------------
CzcA_Phenylobacterium zucineum HLK1      TVRGYSFLGDSFVYVLFEDGTDLYWARSRVLEYLNQVQSRLPEQARSSLGPDATGVGWVFEYALVDR------------
CzcA_Asticcacaulis excentricus CB 48     TVRGYSFFGDSFVYVLFEDGTDLYWARSRVLEYLNQVQGRLPAEAKPSLGPDATGVGWVYEYALVDK------------
CzcA_Pseudomonas fluorescens Pf0-1       TVRGYSFFGDSFVYVLFEDGTDQYWARSRVLEYLSQIQSRLPAGVKPGLGPDATGVGWIYQYALVDR------------
CzcA_Thiobacillus denitrificans          TVRGFSFFGDSFVYVIFEDGTDLYWARSRVLEYLSQVQARLPATARPALGPDATGVSWIYQYALVDR------------
CzcA_Stenotrophomonas sp. SKA14          TVRGFSFFGDSFVYVLFEDGTDLYWARSRVIEYLNQVQGRLPATAKPALGPDATGVGWIFQYALVDR------------
CzcA_ Acidovorax sp. JS42                TVRGFSFFGDSFVYVLFEDGTDLYWARSRVLEYLNQVQGRLPATAKPALGPDATGVGWIYEYALVDR------------
CzcA_Leptothrix cholodnii SP-6           TVRGFSFFGDSFVYVLFDDGTDLYWARSRVLEYLNQVQGRLPASAKTSLGPDATGVGWIFQYALVCRPPGAARQPPEGAS
CusA_curvibacter                         TVRGFSFFGDSFVYILFDDATDLYWARSRVLEYLNQVQGRLPVGAKSALGPDATGVGWIYQYALVDR------------
CzcA_Ralstonia pickettii 12J             TVRGYSFFGDSFVYVLFEDGTDLYWARSRVLEYLNQVQSRLPAAAKPALGPDATGVGWIYEYALVDK------------
SilA_Ralstonia metallidurans CH34        TVRGYSFFGDSYVYVLFEDGTDLYWARSRVLEYLNQVQSRLPAAAKPALGPDATGVGWVYEYALVDK------------
Putative_Methylibium petroleiphilum PM1  VVRGYSFFGDSFVYVLFDDGTDPYWARSRVLEYLNQVQSRLPAAAKPALGPDATGVGWIYQYALVDR------------
CzcA_Delftia acidovorans SPH-1           AVRGYSFFGDSFVYVLFEDGTDPYWARSRVLEYLNQVQSRLPAQAKASLGPDATGVGWIYEYALIDR------------
CzcA_Yersinia kristensenii               TVRGFSMFGDAYVYVLFDDGTDPYWARSRVLEYLSQVQSTLPAEAKAALGPDATGVGWIYEYALIDR------------
CusA_Klebsiella pneumoniae               TVRGFSQFGDSYVYVIFEDGTDPYWARSRVLEYLNQVQGKLPAGVSAEMGPDATGVGWVFEYALVDR------------
CzcA_Polaromonas naphthalenivorans CJ2   TVRGYSFFGDSFVYVLFEDGTDLYWARSRVLEYLNQVQSRLPAQAKASLGPDATGVGWIYQYALVDR------------
CusA_Edwardsiella ictaluri               TVRGFSQFGTSYVYVIFADGTDLYWARSRVLEYLNQVQGKLPAGVSAEIGPDATGVGWIFEYALQDK------------
CusA_Enhydrobacter aerosaccus SK60       TVRGYSFFGDSFVYVIFDEHTDLYWARSRVLEYLNQIQGRIPANAKSSLGPDATGVGWVYEYALVDP------------
CusA_Citrobacter sp. 30-2                TVRGFSQFGDSYVYVIFEDGTDPYWARSRVLEYLNQVQGKLPAGVSAEMGPDATGVGWIFEYALVDR------------
CzcA_Acinetobacter junii SH205           TVRGYSFFGDSFVYVIFDEHTDLYWARSRVLEYLNQIQGKMPANAKSSLGPDATGVGWVYEYALVDP------------
Putative_Pectobacterium  carotovorum     TVRGFSMFGDAYVYVLFEDGTDPYWARSRVLEYLSQVQSSLPADAKTSLGPDATGVGWIYEYALVDR------------
CusA_Providencia rettgeri DSM1131        TVRGFSAFGDSYVYVIFEDNTDLYWARSRVLEYLNQVQNQLPKGAVASIGPDATGVGWIFEYALVDK------------
                                         .***:* :* ::**::* : ** *******:* *.*:*  :*  . . :*******.*:::***

CusA_Escherichia coli K12                SGK--------------HDLADLRSLQDWFLKYELKTIPDVAEVASVGGVVKEYQVVIDPQRLAQYGISLAEVKSALDAS 213
Putative_Shigella sonnei                 SGK--------------HDLADLRSLQDWFLKYELKTIPDVAEVASVGGVVKEYQVVIDPQRLAQYGISLAEVKSALDAS
CzcA_Shewanella sp. ANA-3                SGK--------------HDLSELRSLQDWFLKFELKTIPNVAEVASVGGVVKQYQIQLDPVKLTQYGIGLPEVKQALSSS
SilA_Klebsiella pneumoniae               NGK--------------HDLSELRSLQDWFLKFELKTIPNVAEVASVGGVVKQYQIQVNPVKLSQYGISLPEVKQALESS
Putative_Serratia marcescens             SGK--------------HDLSELRSLQDWFLKFELKTIPNVAEVASVGGVVKQYQIQVNPVKLSQYGISLPEVKQALESS
SilA_Salmonella Typhimurium              SGK--------------HDLSELRSLQDWFLKFELKTIPNVAEVASVGGVVKQYQIQVNPVKLSQYGISLPEVKQALESS
CzcA_Erythrobacter sp. NAP1              TGN--------------SDLAGLRSLQDWFLRYELQTIPGIAEVASVGGMVKQYQVVLEPYRMASLGVTYSDVVRAIQAS
CzcA_Sphingopyxis alaskensis RB2256      TGG--------------HDLSQLRSLQDWFLRYELKTIPGVAEVASVGGMVRQYQVVLDPVRLAAYGVTHAQAVEAIRRA
CzcA_Caulobacter sp. K31                 TGR--------------HDLSQLRSLQDWFVRYELKTLPGVAEVASIGGMVRQYQVVLDPQKLAAYGVTHQAVVEALNRA
CzcA_Phenylobacterium zucineum HLK1      SGR--------------HDLAQLRGLQDWFLRYELKTLPGVAEVASIGGMVKQYQVVLDPVKLAAYGVTHQQVTEALRRA
CzcA_Asticcacaulis excentricus CB 48     TGQ--------------HDLSQLRSLQDWFLRYELKSLPGVAEVASIGGMVKQYQVVLDPMKLAAYGITHQQVVSAIQNA
CzcA_Pseudomonas fluorescens Pf0-1       SGG--------------HDLAQLRALQDWFLKFELKTLPDVAEVATVGGMVKQYQVQPDPVRLASLGITLAQVREAIGKA
CzcA_Thiobacillus denitrificans          TGK--------------HDLAQLRSLQDWFLKYELKTLPNVAEVATVGGMVKQVQVMLDPVKLAGFGVTHDQAIAAIRAA
CzcA_Stenotrophomonas sp. SKA14          TGE--------------NDLAQLRALQDWFLKFELKSLPNVAEVASVGGMVKQYQVVLDPIKLASYGLSQAQVRDALMGA
CzcA_ Acidovorax sp. JS42                TGK--------------NDLAQLRALQDWFLKFELKSLPNVAEVASVGGMVKQYQVVLDPIKLASYGLSQAQVRDALMAA
CzcA_Leptothrix cholodnii SP-6           TGLGAARRPVLSDRGCEQDLSQLRTLQDWFLKYELKSLPDVAEVASVGGMVRQYQVVLDPTKLAAYGITYAQVRDALMAG
```

```
CusA_curvibacter                          TGG--------------HDLSQLRALQDWFLKFELKTLPNVAEVASVGGMVKQYQVVLDPLKLNGYGITYEQVRQALTNG
CzcA_Ralstonia pickettii 12J              TGR--------------HDLAQLRALQDWFLRFELKALPNVAEVASVGGMVKQFQVVLQPDRLRAFNLTQAKVLAALKGA
SilA_Ralstonia metallidurans CH34         SGQ--------------HDLSQLRALQDWFLRFELKSLPNVAEVASLGGMVKQFQIVLLPDRLRAYNLSQGKVLAALKGA
Putative_Methylibium petroleiphilum PM1   SGT--------------MDAGQLRALQDWFLKYELKTVPNVAEVASVGGMVRQYQVLLDPDKLAAYNVPHGAVIDAIRNA
CzcA_Delftia acidovorans SPH-1            SGK--------------MDISQLRALQDWFLKYELKTVPDVAEVASVGGMVRQYQIVLDPDKLAAYGIPHTKVVEAIQRA
CzcA_Yersinia kristensenii                TGK--------------HSLADLRALQDWTLKFELKTVPNVSEVASVGGMVRQYQVVLDPERMRALNLSHQQIASAIADS
CusA_Klebsiella pneumoniae                SGK--------------HDLAELRSLQDWFLKYELKTIPNVSEVASVGGVVKEYQIVVDPMKLTQYGISLGEVKSALDAS
CzcA_Polaromonas naphthalenivorans CJ2    SGT--------------QDLGQLRALQDWFLKYELKTVPNVAEVASIGGMVRQYQIVLDPQKLAAYAIPHTKVAEAVQKA
CusA_Edwardsiella ictaluri                SGQ--------------HDLAELRSLQDWFLKYELKTIPNVAEVAAVGGVVKQYQIQVDPLKLAQYGISLAEVKRAIGAA
CusA_Enhydrobacter aerosaccus SK60        TGQ--------------HDLAQLRSIQDWFLKYELKTLPNVAEVATIGGMVKQYQVVLDPSKMAALGVTQNNVIEAIQKA
CusA_Citrobacter sp. 30-2                 SGK--------------HDLAELRSLQDWFLKYELKTIPNVAEVASVGGVVKQYQVVIDPMKLTQYGISLADVKSALDTS
CzcA_Acinetobacter junii SH205            TGQ--------------HDLSQLRSIQDWFLKYELKTLPNVAEVATIGGMVKQYQVVLDPSKMAALGVTQNNVIEAIQKA
Putative_Pectobacterium  carotovorum      SGK--------------YSLADLRGFQDWLLKYELKTVPDVAEVASVGGMVKQYQIVVDPERMRTLGITHQQIVSAVKAA
CusA_Providencia rettgeri DSM1131         TGK--------------HNLAELRSLQDWFLKYELKALPNVSEVATVGGVVKSYQILVDPLKLSQFSVTLPEIKQAVEMA
                                          .*                . . ** :*** :::**:::*.::***::**:*:. *:   * ::    :       *:  .

CusA_Escherichia coli K12                 NQEAGGSSIELAEAEYMVRASGYLQTLDDFNHIVLKASENGVPVYLRDVAKVQIGPEMRRGIAELNGEGEVAGGVVILRS 293
Putative_Shigella sonnei                  NQEAGGSSIELAEAEYMVRASGYLQTLDDFNHIVLKARENGVPVYLRDVAKVQIGPEMRRGIAELNGEGEVAGGVVILRS
CzcA_Shewanella sp. ANA-3                 NQEAGGSSVEIAESEYMVRASGYLQTIDDFKNIVLKTGENGVPVYLRDVARIQMGPEMRRGIAELNGQGEVAGGVVILRS
SilA_Klebsiella pneumoniae                NQEAGGSSVEMAEAEYMVRASGYLQSIDDFNNIVLKTGENGVPVYLRDVARVQTGPEMRRGIAELNGQGEVAGGVVILRS
Putative_Serratia marcescens              NQEAGGSSVEMAEAEYMVRASGYLQSIDDFNNIVLKTGENGVPVYLRDVARVQTGPEMRRGIAELNGQGEVAGGVVILRS
SilA_Salmonella Typhimurium               NQEAGGSSVEIAEAEYMVRASGYLQSIDDFNNIVLKTGENGVPVYLRDVARVQTGPEMRRGIAELNGQGEVAGGVVILRS
CzcA_Erythrobacter sp. NAP1               NQEAGGSVVEMGEAEFMVRASGYLTSLNDFRQIPLKSVGNGIPVTLSDVATIQLGPEMRRGIAELNGEGEVAGGIVVLRQ
CzcA_Sphingopyxis alaskensis RB2256       NQEAGGSVLELAEAEYMVRASGYLRSLADFRAIPLRTASGGIPVTLGDVATIQLGPEMRRGIADLNGEGEVAGGIIVLRQ
CzcA_Caulobacter sp. K31                  NQEAGGSVVEMAEAEYMVRASGYLSSLDDFAAVPVKTAAGGVPIALGQVATIQIGPEMRRGVAELNGQGEVTGGVVVLRS
CzcA_Phenylobacterium zucineum HLK1       NQEAGGSVLELGEAEYMVRASGYLKTLEDFEAVPLRTAAGGVPVRLGDVAFVQLGPEMRRGVAELNGEGEVAGGVVILRS
CzcA_Asticcacaulis excentricus CB 48      NGESGGSVLELAEAEYMVRAGGYLKTLDDFRAIPLKTAAGGVPVTLGEVATVQIGPEMRRGVAELNGQGEVAGGVVILRS
CzcA_Pseudomonas fluorescens Pf0-1        NQETGGAVLEMAETEFIVRASGYLKTLDDFRAIPLKLGAGGVPVTLGDVATVQTGPDMRRGITELDGQGETVGGVVILRS
CzcA_Thiobacillus denitrificans           NQETGGAVLELAETELMVRASGYLESVADFRAIPLKL-AGTTPVSLGDVAHIQLGPEMRRGIGELDGEGEAVGGVVVLRS
CzcA_Stenotrophomonas sp. SKA14           NQETGGSVLELSGAEYMVRASGYLKTLDEFREIPLTA-RGGVPVRLGDVATLQIGPEMRRGIAELDGEGEVAGGVVVLRS
CzcA_ Acidovorax sp. JS42                 NQETGGSVLELSGAEYMVRASGYLKTLDEFREIPLTA-RGGVPVRLGDVAMLQIGPEMRRGIAELDGEGEVAGGVVVLRS
CzcA_Leptothrix cholodnii SP-6            NQETGGSVLELAEVEYMVRASGYLRSLDDFRTIPLAA-RGGIPVKLGDVATVQIGPEMRRGIAELDGEGEVAGGVVILRS
CusA_curvibacter                          NQETGGSVLELAEAEYMVRVNGYLRTLEDFRAIPLSS-RGGTAVRLGDVATVQVGPEMRRGVAELDGQGEVAGGVVLLRS
CzcA_Ralstonia pickettii 12J              NQETGGSVLELGEAEYMVRASGYLKTLDDFRQIPLMTNDAGIAVHLGDVATVQLGPEMRRGIAELNGQGEVAGGVVILRS
SilA_Ralstonia metallidurans CH34         NQETGGSVLELGEAEYMVRATGYLKTLDDFRQVPIVTSDAGIPVRLGDVAVIQLGPEMRRGIAELNGQGEVAGGVIILRS
Putative_Methylibium petroleiphilum PM1   NQEAGGSVLELGEAEYVVRASGLLATLDDFRKIPLSATDAGVSVRLGDVARIQVGPEMRRGIGELDGEGEATGGVIVMRS
CzcA_Delftia acidovorans SPH-1            NQETGGSVLELGEAEYMVRASGYLGSLEDFRKVPLMTTAAGVSVRLGDVARVQIGPEMRRGIGELNGEGEAVGGVIVMRS
CzcA_Yersinia kristensenii                NQEGGGSVLEMGAAEYMVRASGYLKTLDDFRNIVITV-REGIPILLSDVATVRIGPEMRRGVAELNGEGEVAGGIIVMRY
CusA_Klebsiella pneumoniae                NQEAGGSSVELAEAEYMVRASGYLQTLDDFKNIVLKTGDNGVPVYLGDVARVQIGPEMRRGIAELNGEGEVAGGVVILRS
CzcA_Polaromonas naphthalenivorans CJ2    NQEAGGSVLELGEAEYMVRATGYLKGLEDFRAIPLTTTAGGVSVRLGDVARIQIGPEMRRGIGELDGEGEAVGGVIIMRS
CusA_Edwardsiella ictaluri                NQEAGGASLELAEAEYMVRASGYLRTLDDFNHIVLKSGQDGVPITLQDVARLQIGPEMRRGIAELNGEGEVAGGVVILRS
CusA_Enhydrobacter aerosaccus SK60        NQETGGSVLEMAETEYMVRASGYLKTLDDFRQIPLRTNSLGVPVSLGDVATIQLGPEMRRGITELNGQGETVGGVVILRA
CusA_Citrobacter sp. 30-2                 NQEAGGSSVEMAEAEYMVRASGYLQTLDDFNNIVLKTGADGVPVYLRDVARVQIGPEMRRGIAELNGEGEVAGGVVILRS
CzcA_Acinetobacter junii SH205            NQETGGSVLEMAETEYMVRASGYLKTLEDFRQIPIKTNSFGIPVTLGDVATIQLGPEMRRGITELNGQGETVGGVVILRA
Putative_Pectobacterium  carotovorum      NQENGGSVLELGEAEYMVRTTGYLKSMQDFNHVVITTRN-GIPVLLQDVATLREGPEMRRGIAELNGEGEVAGGIIVLRY
CusA_Providencia rettgeri DSM1131         NQEAGGSSIEIAEAEYMVRASGYLQSIDDFNKIYLKTPENGVPIYLQDVARIQEGPEMRRGVAELNGEGEVVGGVILLRS
                                          * * **: :*:.  * :**. * *  : :*  : :       .: * :** :: **:****: :*:*:**..**::::*

CusA_Escherichia coli K12                 GKNAREVIAAVKDKLETLKSSLPEGVEIVTTYDRSQLIDRAIDNLSGKLLEEFIVVAVVCALFLWHVRSALVAIISLPLG 373
Putative_Shigella sonnei                  GKNAREVIASVKDKLETLKSSLPEGVEIVTTYDRSQLIDRAIDNLSGKLLEEFIVVAVVCALFLWHVRSALVAIISLPLG
CzcA_Shewanella sp. ANA-3                 GKNAREVITAVRDKLDTLKASLPEGVEIVTTYDRSQLIDRAIDNLSYKLLEEFIVVAVVCALFLWHVRSALVAIISLPLG
SilA_Klebsiella pneumoniae                GKNARDVITAVRDKLETLKASLPEGVEIVTTYDRSQLIDRAIDNLSYKLLEEFIVVAVVCALFLWHVRSALVAIISLPLG
Putative_Serratia marcescens              GKNARDVITAVRDKLETLKASLPEGVEIVTTYDRSQLIDRAIDNLSSKLLEEFIVVAIVCALFLWHVRSALVAIISLPLG
SilA_Salmonella Typhimurium               GKNARDVITAVRDKLETLKASLPEGVEIVTTYDRSQLIDRAIDNLSSKLLEEFFVVAIVCALFLWHVRSALVAIISLPLG
CzcA_Erythrobacter sp. NAP1               GEDARATIAAVEEKLDVLQASLPEGVEIVTTYDRSKLIDASIENLTGKLIAEFIIVAIVCALFLWHVRSALVAIVTLPLG
CzcA_Sphingopyxis alaskensis RB2256       GADARSAIMAVEAKLAELKKGLPKGVEVVTTYDRSQLIDHAVENLTHKLIEEFIVVALVCALFLWHVRSALVAIVTLPLG
CzcA_Caulobacter sp. K31                  GEDARATLKAVQDKLKTLKASLPPGVEIVTTYDRSGLIDRAIDNLKSKLIEEFIVVALVCALFLWHLRSALVAIIALPLG
CzcA_Phenylobacterium zucineum HLK1       GKNARETIQAVRGKLEELKRSLPPGVEVVTTYDRSQLIDRAIANLSQKLLEEFVVVAIVCGLFLWHARSALVAILTLPLG
CzcA_Asticcacaulis excentricus CB 48      GKNAMETISAVKAKLAELKKSLPPGVEVVTTYDRSQLIGRAIGNLREKLIEEFLVVAIVCALFLWHVRSALVAILTLPIG
CzcA_Pseudomonas fluorescens Pf0-1        GKNARETIAAVKAKLDDMKSSLPPGVEIVTTYDRSKLIDRAVENLSHKLLEEFIVVALVCGIFLWHLRSSLVAIISLPVG
CzcA_Thiobacillus denitrificans           GKNARETIAAVKAKLDTLKVSLPAGVEIVPTYDRSQLIDRAIDNLSDKLVEEFIVVALVCALFLWHLRSSLVAIVSLPLG
CzcA_Stenotrophomonas sp. SKA14           GKNAQETIAAVKAKLAELQGSLPPGVEIVTTYDRSALIERAIRNLTTKLGEEFLVVALVCALFLWHLRSALVAIISLPLG
CzcA_ Acidovorax sp. JS42                 GKNAQETIAAVKAKLAELQGSLPPGVEIVTTYDRSALIERAIRNLTTKLGEEFLVVALVCALFLWHLRSALVAIISLPLG
CzcA_Leptothrix cholodnii SP-6            GKNAQSTITAVKAKLAELQKSLPAGVEIVTTYDRSALIERAIENLTHKLIEEFIVVAAVCALFLWHLRSALVAIIALPLG
CusA_curvibacter                          GKNAQETIRAVKTKLAELQKSLPPGVEVVTTYDRSALIARAIDNLSAKLLEEFVVVALVCVLFLGHLRSALVAIISLPLG
CzcA_Ralstonia pickettii 12J              GKNALETIEAVKAKLATLRTSLPEGVEIVPVYDRSGLIKRAVDNLTHKLIEEFIVVAVVCLVFLFHLRSALVAIVSLPLG
SilA_Ralstonia metallidurans CH34         GKNALETINAVKAKLQTLQKSLPDGVEVVTVYDRSALISRAVDNLTTKLLEEFAVVAVVCLLFLFHLRSALVAIVSLPLG
Putative_Methylibium petroleiphilum PM1   GKNALETIAAVKTKIASLQASLPKGVEIVPTYDRSSLIERAVENLSHKLIEEFIVVALVCVVFLFHLRSAFVAIVTLPLG
CzcA_Delftia acidovorans SPH-1            GKNALQTIAAVKGKLQGLASSLPRGVEIVPVYDRSGLIERAVENLTHKLIEEFIVVAVVCFLFLFHLRSALVAIISLPLG
CzcA_Yersinia kristensenii                GKNALETINGVKEKLQQIQRSLPAGVEIVPVYDRSHLITQAIDSLSFKLLEEFLVVAVICSLFLFHFRSALVAIITLPLG
CusA_Klebsiella pneumoniae                GKNAREVISAVKAKLASLQSSLPEGVEVVTTYDRSQLIDRAIDNLSHKLLEEFIVVALVCALFLWHVRSALVAIISLPLG
CzcA_Polaromonas naphthalenivorans CJ2    GKNALETIAAVKAKMAQLQASLPQGVEVVTTYDRSGLINRAVDNLTYKLLEEFLVVAVVCFVFLFHLRSALVAIISLPLG
CusA_Edwardsiella ictaluri                GENARQVITAVKAKLAALQGSLPPGVEVVTTYDRSQLIDRAIDNLSTKLIEEFIVVALVCALFLWHVRSALVAIVSLPLG
CusA_Enhydrobacter aerosaccus SK60        GKNARETITAVKAKLAELQQSLPKGVQVVPVYDRSKLIDRAVENLSHKLIEEFIVVALVCVLFLWHLRSAMVAIVSLPLG
CusA_Citrobacter sp. 30-2                 GKNAREVISAVKAKLDTLKSSLPEGVEVVTTYDRSQLIDRAIDNLSYKLLEEFIVVALVCALFLWHLRSALVAIISLPLG
CzcA_Acinetobacter junii SH205            GKNARETITAVKAKLAELQQSLPKGVQVVPVYDRSKLIDRAVENLSHKLIEEFIVVALVCGLFLWHLRSAMVAIVSLPLG
Putative_Pectobacterium  carotovorum      GKNALNTLHAVKARLQEIQKSLPAGVEIVPTYDRSQLIEHAIDTLSFKLLEEFVVVAIICALFLFHFRSALVAIISLPLG
CusA_Providencia rettgeri DSM1131         GENARNVIQDVKQKLEDLSASLPEGIEIITTYDRSILIDNAIDNLSYKLLEEFIVVALVCAVFLWHFRSALVAIISLPLG
                                          * :*  .:  *. ::  :  .** *::::..**** **  :: .*  **  ** :** :* :** * **::***::**:*
```

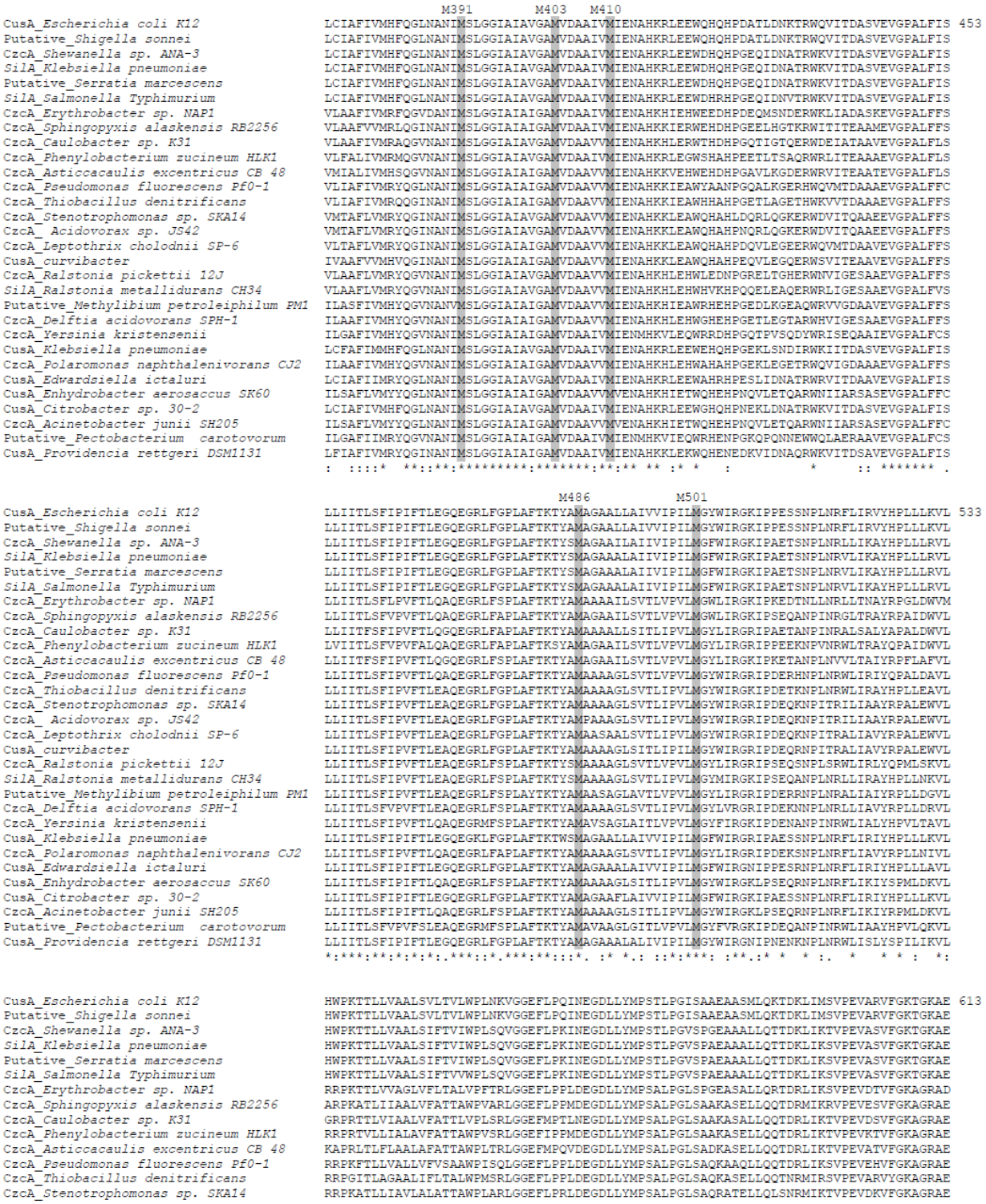
M391
M403
M410
CusA_Escherichia coli K12 LCIAFIVMHFQGLNANIMSLGGIAIAVGAMVDAAIVMIENAHKRLEEWQHQHPDATLDNKTRWQVITDASVEVGPALFIS 453
Putative_Shigella sonnei LCIAFIVMHFQGLNANIMSLGGIAIAVGAMVDAAIVMIENAHKRLEEWQHQHPDATLDNKTRWQVITDASVEVGPALFIS
CzcA_Shewanella sp. ANA-3 LCIAFIVMHFQGLNANIMSLGGIAIAVGAMVDAAIVMIENAHKRLEEWDHQHPGEQIDNATRWKVITDASVEVGPALFIS
SilA_Klebsiella pneumoniae LCIAFIVMHFQGLNANIMSLGGIAIAVGAMVDAAIVMIENAHKRLEEWDHQHPGEQIDNATRWKVITDASVEVGPALFIS
Putative_Serratia marcescens LCIAFIVMHFQGLNANIMSLGGIAIAVGAMVDAAIVMIENAHKRLEEWDHQHPGEQIDNATRWKVITDASVEVGPALFIS
SilA_Salmonella Typhimurium LCIAFIVMHFQGLNANIMSLGGIAIAVGAMVDAAIVMIENAHKRLEEWDHRHPGEQIDNVTRWKVITDASVEVGPALFIS
CzcA_Erythrobacter sp. NAP1 VLAAFIVMRFQGVDANIMSLGGIAIAIGAMVDAAIVMIENAHKHIEHWEEDHPDEQMSNDERWKLIADASKEVGPALFFS
CzcA_Sphingopyxis alaskensis RB2256 VLAAFVVMRLQGINANIMSLGGIAIAIGAMVDAAIVMIENAHKKIERWEHDHPGEELHGTKRWITITEAAMEVGPALFFS
CzcA_Caulobacter sp. K31 VLAAFIVMRAQGVNANIMSLGGIAIAVGAMVDAAVVMIENAHKHLERWTHDHPGQTIGTQERWDEIATAAVEVGPALFLS
CzcA_Phenylobacterium zucineum HLK1 VLFALIVMRMQGVNANIMSLGGIAIAVGAMVDAAIVMIENAHKRLEGWSHAHPEETLTSAQRWRLITEAAAEVGPALFLS
CzcA_Asticcacaulis excentricus CB 48 VMIALIVMHSQGVNANIMSLGGIAIAIGAMVDAAVVMIENAHKKVEHWEHDHPGAVLKGDERWRVITEAATEVGPALFLS
CzcA_Pseudomonas fluorescens Pf0-1 VLIAFIVMRYQGLNANIMSLGGIAIAIGAMVDAAVVMIENAHKKIEAWYAANPGQALKGERHWQVMTDAAAEVGPALFFC
CzcA_Thiobacillus denitrificans VLIAFIVMRQQGINANIMSLGGIAIAIGAMVDAAVVMIENAHKKIEAWHHAHPGETLAGETHWKVVTDAAAEVGPALFFS
CzcA_Stenotrophomonas sp. SKA14 VMTAFLVMRYQGINANIMSLGGIAIAVGAMVDAAVVMIENAHKKLEAWQHAHLDQRLQGKERWDVITQAAEEVGPALFFS
CzcA_ Acidovorax sp. JS42 VMTAFLVMRYQGINANIMSLGGIAIAVGAMVDAAVVMIENAHKKLEAWQHAHPNQRLQGKERWDVITQAAEEVGPALFFS
CzcA_Leptothrix cholodnii SP-6 VLTAFLVMRYQGINANIMSLGGIAIAIGAMVDAAVVMIENAHKKLEAWQHAHPDQVLEGEERWQVMTDAAVEVGPALFFS
CusA_curvibacter IVAAFVVMHVQGINANIMSLGGIAIAIGAMVDAAVVMIENAHKKLEAWQHAHPEQVLEGQERWSVITEAAVEVGPALFFS
CzcA_Ralstonia pickettii 12J VLAAFLVMRYQGVNANIMSLGGIAIAVGAMVDAAVVMIENAHKHLEHWLEDNPGRELTGHERWNVIGESAAEVGPALFFS
SilA_Ralstonia metallidurans CH34 VLAAFLVMRYQGVNANIMSLGGIAIAVGAMVDAAVVMIENAHKHLEHWHVKHPQQELEAQERWRLIGESAAEVGPALFVS
Putative_Methylibium petroleiphilum PM1 ILASFIVMHYQGVNANVMSLGGIAIAIGAMVDAAVVMIENAHKHIEAWRHEHPGEDLKGEAQWRVVGDAAEVGPALFFS
CzcA_Delftia acidovorans SPH-1 ILAAFIVMHYQGVNANIMSLGGIAIAIGAMVDAAVVMIENAHKHLEHWGHEHPGETLEGTARWHVIGESAAEVGPALFFS
CzcA_Yersinia kristensenii ILGAFIVMHYQGVNANIMSLGGIAIAIGAMVDAAIVMIENMHKVLEQWRRDHPGQTPVSQDYWRISEQAAIEVGPALFCS
CusA_Klebsiella pneumoniae LCFAFIMMHFQGLNANIMSLGGIAIAVGAMVDAAIVMIENAHKRLEEWEHQHPGEKLSNDIRWKIITDASVEVGPALFIS
CzcA_Polaromonas naphthalenivorans CJ2 ILAAFIVMHYQGVNANIMSLGGIAIAIGAMVDAAVVMIENAHKHLEHWAHAHPGEKLEGETRWQVIGDAAAEVGPALFFS
CusA_Edwardsiella ictaluri LCIAFIIMRYQGLNANIMSLGGIAIAVGAMVDAAIVMIENAHKRLEEWAHRHPESLIDNATRWRVITDAAVEVGPALFIS
CusA_Enhydrobacter aerosaccus SK60 ILSAFLVMYYQGLNANIMSLGGIAIAIGAMVDAAVVMVENAHKHIETWQHEHPNQVLETQARWNIIARSASEVGPALFFC
CusA_Citrobacter sp. 30-2 LCIAFIVMHFQGLNANIMSLGGIAIAVGAMVDAAIVMIENAHKRLEEWGHQHPNEKLDNATRWKVITDASVEVGPALFIS
CzcA_Acinetobacter junii SH205 ILSAFLVMYYQGLNANIMSLGGIAIAIGAMVDAAVVMVENAHKHIETWQHEHPNQVLETQARWNIIARSASEVGPALFFC
Putative_Pectobacterium carotovorum ILGAFIIMRYQGVNANIMSLGGIAIAIGAMVDAAIVMIENMHKVIEQWRHENPGKQPQNNEWWQLAERAAVEVGPALFCS
CusA_Providencia rettgeri DSM1131 LFIAFIVMRYQGINANIMSLGGIAIAIGAMVDAAIVMIENAHKKLEKWQHENEDKVIDNAQRWKVITDSAVEVGPALFIS
: ::::* **::**:*********:*******:**:** ** :* * : * :: ******* .
M486
M501
CusA_Escherichia coli K12 LLIITLSFIPIFTLEGQEGRLFGPLAFTKTYAMAGAALLAIVVIPILMGYWIRGKIPPESSNPLNRFLIRVYHPLLLKVL 533
Putative_Shigella sonnei LLIITLSFIPIFTLEGQEGRLFGPLAFTKTYAMAGAALLAIVVIPILMGYWIRGKIPPESSNPLNRFLIRVYHPLLLKVL
CzcA_Shewanella sp. ANA-3 LLIITLSFIPIFTLEGQEGRLFGPLAFTKTYSMAGAAILAIIVIPILMGFWIRGKIPAETSNPLNRLLIKAYHPLLLRVL
SilA_Klebsiella pneumoniae LLIITLSFIPIFTLEGQEGRLFGPLAFTKTYSMAGAAALAIIVIPILMGFWIRGKIPAETSNPLNRVLIKAYHPLLLRVL
Putative_Serratia marcescens LLIITLSFIPIFTLEGQEGRLFGPLAFTKTYSMAGAAALAIIVIPILMGFWIRGKIPAETSNPLNRVLIKAYHPLLLRVL
SilA_Salmonella Typhimurium LLIITLSFIPIFTLEGQEGRLFGPLAFTKTYSMAGAAALAIIVIPILMGFWIRGKIPAETSNPLNRVLIKAYHPLLLRVL
CzcA_Erythrobacter sp. NAP1 LLIITLSFLPVFTLQAQEGRLFSPLAFTKTYAMAAAAILSVTLVPVLMGWLIRGKIPKEDTNLLNRLLTNAYRPGLDWVM
CzcA_Sphingopyxis alaskensis RB2256 LLIITLSFVPVFTLQAQEGRLFAPLAFTKTYAMAGAAILSVTLVPVLMGWLIRGKIPSEQANPINRGLTRAYRPAIDWVL
CzcA_Caulobacter sp. K31 LLIITFSFIPVFTLQGQEGRLFAPLAFTKTYAMAAAALLSITLIPVLMGYLIRGRIPAETANPINRALSALYAPALDWVL
CzcA_Phenylobacterium zucineum HLK1 LVIITLSFVPVFALQAQEGRLFAPLAFTKSYAMAGAAILSVTLVPVLMGYLIRGRIPPEEKNPVNRWLTRAYQPAIDWVL
CzcA_Asticcacaulis excentricus CB 48 LLIITFSFIPVFTLQGQEGRLFSPLAFTKTYAMAGAAILSVTLVPVLMGYLIRGKIPKETANPLNVVLTAIYRPFLAFVL
CzcA_Pseudomonas fluorescens Pf0-1 LLIITLSFIPVFTLQAQEGRLFGPLAFTKTYAMAAAAGLSVTLVPVLMGYWIRGRIPDERHNPLNRWLIRIYQPALDAVL
CzcA_Thiobacillus denitrificans LLIITLSFIPVFTLEAQEGRLFGPLAFTKTYAMAAAAGLSVTLIPVLMGYWIRGKIPDETKNPLNRWLIRAYHPLLEAVL
CzcA_Stenotrophomonas sp. SKA14 LLIITLSFIPVFTLEAQEGRLFGPLAFTKTYAMAAAAGLSVTLIPVLMGYWIRGRIPDEQKNPITRILIAAYRPALEWVL
CzcA_ Acidovorax sp. JS42 LLIITLSFIPVFTLEAQEGRLFGPLAFTKTYAMPAAAGLSVTLIPVLMGYWIRGRIPDEQKNPITRILIAAYRPALEWVL
CzcA_Leptothrix cholodnii SP-6 LLIITLSFIPVFTLEAQEGRLFGPLAFTKTYAMAASAALSVTLIPVLMGYWIRGRIPDEQKNPITRALIAVYRPALEWVL
CusA_curvibacter LLIITLSFIPVFTLEAQEGRLFGPLAFTKTYAMAAAAGLSITLIPILMGYWIRGRIPDEQRNPITRALIAVYRPALEWVL
CzcA_Ralstonia pickettii 12J LLIITLSFIPVFTLEAQEGRLFSPLAFTKTYSMAAAAGLSVTLVPVLMGYLIRGRIPSEQSNPLSRWLIRLYQPMLSKVL
SilA_Ralstonia metallidurans CH34 LLIITLSFIPVFTLEAQEGRLFSPLAFTKTYSMAAAAGLSVTLIPVLMGYMIRGKIPSEQANPLNRLLIRAYHPLLNKVL
Putative_Methylibium petroleiphilum PM1 LLIITLSFIPVFTLEAQEGRLFSPLAYTKTYAMAASAGLAVTLVPVLMGYLIRGRIPDERRNPLNRALIAIYRPLLDGVL
CzcA_Delftia acidovorans SPH-1 LLIITLSFVPVFTLEAQEGRLFSPLAFTKTYAMAAAAGLSVTLIPVLMGYLVRGRIPDEKNNPLNRLLIAVYRPLLDRVL
CzcA_Yersinia kristensenii LLIITLSFIPVFTLQAQEGRMFSPLAFTKTYAMAVSAGLAITLVPVLMGYFIRGKIPDENANPINRWLIALYHPVLTAVL
CusA_Klebsiella pneumoniae LLIITLSFIPIFTLEGQEGKLFGPLAFTKTWSMAGAALLAIVVIPILMGFWIRGRIPAESSNPLNRFLIRIYHPLLLKVL
CzcA_Polaromonas naphthalenivorans CJ2 LLIITLSFIPVFTLQAQEGRLFAPLAFTKTYAMAAAAGLSVTLIPVLMGYLIRGRIPDEKSNPLNRFLIAVYRPLLNIVL
CusA_Edwardsiella ictaluri LLIITLSFIPIFTLEGQEGRLFGPLAFTKTYAMAGAAALAIVVIPILMGFWIRGNIPPESRNPLNRFLIRIYHPLLLAVL
CusA_Enhydrobacter aerosaccus SK60 LLIITLSFIPIFTLQAQEGRLFSPLAFTKTYAMAAAAGLSITLIPVLMGYWIRGKLPSEQRNPLNRFLIKIYSPMLDKVL
CusA_Citrobacter sp. 30-2 LLIITLSFIPIFTLEGQEGRLFGPLAFTKTYAMAGAAFLAIVVIPILMGFWIRGKIPAESSNPLNRFLIRIYHPLLLKVL
CzcA_Acinetobacter junii SH205 LLIITLSFIPIFTLQAQEGRLFSPLAFTKTYAMAAAAGLSITLIPVLMGYWIRGKLPSEQRNPLNRFLIKIYRPMLDKVL
Putative_Pectobacterium carotovorum LLIITLSFVPVFSLEAQEGRMFSPLAFTKTYAMAVAAGLGITLVPVLMGYFVRGKLPDEQANPINRWLIAAYHPVLQKVL
CusA_Providencia rettgeri DSM1131 LLIITLSFIPIFTLEGQEGRLFGPLAFTKTYAMAGAAALALIVIPILMGYWIRGNIPNENKNPLNRWLISLYSPILIKVL
*:***:**:*:*:*:.***::*.***:**:::*. :* *.: ::*:***: :**.:* * * :. * * * : *:
CusA_Escherichia coli K12 HWPKTTLLVAALSVLTVLWPLNKVGGEFLPQINEGDLLYMPSTLPGISAAEAASMLQKTDKLIMSVPEVARVFGKTGKAE 613
Putative_Shigella sonnei HWPKTTLLVAALSVLTVLWPLNKVGGEFLPQINEGDLLYMPSTLPGISAAEAASMLQKTDKLIMSVPEVARVFGKTGKAE
CzcA_Shewanella sp. ANA-3 HWPKTTLLVAALSIFTVIWPLSQVGGEFLPKINEGDLLYMPSTLPGVSPGEAAALLQTTDKLIKTVPEVASVFGKTGKAE
SilA_Klebsiella pneumoniae HWPKTTLLVAALSIFTVIWPLSQVGGEFLPKINEGDLLYMPSTLPGVSPAEAAALLQTTDKLIKSVPEVASVFGKTGKAE
Putative_Serratia marcescens HWPKTTLLVAALSIFTVIWPLSQVGGEFLPKINEGDLLYMPSTLPGVSPAEAAALLQTTDKLIKSVPEVASVFGKTGKAE
SilA_Salmonella Typhimurium HWPKTTLLVAALSIFTVVWPLSQVGGEFLPKINEGDLLYMPSTLPGVSPAEAAALLQTTDKLIKSVPEVASVFGKTGKAE
CzcA_Erythrobacter sp. NAP1 RRPKTTLVVAGLVFLTALVPFTRLGGEFLPPLDEGDLLYMPSALPGLSPGEASALLQRTDRLIKSVPEVDTVFGKAGRAD
CzcA_Sphingopyxis alaskensis RB2256 ARPKATLIIAALVFATTAWPVARLGGEFLPPMDEGDLLYMPSALPGLSAAKASELLQQTDRMIKRVPEVESVFGKAGRAE
CzcA_Caulobacter sp. K31 GRPRTTLVIAALVFATTLVPLSRLGGEFMPTLNEGDLLYMPSALPGLSAAKASALLQQTDRLIKTVPEVDSVFGKAGRAE
CzcA_Phenylobacterium zucineum HLK1 RRPRTVLLIALAVFATTAWPVSRLGGEFIPPMDEGDLLYMPSALPGLSAAKASELLQQTDRLIKTVPEVKTVFGKAGRAE
CzcA_Asticcacaulis excentricus CB 48 KAPRLTLFLAALAFATTAWPLTRLGGEFMPQVDEGDLLYMPSALPGLSADKASELLQQTDRLIKTVPEVATVFGKAGRAE
CzcA_Pseudomonas fluorescens Pf0-1 RRPKFTLLVALLVFVSAAWPISQLGGEFLPPLDEGDLLYMPSALPGLSAQKAAQLLQQTDRLIKSVPEVEHVFGKAGRAE
CzcA_Thiobacillus denitrificans RRPGITLAGAALIFLTALWPMSRLGGEFLPPLDEGDLLYMPSALPGLSAQKASELLQQTNRMIRSVPEVARVYGKAGRAE
CzcA_Stenotrophomonas sp. SKA14 RRPKATLLIAVLALATTAWPLARLGGEFLPRLDEGDLLYMPSALPGLSAQRATELLQLSNRMIKTVPEVDKVFGKAGRAE

```
CzcA_ Acidovorax sp. JS42                RRPKATLLIAVLALATTAWPLARLGGEFLPRLDEGDLLYMPSALPGLSAQRATELLQLSNRMIKTVPEVDKVFGKAGRAE
CzcA_Leptothrix cholodnii SP-6           RWPKATLAAALLVLATTAWPLMQLGGEFLPKLDEGDLLYMPSALPGLSAQKAGELLQLTNRMIKTVPEVERVFGKAGRAE
CusA_curvibacter                         LRPKSTLAIAVLAFATTLWPVSQLGGEFLPPLDEGDLLYMPSALPGLSAQKASELLQITNRMIRTVPEVERVFGKAGRAE
CzcA_Ralstonia pickettii 12J             AYPKATVAIAIVLLGATAWPILRTGGEFMPPLDEGDLLYMPSALPGLSAGKAAQLLQQTDRLIKTVPEVASVYGKAGRAD
SilA_Ralstonia metallidurans CH34        RYPKTTVALAGVLLVATAWPIMRTGGEFMPPLDEGDLLYMPSALPGLAAGKASQLLQQTDRLIKTVPEVASVFGKAGRAD
Putative_Methylibium petroleiphilum PM1  AWPKATIAVALLLLASTAWPILKIGGEFMPPLDEGDLLYMPTALPGLSAGKAAELLQQTDRLIKTLPEVQSVYGKAGRAE
CzcA_Delftia acidovorans SPH-1           RAPKLTLVVALVVLATSLWPLRHIGGEFMPRLDEGDLLYMPSALPGLSAGKAAELLQQTDRLIKTVPEVASVYGKAGRAE
CzcA_Yersinia kristensenii               ARPKTTLAIAGMLLLATLYPLSRLGSEFMPALDEGDLLYMPSTLPGISVREASHLLQQTDRLIKTVPEVDTVFGKAGRAE
CusA_Klebsiella pneumoniae               HWPKTTLLIALLSILTVAWPLNRVGGEFLPQINEGDLLYMPSTLPGISAAQAADMLQKTDKLIMTVPEVARVFGKTGKAE
CzcA_Polaromonas naphthalenivorans CJ2   RAPKMTLVVAGIVLATSLWPLQHIGGEFMPRLDEGDLLYMPSALPGLSSGKAGELLQQTDRLIKTVPEVASVYGKAGRAE
CusA_Edwardsiella ictaluri               RWPRMTLLVAAFSIVTVIWPLERLGGEFLPNINEGDLLYMPSTLPGISPAQAAQLLQTTDKLIRQVPEVASVFGKSGKAE
CusA_Enhydrobacter aerosaccus SK60       AHPKTIILGALLIFLISLFPLTRLGGEFLPNMDEGDLLYMPSALPGLSAAKASELLQQTDRMIKTVPEVATVFGKAGRAE
CusA_Citrobacter sp. 30-2                HWPKTTILVAVLSILTVVYPLNKVGGEFLPQINEGDLLYMPSTLPGISAAQAADMLQKTDKLIMTVPEVARVFGKTGKAE
CzcA_Acinetobacter junii SH205           AYPKTTLLVALLIFLVSLYPLTRLGGEFLPNMDEGDLLYMPSALPGLSAAKASELLQQTDRMIKTVPEVATVFGKAGRAE
Putative_Pectobacterium  carotovorum     SYPKTTLLVSGLLLLLTLFPLSRLGSEFMPPLDEGDLLYMPSTLPGISAREAGRLLQQTDRLIKTVPEVESVFGKAGRAE
CusA_Providencia rettgeri DSM1131        AWPKTTLLIGFLSLFTVIWPLKHLGGEFLPAINEGDLLYMPSTLPGVSPAQAAFLLQNTDKLIKTIPEVDTVFGKVGKAE
                                           *   :  .   .     *. : *.**:* ::********::***::  .*  :** ::::*  :***  *:** *:*:

CusA_Escherichia coli K12                TATDSAPLEMVETTIQLKPQEQWRPGMTMDKIIEELDNTVRLPGLANLWVPPIRNRIDMLSTGIKSPIGIKVSGTVLADI 693
Putative_Shigella sonnei                 TATDSAPLEMVETTIQLKPQDQWRPGMTMDKIIEELDNTVRLPGLANLWVPPIRNRIDMLSTGIKSPIGIKVSGTVLADI
CzcA_Shewanella sp. ANA-3                TATDSAPLEMMETTIQLKPEDQWRPGMTIDKIIEELDRTVRLPGLANLWVPPIRNRIDMLSTGIKSPIGIKVSGTVLSDI
SilA_Klebsiella pneumoniae               TATDSAPLEMVETTIQLKPEDQWRPGMTIDKIIDELDRTVRLPGLANLWVPPIRNRIDMLSTGIKSPIGIKVSGTVLSDI
Putative_Serratia marcescens             TATDSAPLEMVETTIQLKPEDQWRPGMTIDKIIEELDRTVRLPGLANLWVPPIRNRIDMLSTGIKSPIGIKVSGTVLSDI
SilA_Salmonella Typhimurium              TATDSAPLEMVETTIQLKPEDQWRPGMTIDKIIDELDRTVRLPGLANLWVPPIRNRIDMLSTGIKSPIGIKVSGTVLSDI
CzcA_Erythrobacter sp. NAP1              TATDPAPLTMFETTIRFKPREEWRPGMTPEKLVEELDRAVQVPGLANVWVPPIRNRIDMLATGIKSPIGVKVSGENLGEI
CzcA_Sphingopyxis alaskensis RB2256      TATDPAPLEMFETTIHFKPRDQWRPGMTPEKLVEELDAKVKVPGLANIWIPPIRNRIDMLATGIKSPIGVKVSGSDLAEL
CzcA_Caulobacter sp. K31                 SATDPAPLEMFETTIRFKPRDQWRPGMTPEKLVEELDRTVAVPGLSNVWVPPIRNRIDMLATGIKSPIGVKVSGADLAQL
CzcA_Phenylobacterium zucineum HLK1      TATDPAPLEMFETTIQFKPRGEWRPGMTPEKLVEELDRAVQVPGLANVWVPPIRNRIDMLATGIKSPIGVKVSGPDLAQL
CzcA_Asticcacaulis excentricus CB 48     SATDPAPMEMFETTIQFKPRDQWRPGMTPDKLVEELDRTVKVPGLANVWVPPIRNRIDMLATGIKSPIGVKVSGSNLAEL
CzcA_Pseudomonas fluorescens Pf0-1       TATDPAPLEMFETTIQFKPHDQWRPGMTPEKLVEELDRVVRVPGLTNIWIPPIRNRIDMLATGIKSPIGVKVAGNDLAQI
CzcA_Thiobacillus denitrificans          TATDPAPLEMFETTIQFKPREQWRAGMTPDELVEELDRAVRVPGLANIWVPPIRNRIDMLATGIKSPVGVKIAGSHLADI
CzcA_Stenotrophomonas sp. SKA14           TATDPAPLEMFETTVKLKPREQWRPGMTPEKLVEELDRAVKIPGLSNIWIPPIRNRIDMLATGIKSPIGVKVTGNDLGVI
CzcA_ Acidovorax sp. JS42                TATDPAPLEMFETTVKLKPREQWRPGMTPEKLVEELDRAVKIPGLSNIWIPPIRNRIDMLATGIKSPIGVKVTGNDLGVI
CzcA_Leptothrix cholodnii SP-6           SATDPAPIEMFETTIQLKPREQWRAGMTPDKLVEELDRAVKVPGLSNLWVPPIRNRIDMLATGIKSPIGVKVTGGDLAAI
CusA_curvibacter                         TATDPAPMEMFETTVQLKPREQWRVGMTPEKLIETLDQAVKVPGLSNIWIPPIRNRIDMLATGVKSLIGVKVNGTDLATI
CzcA_Ralstonia pickettii 12J             SATDPAPIEMFETTIQFKPHDQWRPGMTTDKLVEELDRVVKVPGLSNIWVPPIRNRIDMLATGIKSPVGIKVAGTDLKEI
SilA_Ralstonia metallidurans CH34        SATDPAPIEMFETTIRFKPKDQWRPGMTTDKLVEELDRIVKVPGLSNIWVPPIRNRIDMLATGIKSPVGIKVAGTDLKEI
Putative_Methylibium petroleiphilum PM1  TATDPAPMEMFETTIQFKPKDQWRDGMTSDRLVEELDRIVKVPGLSNIWVPPIRNRIDMLATGIKSPVGVKVAGTDLAEI
CzcA_Delftia acidovorans SPH-1           SATDPAPLEMFETTIQFKPRDQWRAGMTTDKLVEELDRIVKVPGLSNIWVPPIRNRIDMLATGIKSPVGVKVAGTDLATI
CzcA_Yersinia kristensenii               TATDPAPLTMIETTIRFKPKDQWRPGMTMDKLIEELDATVKVPGIANLWVPPIRNRLDMLSTGIKSPVGIKVNGKNVQQI
CusA_Klebsiella pneumoniae               TATDSAPLEMVETTIQLKPQDQWRPGMTMEKIVEELDKTVRLPGLANLWVPPIRNRIDMLSTGIKSPIGVKVSGTNLADI
CzcA_Polaromonas naphthalenivorans CJ2   TATDPAPMEMFETTIQFKPKDQWRAGMTQDQLVEELDRIVQVPGLSNIWVPPIRNRIDMLATGIKSPVGVKVAGTDLQTI
CusA_Edwardsiella ictaluri               TATDSAPLEMIETTIQLKPQEQWRPGMTMDRIIAELDATVRLPGLANLWVPPIRNRIDMLSTGIKSPIGIKVSGTVLADI
CusA_Enhydrobacter aerosaccus SK60       SATDSAPLEMFETTIQFKPRSEWRSGMTPDKLVKELDKAVQVPGLTNIWVPPIRNRIDMLATGVKSPIGIKISANDLQDI
CusA_Citrobacter sp. 30-2                TATDSAPLEMVETTIQLKPQDQWRPGMTMDKIIAELDKTVRLPGLANLWVPPIRNRIDMLSTGIKSPIGIKVSGNVLADI
CzcA_Acinetobacter junii SH205           SATDPAPLEMFETTIQFKPRSEWRSGMTPDKLVKELDKAVQVPGLTNIWVPPIRNRIDMLATGVKSPIGIKISANDLQDI
Putative_Pectobacterium  carotovorum     TATDPAPLTMLESTIRLKPRNQWREGMTMDKLVAELDRTVSLPGIVNVWVPPIRNRLDMLATGIKSPVGIKVNGNNLADI
CusA_Providencia rettgeri DSM1131        TATDSAPMEMIETTIRLKPQAQWREGMTLEKIIDELDETVRLPGVANLWVPPIRNRIDMLSTGVKSPIGIKVSGRDLEEI
                                         :***.**: *.*:*:::**. :** *** :.::  **  * :**: *:*:******:***:**:** :*:*: .  :  :

CusA_Escherichia coli K12                DAMAEQIEEVARTVPGVASALAERLEGGRYINVEINREKAARYGMTVADVQLFVTSAVGGAMVGETVEGIARYPINLRYP 773
Putative_Shigella sonnei                 DAMAEQIEEVARTVPSVASALAERLEGGRYINVEINREKAARYGMTVADVQLFVTSAVGGAMVGETVEGIARYPINLRYP
CzcA_Shewanella sp. ANA-3                DVTAQSIEAVAKTVPGVVSALAERLEGGRYIDVDINREKASRYGMTVGDVQLFVSSAIGGAMVGETVEGVARYPINIRYP
SilA_Klebsiella pneumoniae               DATAQSIEAVAKTVPGVVSVLAERLEGGRYIDIDINREKASRYGMTVGDVQLFVSSAIGGAMVGETVEGVARYPINIRYP
Putative_Serratia marcescens             DATAQSIEAVAKTVPGVVSALAERLEGGRYIDVDINREKASRYGMTVGDVQLFISSAIGGATVGETVEGVARYPINIRYP
SilA_Salmonella Typhimurium              DATAQSIEAVAKTVPGVVSVLAERLEGGRYIDIDINREKASRYGMTVGDVQLFVSSAIGGAMVGETVEGVARYPINIRYP
CzcA_Erythrobacter sp. NAP1              ERVALQVENVAKQVPGVSSALAERLSGGRYVDVDIDRVAAARFGLNIADVQQIVSGAIGGANIGRTVEGLARYPINVRYP
CzcA_Sphingopyxis alaskensis RB2256      DRIAHDVETAAKAVPGVSSALAERLTGGRYVDVEIDRLAAARFGLNIADVQEIVAGAIGGENVGQTVEGLARYPINVRYP
CzcA_Caulobacter sp. K31                 DRVAQQIAQVAKTVPGVSSALAERLAGGRYVDVRIDRAAAGRYGLNIADVQAIVSGAIGGQTVGETVEGLARYPISVRYP
CzcA_Phenylobacterium zucineum HLK1      DRVAAQVEAVARRTPGVSSALAERLTGGRYVDVSIDRSAAARFGLNIADVQEIVSGAVGGETIGETVEGVARYPISVRYP
CzcA_Asticcacaulis excentricus CB 48     DRIAHDVETVAKTVPGVSSALAERLTGGRYVDVDIDRAAAGRYGLNTSDVQSIISGAVGGENVGETVDGLARYPINVRYP
CzcA_Pseudomonas fluorescens Pf0-1       DAATQAVERVAKGVPGVSSALAERLTGGRYIDVDIDRNAAGRYGLNISDVQSIVSGAIGGENIGETIEGLARFPINIRYP
CzcA_Thiobacillus denitrificans          DRIAQDVERVAKTVPGVSSALAERLTGGRYVDVDIDRAAAARYGMNIGDVQSAVANLIGGENIGETVEGLARYPINVRYP
CzcA_Stenotrophomonas sp. SKA14           DRIAAEVEQVAKGIPGVTSSLAERLTGGRYVDVQIDRVAAGRYGLNIADVQAVIAGAVGGENVSETVEGLARFPINLRYA
CzcA_ Acidovorax sp. JS42                DRIAAEVEQVAKGIPGVTSSLAERLTGGRYVDVQIDRVAAGRYGLNIADIQAVIAGAVGGENVSETVEGLARFPINLRYA
CzcA_Leptothrix cholodnii SP-6           DRVAARIEQVAKGVPGVSSALAERLTGGRYVDVQIDRAAASRYGLNIADVQALVAGAIGGENVTETIEGRARFPVNLRYP
CusA_curvibacter                         DRIASQIEQVAKSVPGVSSALAERLTGGRYVDVQIDRVAAGRYGLNINDVQALVSGAIGGENVAETIEGLARFPINLRYP
CzcA_Ralstonia pickettii 12J             DRLTTRIEETVKTVPGVTSALAERLSGGRYIDVDINRQAAGRYGLNIDDVQSIVSSAIGGDNVGEVVDGLARFPINLRYP
SilA_Ralstonia metallidurans CH34        DRLATRIEEAVKTVPGVTSALAERLTGGRYIDVDIDRAAAGRYGLNIEDVQSIVSSAIGGETVGEVVDGLARFPINVRYP
Putative_Methylibium petroleiphilum PM1  DRIASEVEKAVRGVPGVSSALAERLTGGRYVDVNINRDTAARYGMNIADVQSVISTAVGGDNVGETVEGLQRFPINVRYP
CzcA_Delftia acidovorans SPH-1           DRLTGEIERTLKDVPGVSSALAERLTGGRYVDVNIRRDDAARYGLNIADVQSVVSSAVGGENIGETVEGLQRFPINLRYP
CzcA_Yersinia kristensenii               EQVAQKIEQVVRKVPGVTSALSERLAGGRYVDIDIDRKRAARYGVSVKELQSLVETVIGGQNIGETIEGRERYPINLRYP
CusA_Klebsiella pneumoniae               DAIAEQIEGVARTVPGVTSALAERLVGGRYLNIDIQREKAARYGMTVGDVQLFVSSAIGGAMVGETVEGVERYPINIRYP
CzcA_Polaromonas naphthalenivorans CJ2   DKLSSEIERALKDVPGVSSALAERLTGGRYVDVNIKRDAAASFGLNIADVQSVISSAVGGENIGETVEGLQRFPINMRYP
CusA_Edwardsiella ictaluri               DATAQRIEAVARGVPGVVSALAERLEGGRYIDIQIQRQRAARYGMTVADVQLFVSSAIGGAMVGETVEGVARYPIALRYP
CusA_Enhydrobacter aerosaccus SK60       DRVAQQIEQVAKQVPGVSSALAERLTGGRYVDVDINRMQAARYGLNINDVQQIVSSAIGGENIGETVEGLARYPINVRYP
CusA_Citrobacter sp. 30-2                DATAEQIEEVARTVPGVSSALAERLVGGRYLNVDINRERAARYGMTVGAVQLFVTSAVGGAMVGETVEGIARYPINLRYA
CzcA_Acinetobacter junii SH205           DRVAQQIEQVAKQVPGVSSALAERLTGGRYVDVDINRMQAARYGLNINDVQQIVSSAIGGENIGETVEGLARYPINVRYP
Putative_Pectobacterium  carotovorum     ERTAAQIEQVVKQVPGVTSALAERLAGGRYIDIDIDRQRAARYGVSVEELQSVVSTLIGGQNIGETIEGRQRYPINIRYP
CusA_Providencia rettgeri DSM1131        DALAQEIEKVTKSVPGVVSVLAERLVGGRYIDVKIDREKAARFGMSVSDVQVYISMATGGEMIGETVEGIERYPISIRYP
                                         :  :  :  . :  *.* * *:*** ****::: * *  *. :*:.   :*  :    **  : ..::*  *:*: :**.
```

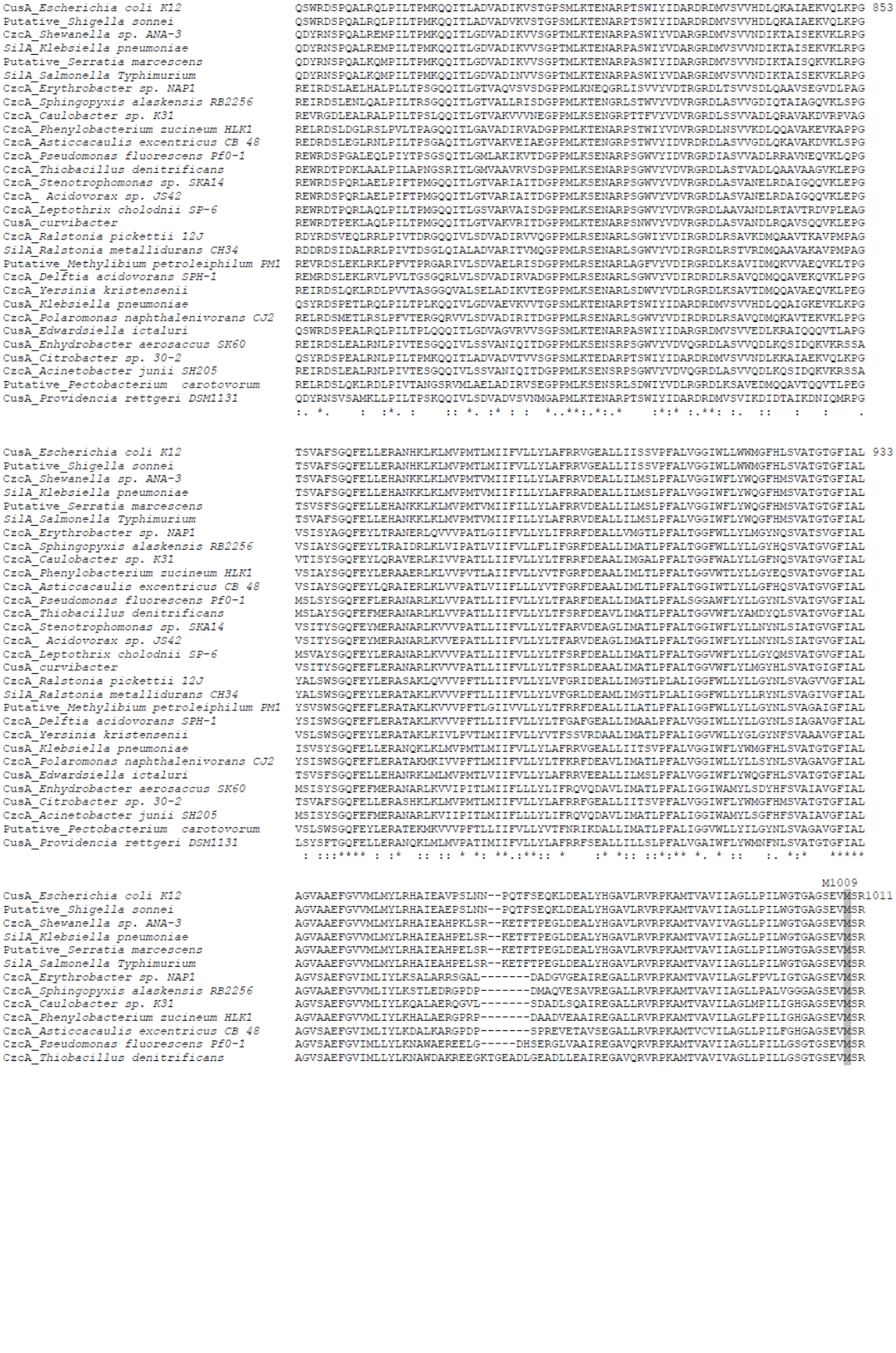
CusA_Escherichia coli K12
Putative_Shigella sonnei
CzcA_Shewanella sp. ANA-3
SilA_Klebsiella pneumoniae
Putative_Serratia marcescens
SilA_Salmonella Typhimurium
CzcA_Erythrobacter sp. NAP1
CzcA_Sphingopyxis alaskensis RB2256
CzcA_Caulobacter sp. K31
CzcA_Phenylobacterium zucineum HLK1
CzcA_Asticcacaulis excentricus CB 48
CzcA_Pseudomonas fluorescens Pf0-1
CzcA_Thiobacillus denitrificans
CzcA_Stenotrophomonas sp. SKA14
CzcA_ Acidovorax sp. JS42
CzcA_Leptothrix cholodnii SP-6
CusA_curvibacter
CzcA_Ralstonia pickettii 12J
SilA_Ralstonia metallidurans CH34
Putative_Methylibium petroleiphilum PM1
CzcA_Delftia acidovorans SPH-1
CzcA_Yersinia kristensenii
CusA_Klebsiella pneumoniae
CzcA_Polaromonas naphthalenivorans CJ2
CusA_Edwardsiella ictaluri
CusA_Enhydrobacter aerosaccus SK60
CusA_Citrobacter sp. 30-2
CzcA_Acinetobacter junii SH205
Putative_Pectobacterium carotovorum
CusA_Providencia rettgeri DSM1131
853
933
M1009
1011

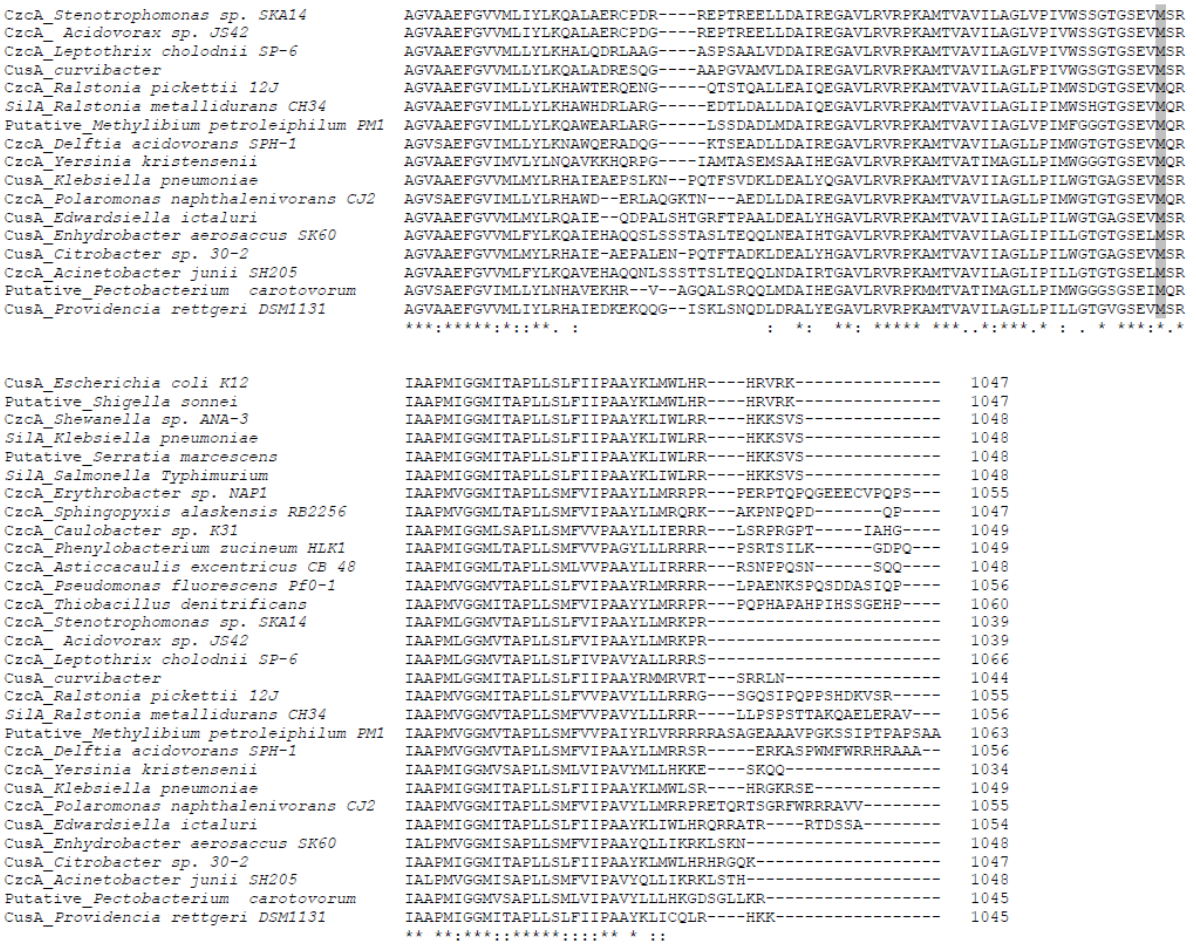


Fig. S7. Alignment of amino acid sequences of the HME-RND-type Cu(I) and/or Ag(I) efflux pumps using CLUSTAL W. *, identical residues; :, >60% homologous residues. The alignment suggests that the methionine residues forming the relay network are conserved among these 30 different pumps. Six of these methionines located at the transmembrane region are highlighted with gray bars.

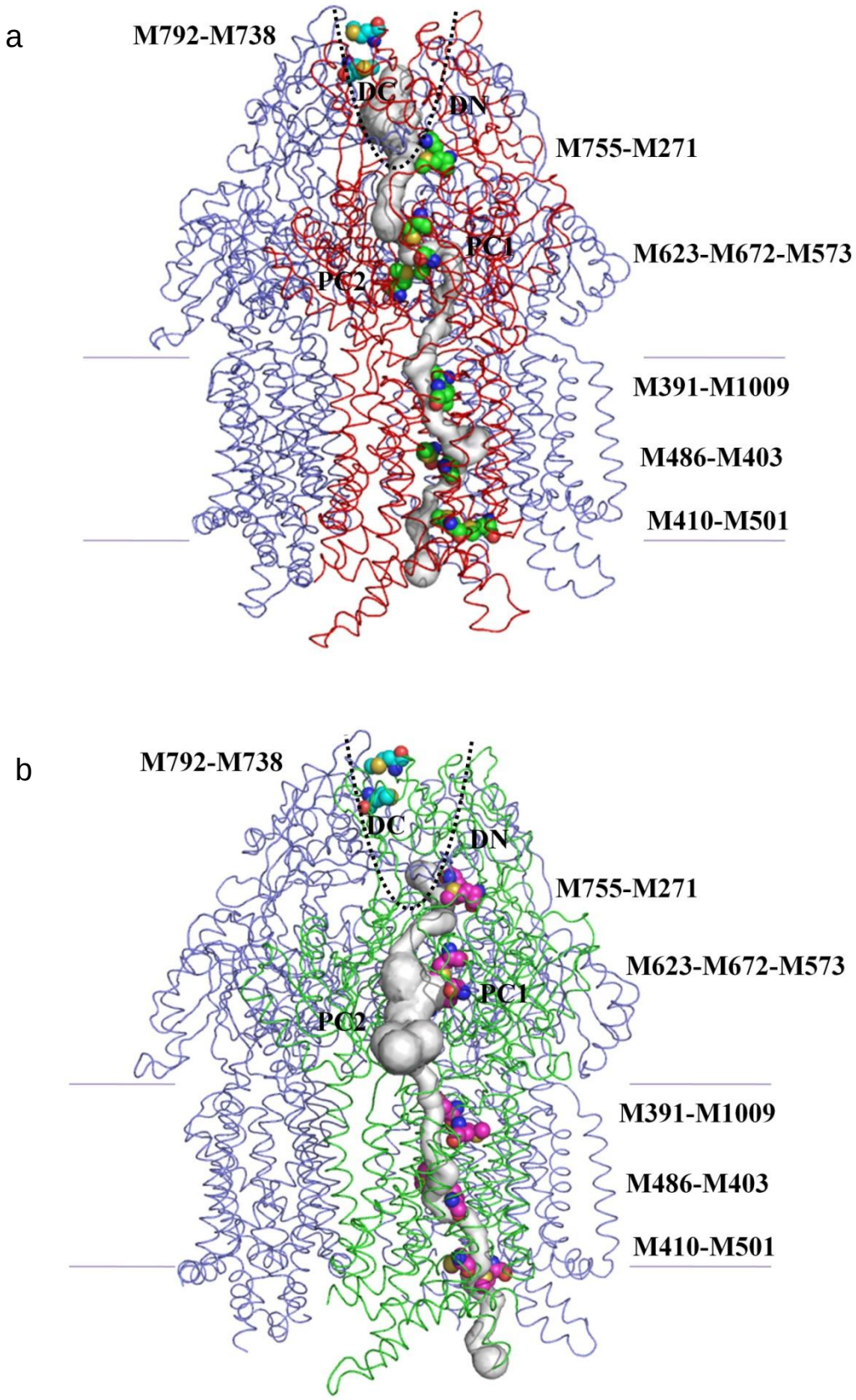
a
M792-M738
DC
DN
M755-M271
PC1
PC2
M623-M672-M573
M391-M1009
M486-M403
M410-M501
b
M792-M738
DC
DN
M755-M271
M623-M672-M573
PC1
PC2
M391-M1009
M486-M403
M410-M501

Fig. S8. Channel in the CusA pump. (a) The channel formed by the front protomer of apo-CusA (red) leading through the transmembrane and periplasmic domains is in gray color. The 11 methionines forming the relay network are in spheres (green, carbon; red, oxygen; blue, nitrogen; orange, sulfur). The Cα atoms of the methionine pair, located at the top of the funnel, which does not involve in creating the channel are colored cyan. Two other CusA protomers behind the front protomer are shown as blue wires. (b) The channel formed by the front protomer of Cu(I) bound-CusA (green) leading through the transmembrane and periplasmic domains is in gray color. The 11 methionines forming the relay network are in spheres (pink, carbon; red, oxygen; blue, nitrogen; orange, sulfur). The Cα atoms of the methionine pair, located at the top of the funnel, which does not involve in creating the channel are colored cyan. Two other CusA protomers behind the front protomer are shown as blue wires. The funnel formed by sub-domains DN and DC is indicated with a dotted curve. For clarity, the channels formed by the other two protomers at the back are omitted. The calculations were done using the program CAVER (http://loschmidt.chemi.muni.cz/caver).

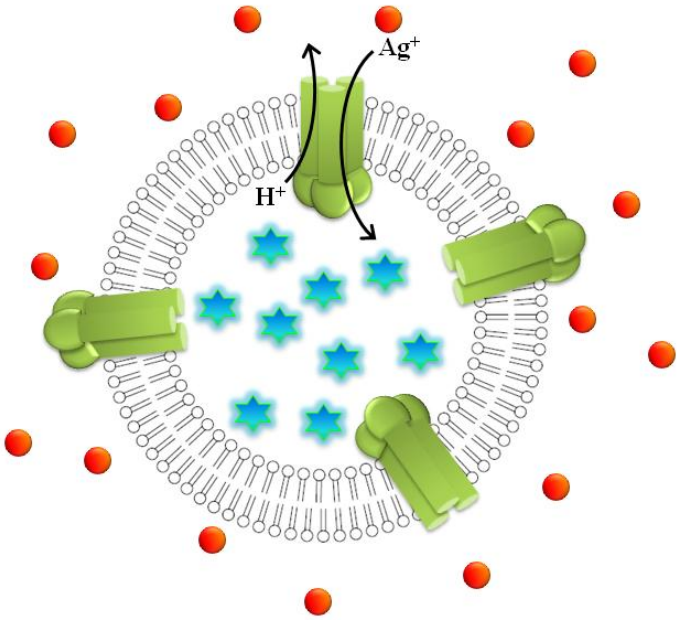


Fig. S9. A cartoon of a proteoliposome containing the CusA trimers. The CusA trimers are in green. The intravesicular space is loaded with the fluorescence indicator PGSK (blue star). $Ag^+$ (red sphere) is then added into the extravesicular medium for metal transport.

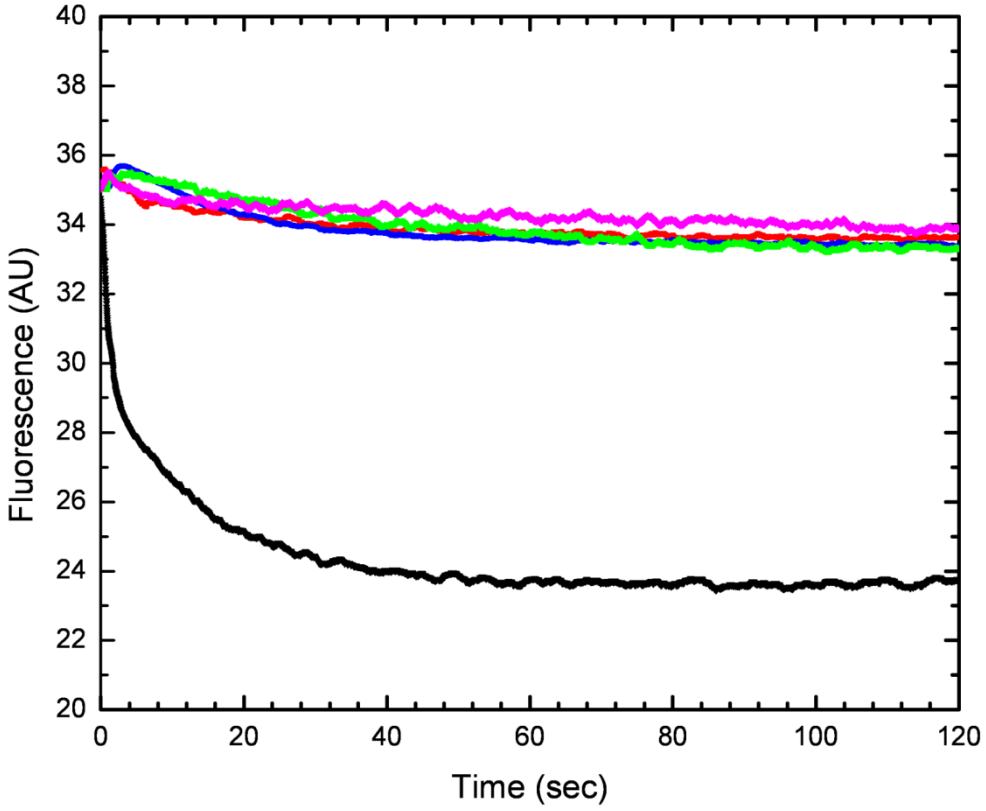


Fig. S10. Stopped-flow transport assay of reconstituted wild-type CusA with extravesicular $Ag^+$ ion at different intravesicular and extravesicular pHs. The stopped-flow traces are the cumulative average of four successive recordings (intravesicular pH = 6.6 and extravesicular pH = 7.0, black curve; intravesicular pH = extravesicular pH = 6.6, blue curve; intravesicular pH = extravesicular pH = 7.0, green curve; intravesicular pH = 7.0 and extravesicular pH = 6.6, pink curve; control liposome, red curve).

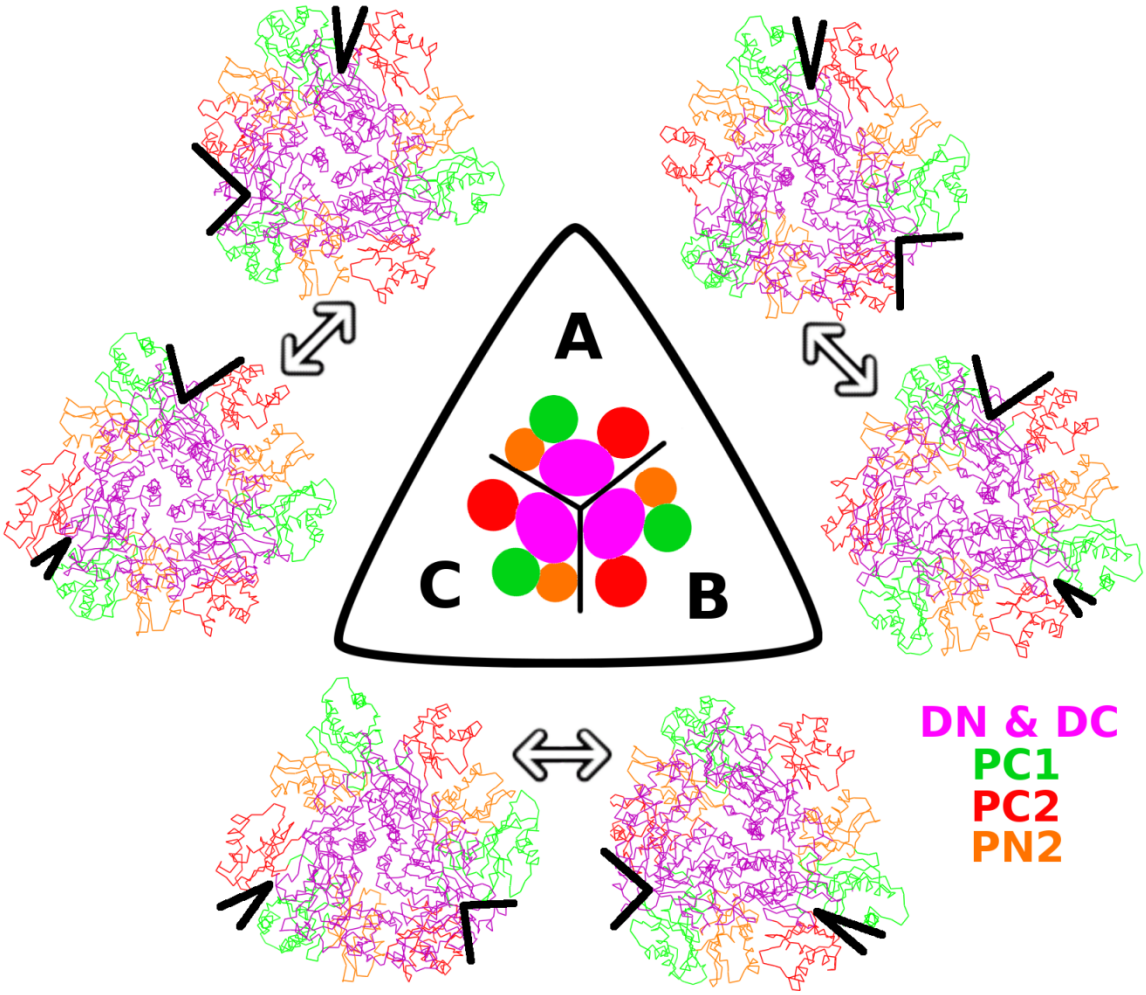


Fig. S11. The neighbor dependent opening closing motions. We show the effects of the strong internal motions on the CusA trimer. In the center is a diagram of the periplasmic domain looking downward, towards the inner membrane. We build an elastic network model using the formalism of Atilgan et al.[34] to predict the natural motions of CusA. On each of three sides we show the effect of two of the structure's natural motions. These motions describe coupled opening and closing of adjacent periplasmic metal entry sites. Black wedges are shown in open and closed form, indicating the approximate angle between the

edges of PC1 and PC2 in each motion. From these the alternating open/close motion is evident.

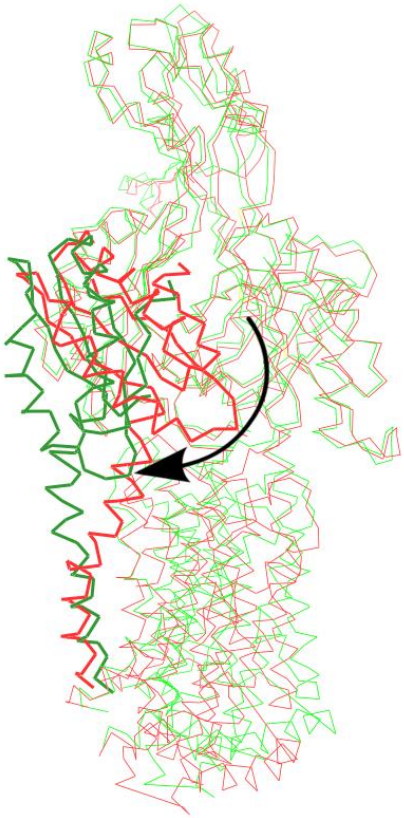

Fig. S12. The swinging motion of PC2 coupled to TM8, as computed with the same elastic network model used for Fig. S11. This motion is similar to the difference between the apo and bound crystal forms displayed in Fig. 2. An arrow indicates the motion of swinging from the red conformation to the green. For clarity PC2 and TM8 are shown in thicker lines than the remainder of the monomer.

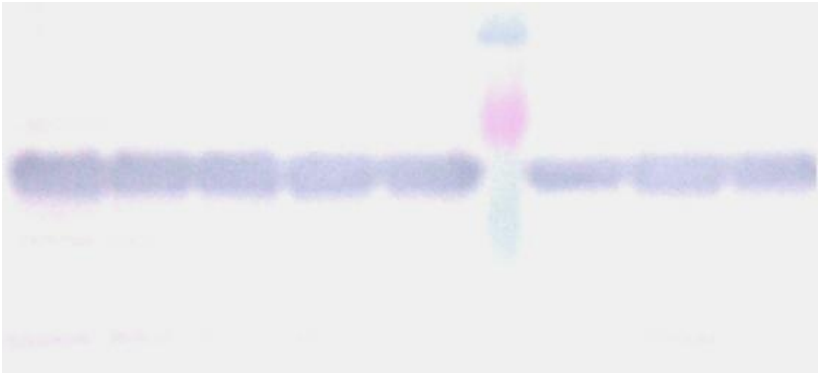

Fig. 13. Expression level of the CusA pumps. An immunoblot against CusA of crude extracts from 50 μg dry cells of strain BL21(DE3)Δ*cueO*Δ*cusA* expressing the CusA pumps (M755I, lane 1; M391I, lane 2; M410I, lane 3; M486I, lane 4; wild-type, lane 5; marker, lane 6; M573I, lane 7; M623I, lane 8; M672I, lane 9) is shown.

# CHAPTER 4. General Conclusions and Future Directions

Multidrug resistance of common pathogens is one of the most serious issues regarding human health. To ensure their survival, bacteria have developed a mechanism that involves the expression of multidrug efflux transporters to subvert antibiotics and other toxic compounds. In this dissertation, several efflux pumps belonging to different transporter families, such as MATE and RND, were functionally and structurally characterized.

We have cloned, expressed and purified the *N. gonorrhoeae* NorM MATE-type transporter. The functions of NorM and its homologous protein *E. coli* YdhE were examined using drug susceptibility and transport assays. Both NorM and YdhE confer resistance to various antimicrobial agents in a similar but slightly different manner. Direct measurements of drug efflux in living cells indicated that NorM behaves as a $Na^+$/drug antiporter, which is consistent with the previous hypothesis that MATE transporters utilize $Na^+$ as the coupling cation. Recently, a few efflux pumps, identified as MATE transporters, have been identified as $H^+$/substrate antiporters. These antiporters include PmpM of *P. aeruginosa* (1), AbeM of *A. baumannii* (2), and hMATE1 from human chromosome 17 (3). The selection of cations for energy coupling is definitely not by random. Thus, the question of how a bacterium selectively chooses a particular cation for better energy coupling remains to be elucidated. To this point, it is expected that the extracellular environment might somehow account for it (4). The functional information of more MATE transporters is needed to uncover this energy coupling mechanism.

The work of NorM of *V. parahaemolyticus* suggested that the three conserved anionic residues (Asp32, Glu251 and Asp367) in the predicted transmembrane regions are important

for the function of the pump (5). Our preliminary results (not shown) from drug susceptibility assay also indicated that the corresponding mutants in *N. gonorrhoeae* NorM (Asp41, Glu261 and Asp377) are defective in drug resistance. It is unclear how these charged residues involve in the operation of the active pumps. Systematic and rational mutations should be made to elucidate the molecular mechanism that NorM utilizes to expel toxic compounds out of the cell. The crystal structure of NorM appears to be essential to address this fundamental question. Until now, the structural information of the MATE family transporters has not yet been available. Preliminary crystallization study of NorM in our laboratory has shown that the best crystal diffracted to a resolution of 3.8 Å, thus providing us with a strong foundation in optimizing the crystallization conditions and hopefully having the crystal structure determined (6).

In this dissertation, we have determined the crystal structure of CusA, which serves as the first three-dimensional structural model of the HME-RND efflux pumps. A major conformational change was revealed by comparing the crystal structures with and without Cu(I) and Ag(I). The metal binding site, located at the periplasmic domain, is formed by three methionines (M573, M623 and M672). Based on the crystal structures, we proposed that the metal ion is exported through a methionine-residue relay network which involves five methionine pairs/clusters in the pump. We also performed metal transport assay using proteoliposomes. The results suggest that these methionine pairs/clusters are essential for the active efflux of silver ions. In addition, we have also identified three charged residues that form the proton relay network of the pump. Sequence alignment among different RND efflux pumps shows these charged residues, located at the transmembrane domain, are conserved among the HME-RND efflux pumps.

It has been generally accepted that the RND-type transporters operate through an alternating-access mechanism that involves the asymmetric conformation of the trimeric pump (7, 8). Thus, CusA may go through a cyclic conformational change, from the "access", through the "binding" and finally to the "extrusion" conformers of the trimeric pump to export metal ions. With the development of the single molecule technique, it is possible to capture the functional dynamics of CusA during metal export.

The study of AcrB tripartite system suggested that AcrB is likely to capture its substrates from the periplasm (9). It is not known if AcrB could pick up drug molecules from the cytoplasm. Our proposed metal export pathway suggests that CusA is capable of accepting the metal ions through both the cytoplasm and periplasm. This may imply that the RND pumps may be able to detoxify the interior of the cell by picking up toxic compounds both from the cytoplasmic and periplasmic spaces. The fact that substrate can be directly transported from the cytoplasm is also supported by the works of other RND transporters. For example, the *C. metallidurans* CzcA HME-RND transporter has been found to export $Zn^{2+}$ ions through the cytoplasm (10). Further, these RND transporters are also found in Gram-positive bacteria (YerP, ActII3) (11, 12), mycobacteria (MmpL7) (13, 14), and human cells (NPC1) (15, 16), in which both of these cells possess only one single layer of cell membrane.

To understand how the RND pumps operate to mediate drug and toxic chemical resistance, the crystal structure of the tripartite efflux complex is essential. Currently, our laboratory is in the process of crystallizing the CusBA and CusCBA complexes. It is expected that the complex structures will allow us to uncover the mechanisms by which the RND transporters employ to export toxic substances.

## References


1. He, G.-X., T. Kuroda, T. Mima, Y. Morita, T. Mizushima, and T. Tsuchiya. 2004. An $H^+$- coupled multidrug efflux pump, PmpM, a member of the MATE family of transporters, from *Pseudomonas aeruginosa*. *J. Bacteriol.* 186:262-265.
2. Su, X.-Z., J. Chen, T. Mizushima, T. Kuroda, and T. Tsuchiya. 2005. AbeM, an $H^+$-coupled *Acinetobacter baumannii* multidrug efflux pump belonging to the MATE family of transporters. *Antimicrob. Agents Chemother.* 49:4362-4364.
3. Otsuka, M., T. Matsumoto, R. Morimoto, S. Arioka, H. Omote, and Y. Moriyama. 2005. A human transporter protein that mediates the final excretion step for toxic organic cations. *Proc. Natl. Acad. Sci. USA* 102:17923-17928.
4. Kuroda, T., T. Tsuchiya. 2009. Multidrug efflux transporters in the MATE family. *Biochim Biophys Acta.* 1794:763-768.
5. Otsuka, M., M. Yasuda, Y. Morita, C. Otsuka, T. Tsuchiya, H. Omote, Y. Moriyama. 2005. Identification of essential amino acid residues of the NorM $Na^+$/multidrug antiporter in *Vibrio parahaemolyticus*. *J. Bacteriol.* 187:1552-8.
6. Su, C.-C., F. Long, G. McDermott, W. M. Shafer, and E. W. Yu. 2008. Crystallization and preliminary X-ray diffraction analysis of the multidrug efflux transporter NorM from *Neisseria gonorrhoeae*. *Acta Cryst. F* 64:289-292.
7. Murakami, S., R. Nakashima, E. Yamashita, T. Matsumoto, and A. Yamaguchi. 2006. Crystal structures of a multidrug transporter reveal a functionally rotating mechanism. *Nature* 443:173-179.

8. Seeger, M. A., A. Schiefner, T. Eicher, F. Verrey, K. Dietrichs, and K. M. Pos. 2006. Structural asymmetry of AcrB trimer suggests a peristaltic pump mechanism. *Science* 313:1295-1298.

9. Nikaido, H. 1996. Multidrug efflux pumps of gram-negative bacteria. *J. Bacteriol.* 178:5853-59.

10. Goldberg, M., Pribyl, T., Juhuke, S. & Nies, D. H. 1999. Energetics and topology of CzcA, a cation/proton antiporter of the resistance-nodulation-cell division protein family. *J. Biol. Chem.* 274:26065-26070.

11. Saier, M. H., Jr., S. R. Goldman, R. R. Maile, M. S. Moreno, W. Weyler, N. Yang, I. T. Paulsen. 2002. Transport capabilities encoded within the *Bacillus subtilis* genome. *J. Mol. Microbiol. Biotechnol.* 4(1):37–67.

12. http://www.tcdb.org/tcdb/index.php?tc=2.A.6

13. Cole, S. T., R. Brosch, J. Parkhill, T. Garnier, C. Churcher, D. Harris, S. V. Gordon, K. Eiglmeier, S. Gas, et al. 1998. Deciphering the biology of *Mycobacterium tuberculosis* from the complete genome sequence. *Nature* 393:537-544.

14. Rasca, M. R., P. Guglierame, E. De Rossi, F. Zara, G. Riccardi. 2005. *mmpL7* gene of *Mycobacterium tuberculosis* is responsible for isoniazid efflux in *Mycobacterium smegmatis*. *Antimicrob Agents Chemother.* 49(11):4775-7.

15. Chang, T. Y., C. C. Chang, N. Ohgami, Y. Yamauchi. 2006. Cholesterol sensing, trafficking, and esterification. *Annu. Rev. Cell Dev. Biol.* 22:129-57

16. Davies, J. P., F. W. Chen, Y. A. Ioannou. 2000. Transmembrane molecular pump activity of Niemann-Pick C1 protein. *Science* 290:2295-8.

# ACKNOWLEDGEMENTS

First, I would like to thank my major advisor, Dr. Edward Yu. I am deeply impressed with his spirit as a scientist who is willing to dedicate his life to science. His penetrating insights into the cutting-edge research of biological science invigorate me. The dissertation research couldn't have been finished successfully without his precious advices and strict requirements. The courage and persistence in front of difficulties which I learned from him will benefit me not only in the research but also in the future life. Heartfelt thanks to him!

I would like to thank all other professors in my POS committee, Dr. Drena Dobbs, Dr. Gregory Phillips, Dr. Kai-Ming Ho, and Dr. Qijing Zhang. Thanks them for their valuable advices and kind help during my Ph.D study.

I also want to thank all of the current and previous lab members. Thanks them for their help in the past six years.

I want to thank the staffs in ISU facilities, including DNA facility, protein facility and proteomic facility, and hybridoma facility. Thanks for their services and help during the progress of my research. I want to thank the staffs of the beamline 24ID-C/E in APS. They helped me a lot regarding collecting and processing the data.

Finally, I want to thank all my family members and my friends. They are always on my side and support me no matter what happens and whenever I confront difficulties. Without them, I could not finish the degree.